

## Response to Referee and Other Comments

An observational constraint on stomatal function in forests: evaluating coupled carbon and water vapor exchange with carbon isotopes in the Community Land Model (CLM 4.5)

Brett Raczka, Henrique F. Duarte, Charles D. Koven, Daniel Ricciuto, Peter E. Thornton, John C. Lin, David R. Bowling

Manuscript #: doi:10.5194/bg-2016-73, submitted Mar 22, 2016

Thank you to the referees, editor and Dr. Keeling for their time and extremely thorough reviews. Their comments have greatly improved the manuscript. A combined response to these comments are below. Line numbers in the author response refer to the revised manuscript (not the track changes version). Also note that the referee comments refer to pages, line numbers and figures from the original manuscript that no longer match with the revised manuscript. Each comment is numbered in the order presented by each referee.

The most important addition to the revised manuscript reflects the potential impact of mesophyll conductance upon the simulations – commented upon by both reviewers. We have addressed this in the manuscript abstract (page 2, lines 13-14) discussion (page 19, lines 3-17) and conclusions (page 25, lines 26-31). Also please see the responses to the reviewer questions related to mesophyll conductance. (Referee 1.4, 1.20, 1.23, 2.8).

Secondly, we have included a new figure (Figure 1) that was suggested by the reviewers and Dr. Keeling to help clarify the carbon flow within the CLM model, including the impact of nitrogen limitation within the two major formulations of CLM in our analysis. We refer to it within the manuscript (page 8, lines 13-14 and page 8, lines 25-26). Also please see the responses to reviewer questions related to this topic. (Referee 1.10, Ralph Keeling 2)

On behalf of all authors,

Dr. Brett Raczka

brett.raczka@utah.edu

University of Utah

---

Response to comments of editor:

Editor 1: Many thanks for your replies to the reviewer comments. Please provide a thoroughly revised version, addressing each of the comments and ensuring that your responses are reflected by changes in the manuscript.

Author: We have provided a fully revised manuscript based upon the reviewers, editor and Dr. Keeling's comments. We also have provided a track changes version of this revised manuscript.

Editor 2: I don't think that the terminology of 'pre-photosynthetic' vs. 'post-photosynthetic' N limitation is useful. Rather I would recommend to state that either photosynthesis or growth is assumed to acclimate to N availability.

Author: We believe the terminology of 'pre-photosynthetic' vs. 'post-photosynthetic' N limitation is the most straightforward way to define the two major model formulations. Admittedly, this description makes the most sense from a modeling point of view and not necessarily from an ecological perspective, however, we devote considerable discussion describing the model formulations from an ecological perspective in Section 2.1.2. We think the editor's suggestion to define the 'post-photosynthetic' formulations as 'acclimating to N availability' is a useful way to distinguish between the two formulations and we have added discussion (page 8, lines 26-29) to reflect this. We caution that to equate the 'post-photosynthetic' formulation as the only formulation that 'acclimates to N availability' is not strictly true – even the 'pre-photosynthetic' formulation which uses a calibrated  $V_{\text{cmax}}$  likely reflects, in part, the influence of nitrogen availability.

Editor 3: The use of gross photosynthesis is not really helpful when defining intrinsic water-use efficiency, because as a consequence of the varying temperature response of  $A$  and leaf dark respiration  $iWUE$  will vary with temperature, which it should not. I do not see a justification for not using  $A_n$ .

Author: We anticipated that the % change of  $iWUE$  whether using net assimilation or gross assimilation rate would remain relatively unchanged given that the modeled climate (and therefore temperature) remained generally constant during the dynamic portion of the simulation. Nevertheless, we re-made Figure 7 using net assimilation instead of gross assimilation and found that the  $iWUE$  increased slightly more, from 15% to 20% from 1960-2000. We have updated Figure 7 and included discussion on page 16, lines 18-20 to reflect this change. We have also edited equation 7 and Table 2 to reflect this change in the definition of  $iWUE$ .

Editor 4: Please provide a reference for the discrimination values.

Author: If we understand the comment correctly, you mean the observed photosynthetic discrimination that we describe in Section 3.2.2, Figure 8 and Figure 10. In all these locations we reference Bowling et al. (2014) as the source for the photosynthetic discrimination values.

Editor 5: Your response to 1.12 is unsatisfying: How can GPP at the ecosystem level not be dependent on  $A_n$  on the leaf level. This makes absolutely no sense at all.

Author: Agreed, this is strange, but it is a result of the CLM model structure and does not reflect the expected ecological linkage. We have added several equations to the manuscript to make this clearer (Equations 6 and 7), not only for this question, but based on reviewer comment 1.11 (see below). The potential GPP is calculated from the potential leaf-level photosynthesis (Equation 6). Next, the potential GPP is downscaled through nitrogen availability (equation 9). This downscaling of potential GPP does not feed back to the leaf-level equations of  $A_n$  and  $g_s$  (equations 1 and 4), which is why CLM is considered a 'partially' coupled model. We have added discussion of this on page 16, lines 26-32, and this also serves as a response to comment 2.9 and Keeling 3.

The editor is correct that from an overall ecological perspective the actual (downscaled) GPP must result from an actual (downscaled) leaf level photosynthesis. This is calculated from CLM as:  $GPP/LAI$ . However, this downscaled leaf level photosynthesis is distinct from the modeled definition of  $A_n$  in

Equation 1, and that is what we are referring to in our response to reviewer 1.12. We have added this caveat in the response to reviewer 1.12.

Editor 6: Your response to 1.16. It should be possible to calculate the fraction of LE which is driven by transpiration and therefore identify whether the canopy or soil fluxes contribute to the WUE bias.

Author: We interpreted comment 1.16 as referring to the observed intrinsic water use efficiency, data for which are not available. We assume from the reviewer comment that the WUE bias that is referred to is the underestimation of the increase in simulated iWUE as described in Figure 7 panel F and discussed in section 3.2.1. Now that we have updated iWUE to be the ratio of the *net* assimilation to stomatal conductance and not *gross* assimilation to stomatal conductance (see editor comment 3) the simulated increase in iWUE (20% -limited nitrogen, 10% unlimited nitrogen) now spans the range from other literature (15-20%), making the simulation and observations indistinguishable. We have updated page 16, lines 16-20 to reflect this change. In response to the reviewer's comment, we did examine the simulated mean fraction of transpired latent heat, which was 70-75% during the summer months. We don't feel it is within the scope of the present manuscript to add this now that the WUE bias is gone, however, we can add it the supplemental material at the editor's discretion.

---

Response to comments of Referee 1:

Referee 1.1: The manuscript by Raczka et al. provides an extensive description of how carbon isotope discrimination is represented in the CLM land surface model and how it can be used as a constraint for evaluating model performance. The model evaluation conducted in this paper provides valuable insights into the representation of physiological processes in process-based models, including potential improvements with regard to model structure and parameterization. This information will be useful to the wider land surface modeling community.

Author: Thank You

Referee 1.2: The abstract could explicitly mention that three different N-limitation formulations were tested in the model. This information is worth to mention, but somewhat hidden in the abstract. E.g. it would make sense to shortly explain what the "alternative nitrogen limitation" formulation in line 29 actually means. To compensate for the additional number of words one could shorten the Vcmax calibration description or try to focus on a few key outcomes.

Author: We have clarified this by using the pre-photosynthetic vs. post-photosynthetic terminology within the abstract, which was used later in the manuscript (page 1-2, line 27-29 and 1). We believe this improves upon the 'alternative nitrogen formulation' description, but leaves a necessarily detailed description for the main body of the manuscript (too long for abstract).

Referee 1.3: The original source of the Ball Berry model (Ball et al. 1987) should be acknowledged. Further,  $h_s$  represents relative, and not specific humidity at the leaf surface. The definition of  $h_s$  is unnecessary.

Author: Citation added. Corrected  $h_s$  to relative humidity. Thanks for catching this.

Referee 1.4:  $c_i$  is intercellular, not intracellular CO<sub>2</sub> partial pressure, unless you consider mesophyll conductance, which seems not to be the case.

Author: Thanks for catching this terminology mistake. This has been corrected, and there now is a paragraph in the discussion (page 19 lines 3-17) highlighting that CLM ignores mesophyll conductance, and discusses the implications.

Referee 1.5: Equation 13: what does  $E_T$  represent? In Table 1 it is listed as leaf transpiration, but that clearly doesn't make sense here. But I wonder if it is ecosystem transpiration or evapotranspiration?

Author:  $E_T$  was changed to ecosystem transpiration in Table 1.

Referee 1.6: Table 1: please check the unit for  $iWUE$ , it shouldn't be  $gC\ gH_2O^{-1}$ . Add CO<sub>2</sub> and O<sub>2</sub> for the Michaelis Menten constants.

Author: The units for  $iWUE$  were changed to  $\mu mol\ C\ mol\ H_2O^{-1}$  and we added CO<sub>2</sub> and O<sub>2</sub> for the constants.

Referee 1.7: In Equation 14, I assume you mean " $A_n$ " rather than " $A$ ". Please clarify.

Author: We have changed Equation 14 to read  $A_n$  and have changed panel F Figure 7 ( $iWUE$ ) to reflect this change.

Referee 1.8: Please provide latin names for the dominant species at the site.

Author: We added latin names on page 9, lines 24-25.

Referee 1.9: Equation 8: please state where the 4.4 and 22.6 come from and which of those represents fractionation due to diffusion and Rubisco. I am not sure if this is clear to all readers.

Author: This is now made clear in the text, (page 7, lines 21-23) that 4.4 and 22.6 represent the diffusional and enzymatic contributions to isotopic discrimination during photosynthesis.

Referee 1.10: 2.1.2: The comparison of different versions of how nitrogen limitation is implemented in the model and its implications is a very interesting aspect covered by the manuscript. Unfortunately, the three different formulations tested (unlimited N, limited N, no downregulation discrimination) are described in a rather confuse way, and I doubt that it will be comprehensible for all readers. I strongly encourage the authors to include the overview figure that they have shown in an earlier comment

Author: We have added a new Figure 1 to help make this clear. We also refer to this figure on page 8, line 13-14 and page 8, line 25-26.

Referee 1.11: I recommend a better explanation of Equation 7. How is N-limitation determined? This is mentioned in the Figure caption, but one could also include this in the manuscript as well. Further, the terms "potential" and "actual photosynthesis" are mentioned on page 7, line 17f, but they haven't been defined before, and they aren't common terms either. In the standard (= limited nitrogen) version, is photosynthesis first calculated without N-limitation, then N-limitation calculated according to Equation 7, and then the actual photosynthesis calculated by  $A_n \cdot (1 - f_{dreg})$ ?

Author: This is now better addressed by adding Figure 1 and associated text (page 8, line 13-14 and page 8, line 25-26), and by adding equations (6 and 9) that define how potential GPP is calculated from  $A_n$ , and that potential GPP is downscaled with  $f_{dreg}$ .

Referee 1.12: How is it possible that a reduction in  $A_n$  caused by N-limitation does not feedback on  $g_s$ ? This should be the case considering Eq. 4. The approach becomes clearer after reading section 3.3, but it would be helpful to explain it better at this point.

Author: ' $A_n$ ' (leaf-level photosynthesis) does not undergo a reduction from N-limitation, only GPP (ecosystem photosynthesis). This should be much clearer now with the addition of Eqs. 6 and 9 as discussed previously. In general, the fact that N-limitation does not feedback on  $A_n$  and  $g_s$ , makes CLM a 'partially' coupled model. We added discussion to reflect this on page 16, line 26-32.

As pointed out by the editor (editor comment 5) to our initial response to comment 1.12, the  $A_n$  we are referring to is from Equation 6, which technically is the 'potential' leaf level photosynthesis, and not the actual leaf level photosynthesis (after N downscaling).

Referee 1.13: 2.2 State here that NEE and other fluxes are observations based on the eddy covariance method. Please clarify here that the NEE partitioning was conducted using two different methods, and briefly mention their approach.

Author: We implemented these changes on page 10, lines 3-7.

Referee 1.14: P.10 line 27ff: that's a very detailed description which seems unnecessary to me. One could shorten this part or omit completely. - Same is true for the last sentence in 2.3 and the first sentences of 2.4., where many technical and CLM-specific details are mentioned that one may consider to omit, as they are of lesser interest to the wider community.

Author: We have simplified the explanation of the synthetic  $CO_2$  and  $\delta^{13}C$  time series in sections 2.3.1, 2.3.2 and moved the details to the Methodological details section of the supplement.

Referee 1.15: Figure 2: I think it would make more sense to show a mean annual course of the three variables rather than the complete time series. The way it is now makes it hard to see by how much GPP, ER, and LE differ from the observations on average.

Author: Good idea. Figure 3 has been updated to show the average seasonal cycle in fluxes. We moved the original figure 2 to the supplement (Figure S1), not only to provide the length of the data record, but also to demonstrate transient behavior as revealed by the flux data (i.e. changes in productivity, or latent heat exchange by drier conditions etc.)

Referee 1.16: An interesting aspect is the underestimation of WUE. Is this more related to evaporation or transpiration? In the latter case this would be strongly related to the stomatal slope parameter " $m$ " in the Ball-Berry model (see later comment), but could have other reasons as well. One could shortly comment on this, up to the authors.

Author: The manuscript does not address the accuracy of modeled WUE, given we don't have observations of transpiration and therefore no observations of WUE, only observations of latent heat flux, which the model simulates quite well after calibration (see Figure 3).

Now that we have updated iWUE to be the ratio of the net assimilation to stomatal conductance and not gross assimilation to stomatal conductance (see editor comment 3) the simulated increase in iWUE (20% -limited nitrogen, 10% unlimited nitrogen) now spans the range from other literature (15-20%), making the simulation and observations indistinguishable. We have updated page 16, lines 16-20 to reflect this change. Diagnosing how much of the latent heat comes from transpiration is now, in our opinion, outside the scope of the manuscript, but we could add this to the supplement at the editor's discretion.

Referee 1.17: P.16 line 13: Please make sure that the iWUE trend reported in the studies cited here refer to the same time period. Over which timespan did the 15-20% increase in iWUE occur according to these studies?

Author: We clarified the text to state this change occurred within the time frame of 1960-2000. (Page 16, Lines 16-18)

Referee 1.18: 3.2.1 you state that "...this trend imposed by iWUE can be neutralized by increasing  $c_a$ ." Firstly, what trend do you mean? The one in  $c_i/c_a$ ?

Author: We mean the established relationship between iWUE and discrimination, that is, as iWUE increases, discrimination weakens (Saurer et al. 2004; equation 19). We discuss this in the previous paragraph (page 17, lines 12-29), and edited the text to emphasize what relationship/trend we mean (page 17, lines 30-31).

Referee 1.19: Secondly, I am struggling with the logic of this sentence, since the principal effect of rising  $c_a$  is stomatal closure, which increases iWUE. So how can  $c_a$  counteract this at the same time? Doesn't that depend on how strong stomata respond to  $c_a$ , as you have mentioned at the beginning of the section? This on the other hand is strongly controlled by the stomatal model used. The Ball-Berry model predicts a proportional decrease of  $g_s$  with  $c_a$  and a constant  $c_i/c_a$ . Please clarify this argument, in particular the role of  $c_a$  for iWUE.

Author: Equation 19 defines an inverse relationship between iWUE and  $c_i^*/c_a$  (full derivation of this relationship can be found in the supplement). Equation 19 suggests that  $c_i^*/c_a$  (discrimination) should decrease as a result of iWUE increasing (constant  $c_a$ ). However, if  $c_a$  is also increasing at the same time this relationship between iWUE and discrimination can weaken. Because iWUE should respond to an increase in  $c_a$  through  $g_s$  (as you have commented), this implies a weak stomatal response to  $c_a$  in the model.

Referee 1.20: I'm also wondering why the effect of mesophyll conductance is not discussed at this point, even though its importance is underlined in one of the studies you have cited (Seibt et al. 2008)? What would change if it was explicitly considered?

Author: Please see added discussion of implications of ignoring mesophyll conductance on page 19, lines 3-17). We also added discussion (page 17: lines 12-21) that explains one of the key reasons that iWUE and discrimination can vary independently is because the model that Seibt et al. 2008 uses that relates iWUE and  $\delta^{13}C$ , includes mesophyll conductance. They demonstrate that trends do emerge that are different from the linear model used by Saurer et al. (2004), consistent with our simulation results

(increasing WUE and increasing discrimination). This finding is largely coincidental, considering that CLM does not include mesophyll conductance, however, it is still important to show the model is not necessarily in conflict with observed trends.

Referee 1.21: 3.2.2 The idea that the stomatal slope may be too high for the site is interesting. Indeed a recent compilation of this parameter (Lin et al. 2015, Nature climate change) showed significantly lower values for coniferous evergreen forests than for other vegetation types (note that the study uses a slightly different model, and that the slopes cannot be compared 1:1, but they should vary in the same manner). One could cite this reference and point out that there is a biological explanation for why the slope should be lower for coniferous vegetation compared to other vegetation types. One could further explicitly mention that a lower stomatal slope would also give a lower stomatal conductance for a given  $A_n$ , and thus reduce the model-observation mismatch. Note that this would also affect  $V_{cmax}$ .

Author: Thank you for bringing this to our attention. The idea that the stomatal slope is too high leading to a stomatal conductance that is too high is also consistent with our simulated mismatch in discrimination (i.e. it is too high). We have added the Lin et al. 2015 paper to page 18-19, lines 27-29, 1-2.

Referee 1.22: Section 3.3 is very interesting, but I wonder if there is some more information on why one approach should be preferred over the other? Here you show that the limited N formulation is inferior to the others, which is nice, but is there also some biological evidence for this? What I mean is that the one reference you cite here (Zaehle et al., 2014) could be backed up by other (non-modeling) studies.

Author: Referee 2 offers DeKauwe et al., (2013) that provides site based observations within the FACE experiment at Duke and Oak Ridge, that indicate that fully coupled  $A_n$ - $g_s$  models tend to perform better in terms of GPP and WUE response to increased  $CO_2$ . We have included discussion of this on pages: 22-23 lines 30-32, 1-3.

Referee 1.23: Conclusions: You state that the isotope measurements suggest a lower  $g_s$  than the flux tower measurements. I'm not sure if I agree with that, since you didn't derive  $g_s$  directly from the eddy covariance measurements, but rather used the Ball-Berry model with an uncalibrated stomatal slope to model  $g_s$ . So if your stomatal slope parameter is inappropriate for the vegetation at the site, then your  $g_s$  will be as well, but that can't be directly related to the eddy covariance data.

Author: After calibration of  $V_{cmax}$  the simulated fluxes matched the flux tower observations much better (Figure 3), which makes our calibrated set of parameters consistent with the eddy covariance flux tower data, and biomass observations. We think it is reasonable to suggest the stomatal slope is too high considering that other studies suggest the stomatal slope should be relatively low for coniferous evergreen species (Lin et al. 2015; Mao et al. 2016) (which we add discussion of page 18-19, lines: 23-29, 1-2), and that the simulation is overestimating discrimination –consistent with a stomatal slope (stomatal conductance) that is too high.

However, we agree with the reviewer that because the stomatal slope parameterization was not taken directly from leaf-gas exchange measurements at the site, therein lies a possibility that calibrating the stomatal slope value to match isotopic discrimination could be in fact compensate for other parametric or structural errors within CLM. We discuss this possibility on page 19, lines 3-17 where we

may be able to correct for bias in discrimination by including a representation of mesophyll conductance in CLM.

Referee 1.24: Figure 1: what do the lines prior to 1850 represent? Is it necessary to show them here?

Author: We changed the limits for the first column to start at 1850 in what is now Figure (2).

Referee 1.25: Figure 8: in Panel A it says fractionation in the heading but discrimination in the caption. Please stick to one.

Author: We changed heading to discrimination in what is now Figure (9).

Referee 1.26: I suggest mentioning the FLUXNET ID of the site (US-NR1) - P.9 line 16: Max Planck Institute for Biogeochemistry - P.9, line 18: remove brackets - P.5 line 13: remove brackets - Omit sentences like "the source code was modified. . ." - The horizontal lines of the error bars seem a bit over-dimensioned - P. 21, line 19: "through", not "though"

Author: All changes were made.

---

#### Response to comments of Referee 2:

Referee 2.1: I found the introduction very clear but I wonder if there is any other literature on how other models have used isotope data? I realize the authors suggest this is the first time it has been attempted in CLM and I realise this paper is primarily targeted at the CLM community, nevertheless I think my one concern would be the lack of literature in relation to other models and isotopes?

Author: As this referee points out later in the review: "... [suggests] cuts that could be made to the text which would make it more digestible."; here is an instance where we felt we needed to be concise. We do make references to previous isotope literature as was relevant to our work, for example Mao et al. (2016) Page 18, Line: 23 and Aranibar et al. (2008) Page 18, Line: 26. Nevertheless, to address the reviewer's concern we have added a sentence that includes a list of isotope enabled land surface models. Lines: page 4, lines 2-6.

Referee 2.2: Equation 1: I don't think you mean  $\text{Resp}_d$  = dark respiration.  $R_{\text{dark}}$  is not the same as day respiration/respiration in the light. Suggest the use of  $R_{\text{day}}$  or  $R_d$ .

Author: Correct. The CLM literature (Oleson et al. 2013) uses the term ' $R_d$ ' to describe this respiration term. For this manuscript, we have purposely named this term ' $\text{Resp}_d$ ' to prevent confusion with the isotope community convention of using ' $R$ ' to describe the ratio of  $^{13}\text{C}$  and  $^{12}\text{C}$  isotopes. To address the reviewer's concern we refer to this term as just 'leaf respiration' in the text and Table (1).

Referee 2.3: Equation 4: I'm pretty sure that "Bt" should be applied to your slope term "m", rather than the minimum stomatal conductance, b? Can you please check you have this correct?

Author: This is correct as we have defined in Equation (4). See Oleson et al. (2013), page 183.



Referee 2.4: Line 23: "tree canopy" is this only true for trees, what happens with grasses in the model? If not, perhaps delete tree and leave just canopy.

Author: We replaced "tree" with "vegetation" to avoid confusion on page 6, line 25-26. In this manuscript CLM simulates the Niwot Ridge vegetation as a temperate evergreen needleleaf forest as stated in page 12, line 11-14. Grasses are not considered in this manuscript, but CLM is capable of simulating grasses.

Referee 2.5: Equation 8 & 9: it would be helpful to the reader to explain where the numbers 4.4, 22.6 and 1000 come from, or what conversions they apply to.

Author: We edited the text (page 7, lines 21-23) to make a clearer linkage between the numbers and the fractionation mechanism they represent.

Referee 2.6: Century model (line 26/27) should have a reference.

Author: We added a reference to page 12 line 3-5.

Referee 2.7: I'm not sure what the length of the paper was but the results/discussion text did feel very long? Similarly the conclusions runs to nearly two pages. This seems excessive to me. I'm fairly confident there are cuts that could be made to the text which would make it more digestible to the reader. I certainly found myself losing track during my reading and I think this is the key area which requires editing during revision.

Author: We found this suggestion difficult to address given its generality. However, where Reviewer 1 made specific suggestions of cuts within the Methods (2.3.1, 2.3.2) we cut roughly 20 lines of text from the Methods section. We also cut ~ 10 lines of text within the conclusions. The revised manuscript has remained the same length (26 pages) even with discussion added in response to other comments.

Referee 2.8: The authors note: "the overestimation of discrimination may suggest the stomatal slope in the Ball-Berry model ( $m=9$  in Eq. 4) used for these simulations was too high." While it may be true that the slope parameter is poorly informed by site data, the logic of this conclusion in itself may not be valid. Isotopic measurements *should* give lower slope values than those one would infer via leaf gas exchange data (i.e. the data used to inform the Ball-Berry model). This is because leaf gas exchange measures the resistance from the intercellular spaces ( $C_i$ ), whereas isotopes measures the resistance from the chloroplast ( $C_c$ ). I see no mention of this in the text and caution against the authors potential drawing the wrong conclusion from the model-data discrepancy.

Author: We now address mesophyll conductance specifically as discussed above. First, our finding that the stomatal slope parameter value is likely too large is a reasonable conclusion for 2 reasons: 1) A lower stomatal slope value is consistent with both model results (Mao et al. 2016) and leaf-gas exchange measurements (Lin et al. 2015). Discussion of the Lin et al paper was added to page 18 lines: 23-29. Second, a lower stomatal slope value will lead to a lower stomatal conductance which will help reduce the overestimation of the modeled isotopic discrimination (Figure 8).

With that being said, we have added to the discussion (page 19, lines 3-17) the possibility that this result may, in part, come from the simplified approach of CLM 4.5, that does not specifically include mesophyll conductance and assumes intercellular  $CO_2$  = intracellular  $CO_2$ . Therefore, we have added the caveat, that the need to reduce the stomatal slope, may be the result of missing mechanisms governing

mesophyll conductance within CLM. We include this possibility in the abstract (page 2, lines 11-14) and conclusions (page 25, lines 28-31).

Referee 2.9: In discussing the "limited nitrogen formulation", the authors note: "In general, there were no categorical differences in behavior between these two classes of models during CO<sub>2</sub> manipulation experiments held at Duke forest and ORNL (Zaehle et al., 2014). CLM 4.0 was one of the few models in that study to consistently underestimate the NPP response to an increase of atmospheric CO<sub>2</sub> due to nitrogen limitation, however this finding was attributed to a lower initial supply of nitrogen." This is not strictly true. As part of the same model-data inter-comparison of the models to the data at the two FACE sites, De Kauwe et al. (2013, *Global Change Biology*), found no support for the implementation whereby assimilation is limited by nitrogen availability, but not stomatal conductance. They concluded: "Stomatal conductance data from both sites were used to test modelled leaf-level responses. The simple stomatal conductance model (Eq. 1) fitted the data well (Fig. 6), supporting the assumption of coupling between assimilation and stomatal conductance. Importantly, at the ORNL site, N content of the foliage declined strongly over the course of the experiment (Norby et al., 2010), but neither the slope of the stomatal model, nor the response of A/gs to CO<sub>2</sub>, was altered by this decline (Fig. 6b). These data indicate that the coupling between stomatal conductance and assimilation is not affected by N-limitation (Fig. 6b). The data therefore tend to support coupled models over uncoupled, or partially coupled, models such as DAYCENT and CLM4." Furthermore, I would question if there is any evidence that plants follow the "limited nitrogen formulation"?

Author: Thank you for bringing De Kauwe et al. 2013 to our attention. First, we may be talking about two different sub-groupings of models: in our manuscript we are comparing pre-photosynthetic (foliar nitrogen) and post-photosynthetic nitrogen limitation models. Almost all of these models regardless of pre/post photosynthetic sub-grouping contain stomatal-photosynthetic coupling though Ball-Berry type assumptions in the stomatal conductance model.

It is true that CLM4 and CLM4.5 in the default model (post-photosynthetic model formulation) is only 'partially' coupled in terms of photosynthetic-stomatal conductance, however the unlimited nitrogen formulation (pre-photosynthetic) in our manuscript is 'fully' coupled ( $A_n$  is consistent and solved simultaneously with  $g_s$ ). Therefore, our simulations were consistent with De Kauwe et al. 2013 in that fully-coupled models matched the observations the best. We add this to the discussion on page 22-23, lines: 30-32, 1-3.

This progressive de-coupling between  $A_n$  and  $g_s$  for our default CLM 4.5 version also explains the difference in transient behavior between  $g_s$  and  $A_n$  and iWUE as shown in Figure (7). We add this to discussion in page: 16, lines: 26-32.

This referee makes another comment that seems to be referring to a 3<sup>rd</sup> sub-grouping of model – models that do not consider nitrogen limitation at all – similar to the simple stomatal-assimilation model in De Kauwe. What role does nitrogen limitation play (if any) in assimilation and stomatal behavior? We are not sure how much our manuscript can inform this question. Clearly, the default version of CLM 4.5 (post-photosynthetic formulation) is strongly influenced by the nitrogen cycle, whereas our pre-photosynthetic formulation is less strictly linked to the nitrogen cycle ( $V_{cmax}$  was calibrated to match eddy covariance flux observations, not according to nitrogen constraints). However, even for the pre-photosynthetic formulation it is plausible that leaf nitrogen content plays a role in the  $V_{cmax}$  value. Therefore within the limitations of this manuscript we don't think we can comment on the significance

of nitrogen limitation on ecosystem behavior, but only that if nitrogen limitation is implemented, it should occur pre-photosynthetically.

Referee 2.10: Figure 2. I realize that a strength of this paper is the long time series; however, showing ~15 years of data like that isn't particularly instructive. It is hard to distinguish the model-obs differences. Perhaps average a day/week or monthly climatology across years would more clearly show differences. This figure could also be kept, perhaps one could go to the supplementary.

Author: As suggested we edited figure 3 to provide a seasonally averaged flux behavior across all years, to better illustrated model-observation differences, and calibrated/uncalibrated model differences. We moved the original figure 2 within the supplement (Figure S1), not only to provide the length of the data record, but also to demonstrate any transient behavior as revealed by the flux data (i.e. changes in productivity, or latent heat exchange by drier conditions etc.)

Referee 2.11: Figure 8e. I find it hard to believe that there is no reduction in the soil moisture availability factor during the whole of the summer? This seems unlikely to me? Could this please be checked?

Author: We thought the same thing. The modeled soil moisture tends to compare favorably to the observed soil moisture as measured at multiple depths both in terms of the magnitude and seasonal trends. In general, the modeled soil moisture tends to simulate slightly wetter conditions as we point out on page 22, lines 3-12, but per discussion with site PI's, the accuracy of the soil moisture sensors is questionable. Therefore we did not attempt to calibrate the hydrology model to best match the soil moisture sensors. We hypothesize that the modeled soil moisture is too wet at depth, thereby leading to little change in BTRAN (soil moisture stress parameter). We chose to limit this discussion in the text to keep the manuscript length in check, a concern for this reviewer.

Referee 2.12: Figure 9. I would suggest the symbol sizes could be reduced, they seem a little large for the figure panels.

Author: Symbol sizes reduced in figure 10.

---

Response to comments by Ralph Keeling:

Ralph Keeling 1: Overall, very nice paper, which I found quite educational. I'm passing on here a few comments that I jotted down as I read through the paper.

Author: Thank you.

Ralph Keeling 2: Perhaps it would be possible (?) to add a figure which diagrams the carbon flows from the atmosphere, through stomata to substrate formation for each of the three formulations. I'm imagining that the diagram would have arrows for each of these quantities:  $A_n$ , GPP,  $CF_{available\_alloc}$ ,

CF\_alloc, CF\_GPPpot, etc. Or maybe one figure would suffice, assuming the knobs to switch between formulations is clear enough.

Author: We have added a new figure (Figure 1) which explicitly tracks the carbon flows through the 2 main nitrogen sub-models used in this study, and illustrates how the nitrogen limitation model interacts with these carbon flows from substrate to biomass. We also added new equations (6, 9) which explicitly show the linkage between  $A_n$  and  $CF_{GPPpot}$  and between  $CF_{GPPpot}$  and GPP. This new figure, and the new equations, combined with the existing Table 2 provides a sufficient overview of the sub-models that complements the text to enhance reader understanding. We refer to this new figure on page: 8, line: 13-14 and page: 8, line: 25-26.

Ralph Keeling 3: ....where is the carbon that is fixed but not allocated ending up? Is it respired? If so, does this respiration return back from the stomata or return through some other pathway?

Author: For the limited nitrogen sub-model (post-photosynthetic limitation), the carbon that is fixed but not allocated, is removed from the system (does not show up as a respired flux). This is arguably a weakness in this version of the model: the downscaled assimilated flux is not consistent with the carboxylation rate ( $A_n$ ) and stomatal conductance ( $g_s$ ) that created the pre-downscaled flux, and is why this version of CLM is considered to be 'partially' coupled (page 16, lines 26-32). The unlimited nitrogen sub-model (pre-photosynthetic limitation) is not subject to this apparent inconsistency and is 'fully' coupled. We have added Figure (1) that shows a valve for this downscaling, and no respired flux. We also added a line on page 8, line 24-25 that states that this excess carbon is lost to the system, and does not show up as a respired flux.

Ralph Keeling 4: Page 6, line 28: I'm missing how  $A_n$  is related to terms in Eq. (6). It would very much help to include an algebraic expression for this.

Author: We added new equation (6) that relates  $A_n$  to potential GPP term  $CF_{GPPpot}$ .

Ralph Keeling 5: Page 6, lines 29-30. From the wording it sounds like maintenance respiration is partly double counted.

Author: The  $CF_{GPP,mr}$  term comes directly from the carbon pool from photosynthesis. When there is no photosynthesis the model calls on a storage carbon pool to meet this demand:  $CF_{GPP,xs}$ . The maintenance respiration is coming from one or the other, never both. We clarify this on page 7, lines 4-6.

Ralph Keeling 6: Page 7, line 11. What does the subscript psn signify? Perhaps could be omitted?

Author:  $P_{sn}$  stands for photosynthetic fractionation. This is implied in the context of the manuscript so it was removed throughout.

Ralph Keeling 7: Page 7, line 15: This formula suggests that  $A_n$  is not equal to the flux through stomata. So what is  $A_n$  equal to? Is it the same as potential photosynthesis? If so, needs stating. See earlier comment also.

Author:  $A_n$ , as defined in equation (1) is the (potential) leaf-level net assimilation rate which is used to calculate potential photosynthesis ( $CF_{GPPpot}$ ). We now specify on page 5, line 21 that  $A_n$  is the leaf-level

net carbon assimilation. We also added equation (6) that connects  $A_n$  with  $CF_{GPP_{pot}}$  based on a previous comment making it clear that  $A_n$  is the assimilation rate that is used to calculate potential GPP.

Ralph Keeling 8: Page 7, lines 22-23: This sentence is a bit ambiguous. Are both given in Eq. 9, or just one. If not both, then how is nitrogen limitation incorporated? Reading below, I see this is probably related to control of  $V_{cmax}$ . If so, this need stating more clearly earlier.

Author: Both formulations follow Equation (9). We made changes in the text to make this clearer on page 8, lines 8-10. "The unlimited nitrogen formulation also follows equation (11), however the vegetation is allowed to have unlimited access to nitrogen."

The following paragraph on page 8 gives a thorough explanation how we used  $V_{cmax}$  in order to take into account for nitrogen limitation, even when the nitrogen downregulation factor is not used.

Ralph Keeling 9: Page 8, line 22. I'm missing an expression for how  $\delta_{GPP}$  is calculated from  $\alpha_{psn}$ . (Okay, I know enough to work this out for myself, but I'm not sure you should assume all readers would).

Author: The fractionation factor  $\alpha$  is defined in the beginning of section 2.1.2 (page 7, lines 15-16), stating that  $\alpha = R_a/R_{GPP}$ . This relates  $\alpha$  to  $R_{GPP}$ . One can then use equation (10) to get from  $R_{GPP}$  to  $\delta_{GPP}$ .

Ralph Keeling 10: Page 8, line 28. It would seem important to clarify what is meant here by GPP. Which of these is it:  $A_n$ ,  $CF_{available\_alloc}$ ,  $CF_{GPP\_pot}$ , etc. ?

Author: This GPP is the final downscaled GPP or actual GPP (ecosystem photosynthesis). We added a new equation (9) that defines how GPP is downscaled through  $f_{dreg}$ , and this downscaled, or 'actual' GPP is what is used in the definition for WUE.

# **An observational constraint on stomatal function in forests: evaluating coupled carbon and water vapor exchange with carbon isotopes in the Community Land Model (CLM 4.5)**

**Brett Raczka<sup>1</sup>, Henrique F. Duarte<sup>2</sup>, Charles D. Koven<sup>3</sup>, Daniel Ricciuto<sup>4</sup>, Peter E. Thornton<sup>4</sup>, John C. Lin<sup>2</sup>, David R. Bowling<sup>1</sup>**

[1]{Dept. of Biology, University of Utah, Salt Lake City, Utah}

[2]{Dept. of Atmospheric Sciences, University of Utah, Salt Lake City, Utah}

[3]{Lawrence Berkeley National Laboratory, Berkeley, California}

[4]{Oak Ridge National Laboratory, Oak Ridge, Tennessee}

Correspondence to: B. Raczka (brett.raczka@utah.edu)

## **Abstract**

Land surface models are useful tools to quantify contemporary and future climate impact on terrestrial carbon cycle processes, provided they can be appropriately constrained and tested with observations. Stable carbon isotopes of CO<sub>2</sub> offer the potential to improve model representation of the coupled carbon and water cycles because they are strongly influenced by stomatal function. Recently, a representation of stable carbon isotope discrimination was incorporated into the Community Land Model component of the Community Earth System Model. Here, we tested the model's capability to simulate whole-forest isotope discrimination in a subalpine conifer forest at Niwot Ridge, Colorado, USA. We distinguished between isotopic behavior in response to a decrease of  $\delta^{13}\text{C}$  within atmospheric CO<sub>2</sub> (Suess effect) vs. photosynthetic discrimination ( $\Delta_{\text{canopy}}$ ), by creating a site-customized atmospheric CO<sub>2</sub> and  $\delta^{13}\text{C}$  of CO<sub>2</sub> time series. We implemented a seasonally-varying  $V_{\text{cmax}}$  model calibration that best matched site observations of net CO<sub>2</sub> carbon exchange, latent heat exchange and biomass. The model accurately simulated observed  $\delta^{13}\text{C}$  of needle and stem tissue, but underestimated the  $\delta^{13}\text{C}$  of bulk soil carbon by 1-2 ‰. The model overestimated the multi-year (2006-2012) average  $\Delta_{\text{canopy}}$  relative to prior data-based estimates by 5-6 ‰. The amplitude of the average seasonal cycle of  $\Delta_{\text{canopy}}$  (i.e. higher in spring/fall as compared to summer) was correctly modeled but only ~~with an alternative when using pre-photosynthetic~~ nitrogen limitation in

contrast to the post-photosynthetic nitrogen limitation used in the default version of the model.  
~~formulation for the model.~~ The model attributed most of the seasonal variation in discrimination to the net assimilation rate ( $A_n$ ), whereas inter-annual variation in simulated  $\Delta_{\text{canopy}}$  during the summer months was driven by stomatal response to vapor pressure deficit. Soil moisture did not influence modeled  $\Delta_{\text{canopy}}$ . The model simulated a 10% increase in both photosynthetic discrimination and water use efficiency (WUE) since 1850 as a result of  $\text{CO}_2$  fertilization, forced by constant climate conditions. This increasing trend in discrimination is counter to well-established relationships between discrimination and WUE. The isotope observations used here to constrain CLM suggest 1) the model overestimated stomatal conductance and 2) the default CLM approach to representing nitrogen limitation (post-photosynthetic limitation) was not capable of reproducing observed trends in discrimination. These findings demonstrate that isotope observations can provide important information related to stomatal function driven by environmental stress from VPD and nitrogen limitation. Future versions of CLM that incorporate carbon isotope discrimination are likely to benefit from explicit inclusion of mesophyll conductance.

## 1 Introduction

The net uptake of carbon by the terrestrial biosphere currently mitigates the rate of atmospheric  $\text{CO}_2$  rise and thus the rate of climate change. Approximately 25% of anthropogenic  $\text{CO}_2$  emissions are absorbed by the global land surface (Le Quéré et al., 2015), but it is unclear how projected changes in temperature and precipitation will influence the future of this land carbon sink (Arora et al., 2013; Friedlingstein et al., 2006). A major source of uncertainty in climate model projections results from the disagreement in projected strength of the land carbon sink (Arora et al., 2013). Thus, it is critical to reduce this uncertainty to improve climate predictions, and to better inform mitigation strategies (Yohe et al., 2007).

An effective approach to reduce uncertainties in terrestrial carbon models is to constrain a broad range of processes using distinct and complementary observations. Traditionally, terrestrial carbon models have relied primarily upon observations of land-surface fluxes of carbon, water and energy derived from eddy-covariance flux towers to calibrate model parameters and evaluate model skill. Flux measurements best constrain processes that occur at diurnal and seasonal time scales (Braswell et al., 2005; Ricciuto et al., 2008). Traditional

Field Code Changed

Field Code Changed

Commented [BR1]: Insert manually

Field Code Changed

1 ecological metrics of carbon pools (e.g. leaf area index (LAI), biomass) are also commonly  
2 used to provide independent and complementary constraints upon ecosystem processes at  
3 longer time scales (Ricciuto et al., 2011; Richardson et al., 2010). However, neither flux nor  
4 carbon pool observations provide suitable constraints for the model formulation of plant  
5 stomatal function and the related link between the carbon and water cycles.

Field Code Changed

6 Stable carbon isotopes of CO<sub>2</sub> are influenced by stomatal activity in C3 plants (e.g.  
7 evergreen trees, deciduous trees), and thus provide a valuable but under-utilized constraint on  
8 terrestrial carbon models. Plants assimilate more of the lighter of the two major isotopes of  
9 atmospheric carbon (<sup>12</sup>C vs. <sup>13</sup>C). This preference, termed photosynthetic discrimination  
10 ( $\Delta_{\text{canopy}}$ ), is primarily a function of two processes, CO<sub>2</sub> diffusion rate through the leaf boundary  
11 layer and into the stomata, and the carboxylation of CO<sub>2</sub>. The magnitude of  $\Delta_{\text{canopy}}$  is controlled  
12 by CO<sub>2</sub> supply (atmospheric CO<sub>2</sub> concentration, stomatal conductance) and demand  
13 (photosynthetic rate; Flanagan et al., 2012). In general, environmental conditions favorable to  
14 plant productivity result in higher  $\Delta_{\text{canopy}}$  during carbon assimilation compared to unfavorable  
15 conditions. Plants respond to unfavorable conditions by closing ~~their~~ stomata and reducing the  
16 stomatal conductance which reduces  $\Delta_{\text{canopy}}$ . Most relevant here,  $\Delta_{\text{canopy}}$  responds to  
17 atmospheric moisture deficit (Andrews et al., 2012; Wingate et al., 2010), soil water content  
18 (McDowell et al., 2010), precipitation (Roden and Ehleringer, 2007) and nutrient availability.  
19 After carbon is assimilated, additional post-photosynthetic isotopic changes occur (Bowling et  
20 al., 2008; Brüggemann et al., 2011), but these impose a small influence on land-atmosphere  
21 isotopic exchange relative to photosynthetic discrimination.

Field Code Changed

Field Code Changed

Field Code Changed

Field Code Changed

Field Code Changed

22 The Niwot Ridge Ameriflux site, located in a sub-alpine conifer forest in the Rocky  
23 Mountains of Colorado, U.S.A., has a long legacy of yielding valuable datasets to test carbon  
24 and water functionality of land surface models using stable isotopes. Niwot Ridge has a 17-  
25 year record of eddy covariance fluxes of carbon, water, and energy, as well as environmental  
26 data (Hu et al., 2010; Monson et al., 2002) and a 10-year record of  $\delta^{13}\text{C}$  of CO<sub>2</sub> in forest air  
27 (Schaeffer et al., 2008). From a carbon balance perspective, Niwot Ridge is representative of  
28 subalpine forests in Western North America that, in general, act as a carbon sink to the  
29 atmosphere (Desai et al., 2011). Western forests, make up a significant portion of the carbon  
30 sink in the United States (Schimel et al., 2002), yet this ~~carbon~~ sink is projected to weaken with  
31 projected changes in temperature and precipitation (Boisvenue and Running, 2010).

Field Code Changed

Field Code Changed

Field Code Changed

Field Code Changed

Field Code Changed



1 The Community Land Model (CLM), the land sub-component of the Community Earth  
2 System Model (CESM) has a comprehensive representation of biogeochemical cycling (Oleson  
3 et al., 2013) that can be applied across a range of temporal (hours to centuries) and spatial  
4 ~~scales~~ (site to global) scales. A mechanistic representation of photosynthetic discrimination  
5 based upon diffusion and enzymatic fractionation (Farquhar et al., 1989) was included in the  
6 latest release of CLM 4.5 (Oleson et al., 2013), ~~and is similar to the formulation implemented~~  
7 in other land surface models (Flanagan et al., 2012; Scholze et al., 2003; Wingate et al., 2010;  
8 van der Velde et al., 2013). An early version of CLM simulated carbon (but not carbon isotope)  
9 dynamics at Niwot Ridge with reasonable skill (Thornton et al., 2002). ~~To date, we are not~~  
10 aware of any CLM-based studies that have used CO<sub>2</sub> isotopes at natural abundance to quantify  
11 the accuracy of the photosynthetic discrimination sub-model, or to evaluate the utility of CO<sub>2</sub>  
12 isotopes to constrain carbon and water cycle coupling.

13 Here, we evaluate the performance of the <sup>13</sup>C/<sup>12</sup>C isotope discrimination sub-model  
14 within CLM 4.5 against a range of isotopic observations at Niwot Ridge, to examine what new  
15 insights an isotope-enabled model can bring upon ecosystem function. Specifically, we test  
16 whether CLM simulates the expected isotopic response to environmental drivers of CO<sub>2</sub>  
17 fertilization, soil moisture and atmospheric vapor pressure deficit (VPD). A previous analysis  
18 at Niwot Ridge showed a seasonal correlation between vapor pressure deficit (VPD) and  
19 photosynthetic discrimination (Bowling et al., 2014) ~~which may~~ suggesting that leaf stomata  
20 are responding to changes in VPD, and influencing discrimination. We use CLM to test  
21 whether VPD is the primary environmental driver of isotopic discrimination, as compared to  
22 soil moisture and net assimilation rate. Next we determine whether including site-specific δ<sup>13</sup>C  
23 of atmospheric CO<sub>2</sub> within the model simulation combined with simulated long term (multi-  
24 decadal to century) photosynthetic discrimination and simulated carbon pool turnover,  
25 accurately reproduces the measured δ<sup>13</sup>C in leaf tissue, roots and soil carbon. We then use CLM  
26 to determine if the increase in atmospheric CO<sub>2</sub> since 1850 has led to an increase in water use  
27 efficiency (WUE), and whether net assimilation or stomatal conductance is the primary driver  
28 of such a change. Finally, we ask what distinct insights site level isotope observations bring in  
29 terms of both model parameterization (i.e. stomatal conductance) and model structure as  
30 compared to the traditional observations (e.g. carbon fluxes, biomass).

Field Code Changed

Field Code Changed

Field Code Changed

Field Code Changed

Field Code Changed

## 2 Methods

We focus the description of CLM 4.5 (Section 2.1) upon photosynthesis, and its linkage to nitrogen, soil moisture and stomatal conductance (Section 2.1.1). Next we describe the model representation of carbon isotope discrimination by photosynthesis (Section 2.1.2). Because preliminary simulations demonstrated that model results were strongly influenced by nitrogen limitation, we used three separate nitrogen formulations (described in Section 2.1.2) to better diagnose model performance. Next, to provide context for subsequent descriptions of site-specific model adjustments we describe the field site, Niwot Ridge, including the site level observations (Section 2.2) used to constrain ~~model behavior~~ and test model ~~the model skill~~.

Patterns in plant growth and  $\delta^{13}\text{C}$  of biomass are strongly influenced by atmospheric  $\text{CO}_2$  and  $\delta^{13}\text{C}$  of atmospheric  $\text{CO}_2$  ( $\delta_{\text{atm}}$ ). Therefore we designed a site-specific synthetic atmospheric  $\text{CO}_2$  product (Section 2.3.1) and  $\delta_{\text{atm}}$  product (Section 2.3.2) for these simulations. The model setup and initialization procedure, intended to bring the system into steady state, is described in Section (2.3.3). This is followed by an explanation of the model calibration procedure that provided a realistic simulation of carbon and water fluxes (Section 2.4).

### 2.1 Community Land Model, Version 4.5

We used the Community Land Model, CLM 4.5 (Oleson et al., 2013), which is the land component of the Community Earth System Model (CESM) version 1.2 (<https://www2.cesm.ucar.edu/models/current>). Details regarding the Community Land Model can be found in ~~Ma~~ Mao et al., (2016) and; Oleson et al., (2013). Here, we emphasize the mechanistic formulation that controls photosynthetic discrimination ( $\Delta_{\text{canopy}}$ ) and factors that influence  $\Delta_{\text{canopy}}$  including photosynthesis, stomatal conductance, water stress and nitrogen limitation. A list of symbols is provided in Table (1).

#### 2.1.1 Net Photosynthetic Assimilation

The ~~net leaf-level net~~ carbon assimilation of photosynthesis,  $A_n$  is based on Farquhar et al., (1980) as,

$$A_n = \min(A_c, A_j, A_p) - \text{Resp}_d, \quad (1)$$

Field Code Changed

Field Code Changed

Field Code Changed

Field Code Changed

where  $A_c$ ,  $A_j$  and  $A_p$  are the enzyme (Rubisco)-limited, light-limited, and product-limited rates of carboxylation respectively, and  $Resp_d$  the leaf-level ~~dark~~ respiration. The enzyme limited rate is defined as

$$A_c = \frac{V_{cmax}(c_i - \Gamma_*)}{c_i + K_c(1 + \frac{o_i}{K_o})}, \quad (2)$$

where  $c_i$  is the ~~intercellular~~~~internal~~ leaf partial pressure of CO<sub>2</sub>,  $o_i = 0.209 P_{atm}$ , ~~where~~  $P_{atm}$  is atmospheric pressure, and  $K_c$ ,  $K_o$  and  $\Gamma_*$  are constants. The maximum rate of carboxylation at 25°C,  $V_{cmax25}$ , is defined as

$$V_{cmax25} = N_a F_{LNR} F_{NR} a_{R25}, \quad (3)$$

where  $N_a$  is the nitrogen concentration per leaf area,  $F_{LNR}$  the fraction of leaf nitrogen within the Rubisco enzyme,  $F_{NR}$  the ratio of total Rubisco molecular mass to nitrogen mass within Rubisco, and  $a_{R25}$  is the specific activity of Rubisco at 25°C. The  $V_{cmax25}$  is adjusted for leaf temperature to provide  $V_{cmax}$  in Eq. 2, used in the final photosynthetic calculation.

The carbon and water balance are linked through  $c_i$  by the stomatal conductance ~~to CO<sub>2</sub>~~,  $g_s$ , following the Ball-Berry model (~~Ball, 1987~~) as defined by Collatz et al., (1991),

$$g_s = m \frac{A_n}{c_s / P_{atm}} h_s + b \beta_t, \quad (4)$$

where  $m$  is the stomatal slope,  $c_s$  the partial pressure of CO<sub>2</sub> at the leaf surface,  ~~$h_s$  the relative humidity at the leaf surface~~ and  $b$  the minimum stomatal conductance when the leaf stomata are closed. ~~The variable  $h_s = e_t / e_s$  is the leaf surface specific humidity with  $e_t$  the vapor pressure at the leaf surface and  $e_s$  the saturation vapor pressure inside the leaf.~~ The variable  $\beta_t$  represents the level of soil moisture availability, which influences stomatal conductance directly, but also indirectly through  $A_n$  by multiplying  $V_{cmax}$  by  $\beta_t$  (Sellers et al., 1996). CLM calculates  $\beta_t$  as a factor (0-1, high to low stress) by combining soil moisture, the rooting depth profile, and a plant-dependent response to soil water stress as

$$\beta_t = \sum_i w_i r_i, \quad (5)$$

where  $w_i$  is a plant wilting factor for soil layer  $i$  and  $r_i$  is the fraction of roots in layer  $i$ . The plant wilting factor is scaled according to soil moisture and water potential, depending on plant functional type (PFT). Soil moisture is predicted based upon prescribed precipitation and vertical soil moisture dynamics (Zeng and Decker, 2009). The root fraction in each soil layer

Formatted: Subscript

Commented [BR2]: Need to add this manually. Look for other citations that may have been manually added are not there anymore due to stupid zotero.

Field Code Changed

Field Code Changed

Field Code Changed

depends upon a vertical exponential profile controlled by PFT dependent root distribution parameters adopted from Zeng (2001).

The version of CLM used here has a 2-layer (shaded, sunlit) representation of the ~~vegetation tree canopy~~. Photosynthesis and stomatal conductance are calculated separately for the shaded and sunlit portion and the total canopy photosynthesis is the potential gross primary productivity (GPP),  $CF_{GPPpot}$ :

$$CF_{GPPpot} = [(A_{ps} + Resp_d)_{sunlit} (LAI)_{sunlit} + (A_{ps} + Resp_d)_{shaded} (LAI)_{shaded}] * 12.011^{-6}, \quad (6)$$

where  $LAI$  is the leaf area index and  $12.011^{-6}$  is a unit conversion factor. The total carbon available for new growth allocation ( $CF_{avail\_alloc}$ ) is defined as

$$CF_{avail\_alloc} = CF_{GPPpot} - CF_{GPP,mr} - CF_{GPP,xs}, \quad (7)$$

where the maintenance respiration is derived either from recently assimilated photosynthetic carbon ( $CF_{GPP,mr}$ ), is the carbon costs for maintenance respiration, if photosynthesis is low or zero (e.g. night), the maintenance respiration is drawn from a carbon storage pool and ( $CF_{GPP,xs}$ ). is the carbon allocated to a pool responsible for meeting maintenance respiration demand during periods with low or zero photosynthesis. In contrast,  $CF_{alloc}$ , is the actual carbon allocated to growth calculated from the available nitrogen and fixed C:N ratios for new growth (e.g. stem, roots, leaves). The downregulation of photosynthesis from nitrogen limitation,  $f_{dreg}$ , is given by

$$f_{dreg} = \frac{CF_{avail\_alloc} - CF_{alloc}}{CF_{GPPpot}}. \quad (8)$$

The actual, nitrogen-limited GPP is defined as:

$$GPP = CF_{GPPpot}(1 - f_{dreg}). \quad (9)$$

## 2.1.2 Photosynthetic Carbon Isotope Discrimination

The canopy-level fractionation factor  $\alpha_{psn}$  is defined as the ratio of  $^{13}C/^{12}C$  within atmospheric  $CO_2$  ( $R_a$ ) and the products of photosynthesis ( $R_{GPP}$ ) as  $\alpha_{psn} = \frac{R_a}{R_{GPP}}$ . The preference of C3 vegetation to assimilate the lighter  $CO_2$  molecule during photosynthesis is simulated in CLM with two steps: diffusion of  $CO_2$  across the leaf boundary layer and into the stomata, followed by enzymatic fixation to give the leaf-level fractionation factor:

Field Code Changed

Formatted: Font: 10 pt

Formatted: Indent: First line: 0"

Formatted: Font: 10 pt

Formatted: Font: 10 pt

Formatted: Font: 10 pt

Formatted: Font: 10 pt

Formatted: Font: 10 pt

Formatted: Font: 10 pt

Formatted: Font: 10 pt

Formatted: Font: 10 pt

Formatted: Font: 10 pt

Formatted: Font: 10 pt

Formatted: Font: 10 pt

Formatted: Font: 10 pt

Formatted: Font: 10 pt

Formatted: Font: 10 pt

Formatted: Font: 10 pt

Formatted: Font: 10 pt

Formatted: Font: 10 pt

Formatted: Font: 10 pt

Formatted: Font: 10 pt

Formatted: Font: 10 pt

Formatted: Font: 10 pt

Formatted: Font: 10 pt

Formatted: Font: 12 pt

Formatted: Superscript

$$\alpha_{psn} = 1 + \frac{4.4 + 22.6 \frac{c_i^*}{c_a}}{1000} \quad (108)$$

where  $c_i^*$  and  $c_a$  are the intracellular and atmospheric CO<sub>2</sub> partial pressure respectively. The numbers 4.4 and 22.6 represent the diffusional and enzymatic contributions to isotopic discrimination respectively. The variable  $c_i^*$  (known in CLM as the ‘revised intracellular CO<sub>2</sub> partial pressure’) is marked with an asterisk to indicate the inclusion of nitrogen downregulation as defined as,

$$c_i^* = c_a - A_n (1 - f_{dreg}) P_{atm} \frac{(1.4g_s) + (1.6g_b)}{g_b g_s} \quad (119)$$

where  $g_b$  is the leaf boundary layer conductance. — The inclusion of the nitrogen downregulation factor  $f_{dreg}$  in the above expression reflects the two-stage process in which the potential photosynthesis (Eq. 6) and the actual photosynthesis (Eq. 9) are calculated within CLM and prevents a mismatch between the actual photosynthesis and the intracellular CO<sub>2</sub>.

The sensitivity of preliminary model results to nitrogen limitation led us to test three distinct discrimination formulations (Figure 1; Table 2). The *limited nitrogen* formulation was based on the default version of CLM 4.5 and included both nitrogen limitation and the nitrogen downregulation factor within the calculation of  $c_i^*$  as given in equation (119). ~~In the~~ The second, *unlimited nitrogen* formulation also follows equation (11); however, we allowed the vegetation ~~is allowed to have~~ unlimited access to nitrogen ( $CF_{GPPpot} = CF_{GPP} GPP$ ,  $f_{dreg} = 0$ ). Finally, in the *no downregulation discrimination* formulation, we included nitrogen limitation, but removed the downregulation factor  $f_{dreg}$  within the isotopic discrimination from equation (119).

In the *unlimited nitrogen* formulation, we use a different modifier on  $V_{cmax25}$  (Figure 1; described in section 2.4 and Fig. S1, S2) in the calibrated runs to give similar carbon flux, water flux and biomass as in the other two formulations, such that all three formulations have fluxes and biomass that are similar to what is observed at the site, and which presumably reflect nitrogen limitation. Thus the distinction between these three formulations can be viewed entirely as of when nitrogen limitation is imposed in relation to photosynthesis: (1) after photosynthesis via a downregulation between potential and actual GPP (equation 97) that feeds back on the  $c_i/c_a$  used for isotopic discrimination but not on the stomatal conductance  $g_s$  or  $A_n$  in the *limited nitrogen* formulation; (2) before photosynthesis via  $-V_{cmax}$ , which limits photosynthetic capacity affecting both  $c_i/c_a$  and  $g_s$  and  $A_n$  ~~stomatal conductance~~ in the *unlimited*

Formatted: Font: Italic

Formatted: Font: Italic

Formatted: Font: Italic

Formatted: Font: Italic, Subscript

Formatted: Font: Italic

Formatted: Font: Italic, Subscript

Formatted: Subscript

Formatted: Font: Italic

Formatted: Font: Italic

Formatted: Font: Italic, Subscript

Formatted: Font: Italic

Formatted: Font: Italic

Formatted: Font: Italic

Formatted: Font: Italic, Subscript

nitrogen formulation; and (3) after photosynthesis with no effect on either the  $c_i/c_a$  for isotopic discrimination or  $g_s$  or  $A_n$  the stomatal conductance in the no downregulation discrimination formulation. The downscaled portion of the carbon during nitrogen limitation ( $CF_{GPPpot} - GPP$ ) is removed from the system and does not appear as a respired flux (Figure 1). In summary, the limited nitrogen (post-photosynthetic) formulation adjusts the photosynthetic rate by explicitly tracking N availability, whereas the unlimited nitrogen (pre-photosynthetic) formulation takes into account any N-limitation through  $V_{cmax}$  parameterization.

Carbon isotope ratios are expressed by standard delta notation,

$$\delta^{13}C_x = \left( \frac{R_x}{R_{VPDB}} - 1 \right) \times 1000, \quad (120)$$

where  $R_x$  is the isotopic ratio of the sample of interest, and  $R_{VPDB}$  is the isotopic ratio of the Vienna Pee Dee Belemnite standard. The delta notation is dimensionless but expressed in parts per thousand (‰) where a positive (negative) value refers to a sample that is enriched (depleted) in  $^{13}C/^{12}C$  relative to the standard. Because this is the only carbon isotope ratio we are concerned with in this paper, the '13' superscript is omitted for brevity in subsequent definitions using the delta notation. The canopy-integrated photosynthetic discrimination,  $\Delta_{canopy}$ , is defined as the difference between the  $\delta^{13}C$  of the atmospheric and assimilated carbon,

$$\Delta_{canopy} = \delta_{atm} - \delta_{GPP}. \quad (134)$$

The difference between  $\delta^{13}C$  of the total ecosystem respiration (ER) and GPP fluxes, called the isotope disequilibrium (Bowling et al., 2014), is defined as,

$$disequilibrium = \delta_{ER} - \delta_{GPP}. \quad (142)$$

The ecosystem-level water use efficiency (WUE) is defined as actual carbon assimilated (GPP) per unit water transpired ( $E_T$ ) per unit land surface area,

$$WUE = \frac{GPP}{E_T}. \quad (153)$$

The intrinsic water use efficiency ( $iWUE$ ) from leaf-level physiological ecology is defined as,

$$iWUE = \frac{A_n}{g_s}, \quad (164)$$

where  $A$  is the net gross carbon assimilated per unit leaf area and  $g_s$  is the stomatal conductance. CLM calculates  $g_s$  (Equation 4) for shaded and sunlit portions of the canopy separately,

Formatted: Font: Italic

Formatted: Font: Italic

Formatted: Font: Italic

Formatted: Font: Italic

Field Code Changed

therefore an overall conductance was calculated by weighting the conductance by sunlit and shaded leaf areas ~~and is used in this manuscript.~~

## 2.2 Niwot Ridge and site-level observations

Site-level observations and modeling were focused on the Niwot Ridge Ameriflux tower ([US-NR1](#)), a sub-alpine conifer forest located in the Rocky Mountains of Colorado, U.S.A. The forest is approximately 110 years old and consists of lodgepole pine (*Pinus contorta*), Engelmann spruce (*Picea engelmanni*), and subalpine fir (*Abies lasiocarpa*). The site is located at an elevation of 3050 m above sea level, with mean annual temperature of 1.5°C and precipitation of 800 mm, in which approximately 60% is snow. More site details are available elsewhere ([Hu et al., 2010](#); [Monson et al., 2002](#)). Flux and meteorological data were obtained from the Ameriflux archive (<http://ameriflux.lbl.gov/>).

Net carbon exchange (NEE) observations ~~were derived from from the~~ flux tower ~~measurements based on the eddy covariance method and~~ were partitioned into component fluxes of GPP and ER according to ~~two separate~~ methods described by [Reichstein et al., \(2005\)](#) and [Lasslop et al., \(2010\)](#) using an online tool provided by the Max Planck Institute ~~for Biogeochemistry~~ (<http://www.bgc-jena.mpg.de/~MDIwork/eddyproc/>). Seasonal patterns in  $\delta_{GPP}$  and  $\delta_{ER}$  were derived from measurements as described by ~~(Bowling et al., (2014))~~. Observations of  $\delta^{13}C$  of biomass ([Schaeffer et al., 2008](#)) and carbon stocks ([Bradford et al., 2008](#); [Scott-Denton et al., 2003](#)) were compared to model simulations. [Schaeffer et al., \(2008\)](#) reported soil, leaf and root observations specific to each conifer species, however, the observed mean and standard error for all species were used for comparison because CLM treated all conifer species as a single PFT.

## 2.3 Atmospheric CO<sub>2</sub>, isotope forcing and initial vegetation state

### 2.3.1 Site-specific atmospheric CO<sub>2</sub> concentration time series

Global average atmospheric CO<sub>2</sub> concentrations increased roughly 40% from 1850 to 2013 (from 280 to 395 ppm). The standard version of CLM 4.5 includes an annually and globally averaged time series of this CO<sub>2</sub> increase, however, this does not capture the observed seasonal ~~cyclevariation~~ of ~10 ppm at Niwot Ridge ([Trolier et al., 1996](#)). Therefore we created a site-specific atmospheric CO<sub>2</sub> time series (Figure [24](#)) to provide a seasonally realistic atmosphere at Niwot Ridge. ~~From 1968-2013 the CO<sub>2</sub> time series was fit to flask observations~~

Formatted: Font: Italic

Formatted: Font: Italic

Formatted: Font: Italic

Field Code Changed

Field Code Changed

Field Code Changed

Field Code Changed

Field Code Changed

Field Code Changed

Formatted: Subscript

(Dlugokencky et al., 2015) from Niwot Ridge. Observations were used to create the synthetic product from 1968–2013 by binning flask observations into 20 evenly spaced points each year. These flask observations were taken weekly from Niwot Ridge (Dlugokencky et al., 2015). Prior to 1968, the CO<sub>2</sub> time series was created by combining the average multi-year seasonal cycle based on the Niwot Ridge flask data to the annual CO<sub>2</sub> product provided by CLM. More details are located in the supplemental material. A polynomial fit of the annualized CLM product was created and then adjusted by 1.5 ppm to account for the average difference between the CLM product and the Niwot Ridge observations during those years. Next, the average multi-year seasonal cycle based on the de-trended flask data after 1968 was added to every year of this annualized polynomial before 1968. Finally, the synthetic atmospheric CO<sub>2</sub> time series (pre 1968) was populated with 20 evenly spaced points in time each year.

Field Code Changed

Formatted: Subscript

Formatted: Subscript

### 2.3.2 Customized $\delta^{13}\text{C}$ atmospheric CO<sub>2</sub> time series

As atmospheric CO<sub>2</sub> has increased, the  $\delta^{13}\text{C}$  of atmospheric CO<sub>2</sub> ( $\delta_{\text{atm}}$ ) has become more depleted (Francey et al., 1999), and this change continues at Niwot Ridge at -0.25 ‰ per decade (Bowling et al., 2014). The  $\delta_{\text{atm}}$  also varies seasonally, and depends on latitude (Troler et al., 1996). However, CLM 4.5 as released assigned a constant  $\delta^{13}\text{C}$  of -6 ‰.

Field Code Changed

We therefore created a synthetic time series of  $\delta_{\text{atm}}$  from 1850–2013 (Figure 24). From 1990–2013 the time series this was fit to based upon the flask observations (White et al., 2015) as described in Section 2.3.1. A similar approach to the atmospheric CO<sub>2</sub> synthetic time series (Section 2.3.1) was applied here to create the synthetic  $\delta_{\text{atm}}$ . After 1990 the flask data were binned into 20 evenly spaced points each year. Prior to 1990 the inter-annual variation within the  $\delta_{\text{atm}}$  time series was fit to the ice core data from Law Dome (Francey et al., 1999; see also Rubino et al., 2013). This annual data product was then combined with the average seasonal cycle at Niwot Ridge as determined by the flask observations to create the synthetic product from 1850–1990. More details are located in the supplemental material. The polynomial was adjusted by 0.20 ‰ to account for the inter-hemispheric difference identified during the common years (1990–1996) between the ice core and flask data. Next the average seasonal cycle (1990–2013) of  $\delta_{\text{atm}}$  was added to the adjusted polynomial prior to 1990. The synthetic time series was populated from 1850–1989 with 20 evenly spaced points each year based upon the adjusted polynomial with seasonal cycle included. As released, CLM 4.5 was not compatible with time varying  $\delta_{\text{atm}}$ , therefore we

Field Code Changed

Field Code Changed



~~modified the source code by following the model procedure for reading in time-varying  $^{14}\text{C}$ . The modified code was designed to temporally interpolate the  $\delta_{atm}$  time-series for each time step of the model. This interpolated value was then passed into the photosynthetic discrimination calculation to represent the time-varying  $\delta_{atm}$ .~~

### 2.3.3 Model Initialization

We performed an initialization to transition the model from near bare-ground conditions to present day carbon stocks and LAI that allowed for proper evaluation of isotopic performance. This was implemented in 4 stages: 1) accelerated decomposition (1000 model years) 2) normal decomposition (1000 model years) 3) parameter calibration (1000 model years) and 4) transient simulation period (1850-2013). The first two stages were pre-set options within CLM with the first stage used to accelerate the equilibration of the soil carbon pools, which require a long period to reach steady state (Thornton and Rosenbloom, 2005). The parameter calibration stage was not a pre-set option but designed specifically for our analysis. For this we introduced a seasonally varying  $V_{cmax}$  that scaled the simulated GPP and ecosystem respiration fluxes to present day observations (Section 2.4). In the transient phase, we introduced time-varying atmospheric conditions from 1850-2013 including nitrogen deposition (CLM provided), atmospheric  $\text{CO}_2$ , and  $\delta_{atm}$  (site-specific as described above). Environmental conditions of temperature, precipitation, relative humidity, radiation, and wind speed were taken from the Niwot Ridge flux tower observations from 1998-2013 and then cycled continuously for the entirety of the initialization process. We used a scripting framework (PTCLM) that automated much of the workflow required to implement several of these stages in a site level simulation (Mao et al., 2016; Oleson et al., 2013).

Field Code Changed

## 2.4 Specific model details and model calibration

~~We used PTCLM (e.g. Mao et al., 2016) to create site specific weather conditions and initial conditions for CLM 4.5.~~ This version of CLM included a fully prognostic representation of carbon and nitrogen within its vegetation, litter and soil biogeochemistry. We used the Century model representation for soil (3 litter and 3 soil organic matter pools) with 15 vertically resolved soil layers (Parton et al. 1987). Nitrification and prognostic fire were turned off. Our

Commented [BR3]: Insert this manually.

initial simulations used prognostic fire, but we found that simulated fire was overactive leading to low simulated biomass compared to observations. Although Niwot Ridge has been subject to disturbance from fire and harvest in the past, ultimately our final simulations did not include either fire or harvest disturbance because the last disturbance occurred over 1100 years ago (early 20th century logging; Monson et al., 2005).

Field Code Changed

Ecosystem parameter values (Table 3) used here were based upon the temperate evergreen needleleaf ~~plant functional type (PFT)~~ within CLM. These values were based upon observations reported by White et al., (2000) intended for a wide range of temperate evergreen forests, and by Thornton et al., (2002) for Niwot Ridge. For this analysis two site-specific parameter changes were made. First, the e-folding soil decomposition parameter was increased from 5 to 20 meters. This parameter is a length-scale for attenuation of decomposition rate for the resolved soil depth from 0 to 5 meters where an increased value effectively increases decomposition at depth, thus reducing total soil carbon and more closely matching observations. Second, we performed an empirical photosynthesis scaling (equation 175, below) that reduced the simulated photosynthetic flux, as guided by eddy covariance observations (Figure 3; Figure S1). Consequently, all downstream carbon pools and fluxes including ecosystem respiration, aboveground biomass, and leaf area index which provided a better match to present day observations. This approach also removed a systematic overestimation of winter photosynthesis. The model simulations without the photosynthetic scaling are referred to within the text and figures as the *uncalibrated* model, whereas model simulations that include the photosynthetic scaling are referred to as the *calibrated* model. The source code was modified for this scaling approach by reducing  $V_{cmax}$  at 25° Celsius,

Field Code Changed

Field Code Changed

$$V_{cmax25} = N_a F_{LNR} F_{NR} a_{R25} f_{df}, \quad (175)$$

where  $f_{df}$  is the photosynthetic scaling factor, and all other parameters are identical to equation (3). These parameters were constant for the entirety of the simulations except for  $f_{df}$ , an empirically derived time dependent parameter ranging from 0-1. The value was set to zero to force photosynthesis to zero between November 13th and March 23rd, consistent with flux tower observations where outside of this range  $GPP > 0$  was never observed. During the growing season period ( $GPP > 0$ ) within days of year 83-316,  $f_{df}$  was calculated as

$$f_{df} = \frac{\text{observed } GPP(\text{day of year})}{\text{simulated } GPP(\text{day of year})}, \quad 82 < \text{day of year} < 317 \quad (186)$$

where the *observed GPP* was the daily average calculated from the partitioned flux tower observations (Reichstein et al., 2005) from 2006-2013, and the *simulated GPP* was the daily average of the unscaled value during the same time. A polynomial was fit to equation (186) that represented  $f_{af}$  for 1) both the *limited nitrogen* and *no downregulation discrimination* formulations and 2) the *unlimited nitrogen* formulation (Figure S24). Note that CLM already includes a *daylength factor* that also adjusts the magnitude of  $V_{cmax}$  according to time of year, however, that default parameterization alone was not sufficient to match the observations.

### 3 Results & Discussion

This section is organized into four parts. First the calibrated model performance is evaluated against observed bulk carbon pool and bulk carbon flux behavior (Section 3.1.1), and against the observed  $\delta^{13}C$  within carbon pools (Section 3.1.2). Second, the simulated photosynthetic discrimination is evaluated for multi-decadal trends (Section 3.2.1), magnitude (Section 3.2.2) and seasonal patterns (Section 3.2.3), including the environmental factors that were most responsible for driving the seasonal discrimination (Section 3.2.4). Third, we discuss how isotope observations can be used to guide model development related to nitrogen limitation (Section 3.3). Finally, we evaluate the capability of the model to reproduce the magnitude and trends of disequilibrium (Section 3.4).

#### 3.1 Calibrated model performance

##### 3.1.1 Fluxes & carbon pools

The CLM model was successful at simulating GPP, ER, and latent heat fluxes (Fig. 32), leaf area index (LAI), and aboveground biomass (Fig. 43), but only following site-specific calibration. The *uncalibrated* simulation (*limited nitrogen* formulation) overestimated LAI (39 %), aboveground biomass (48%), average peak warm season GPP (15%), and average peak warm season ER (40%) and overestimated cold-season GPP by  $200 \text{ g C m}^{-2} \text{ yr}^{-1}$ . The *calibrated* simulation was much closer to the observations for LAI and aboveground biomass (Figure 43). The calibrated peak warm and cold season GPP, and warm season ER matched observations. The simulated latent heat fluxes were relatively insensitive to the calibration. Overall the simulated latent heat during the warm season overestimated the observations by

1 10% and underestimated by 10% during the cold season. Similar improvement was observed  
2 after calibration for the *unlimited nitrogen* run (not shown).

3 The calibration also eliminated erroneous winter GPP. In general, terrestrial carbon  
4 models tend to overestimate photosynthesis during cold periods for temperate/boreal conifer  
5 forests (Kolari et al., 2007), including Niwot Ridge (Thornton et al., 2002). One approach to  
6 correct for this is to include an acclimatization temperature (e.g. Flanagan et al., 2012) that  
7 reduces photosynthetic capacity during the spring and fall. The CLM 4.5 model includes  
8 functionality to adjust the photosynthetic capacity, including both a temperature acclimatization  
9 and a day length factor that reduces  $V_{max}$  (Bauerle et al., 2012; Oleson et al., 2013). However,  
10 this alone was not sufficient to match the observed fluxes. Although our calibration approach  
11 forced  $V_{max}$  to zero during the winter, it did not solve the underlying mechanistic shortcoming.  
12 A more fundamental approach should address either cold inhibition (Zarter et al., 2006) of  
13 photosynthesis or ~~soil water availability associated with snowmelt~~~~root access to soil moisture~~  
14 (Monson et al., 2005) to achieve the photosynthetic reduction. Nevertheless, within the  
15 confines of our study area, our calibration approach was sufficient to provide a skillful  
16 representation of photosynthesis and provided a sufficient testbed for evaluating carbon isotope  
17 behavior.

### 18 3.1.2 $\delta^{13}\text{C}$ of carbon pools

19 The model performed better simulating  $\delta^{13}\text{C}$  biomass of bulk needle tissue, roots and soil  
20 carbon (Figure 54) for the *unlimited nitrogen* and no *downregulation discrimination* cases as  
21 compared to the *limited nitrogen* case. When nitrogen limitation was included the model  
22 underestimated  $\delta^{13}\text{C}$  of sunlit needle tissue (1.8 ‰), bulk roots (1.0 ‰), and organic soil carbon  
23 (0.7‰). All simulations fell within the observed range of  $\delta^{13}\text{C}$  in needles that span from -28.7  
24 ‰ (shaded) to -26.7 (sunlit). This vertical pattern in  $\delta^{13}\text{C}$  of leaves is common (Martinelli et  
25 al., 1998) and results from vertical differences in nitrogen allocation and photosynthetic  
26 capacity. The model results integrated the entire canopy and ideally should be closer to sun  
27 leaves (as in Figure 54) given that the majority of photosynthesis occurs near the top of the  
28 canopy.

29 Model simulations of  $\delta^{13}\text{C}$  of living roots were ~1 ‰ more negative as compared to the  
30 structural roots. This range in  $\delta^{13}\text{C}$  results from decreasing  $\delta_{atm}$  with time (Suess effect, Figure  
31 24). The living roots had a relatively fast turnover time of carbon within the model, whereas

Field Code Changed

Field Code Changed

Field Code Changed

Field Code Changed

Field Code Changed

Field Code Changed

Field Code Changed

the structural roots had a slower turnover time and reflected an older (more enriched  $\delta_{atm}$ ) atmosphere. The *limited nitrogen* simulation was a poor match to observations relative to the others (Figure 54, middle panel).

There was an observed vertical gradient in  $\delta^{13}\text{C}$  of soil carbon (-24.9 to -26 ‰) with more enriched values at greater depth (Figure 54, right panel). This vertical gradient is commonly observed (Ehleringer et al., 2000). Simulated  $\delta^{13}\text{C}$  of soil carbon was most consistent with the organic horizon observations. There are a wide variety of post-photosynthetic fractionation processes in the soil system (Bowling et al., 2008; Brüggemann et al., 2011) that are not considered in the CLM 4.5 model, so the match with observations is perhaps fortuitous.

## 3.2 Photosynthetic discrimination

### 3.2.1 Decadal changes in photosynthetic discrimination and driving factors

All modeled carbon pools showed steady depletion in  $\delta^{13}\text{C}$  since 1850 (coinciding with the start of the transient phase of simulations, Figure 54). For the *limited nitrogen* run, there was a decrease in  $\delta^{13}\text{C}$  of 2.3 ‰ for needles, 2.3 ‰ for living roots, and 0.1 ‰ for soil carbon. This occurred because of 1) decreased  $\delta_{atm}$  (Suess effect, Figure 24) and 2) increased photosynthetic discrimination. We quantified the contribution of the Suess effect by performing a control run with constant  $\delta_{atm}$ , and kept other factors the same (Figure 65). Approximately 70% of the reduction in  $\delta^{13}\text{C}$  of needles occurred due to the Suess effect, and the remaining 30% was caused by increased photosynthetic discrimination. This occurred as plants responded to  $\text{CO}_2$  fertilization as illustrated in Figure 76. The model indicated that plants responded to increased atmospheric  $\text{CO}_2$  (~40% increase) by decreasing stomatal conductance (Equation 4) by 20% for the *limited nitrogen* run and 30% for the *unlimited nitrogen* run (Figure 76B) with associated change in  $c_i/c_a$  (Figure 76A). Other influences upon stomatal conductance were less significant, including  $A_n$  (+ 10% *limited nitrogen*, -10% *unlimited nitrogen*, Figure 76D), soil moisture availability (2-3%, Figure 76E), and negligible changes in relative humidity (potential climate change effects are neglected due to methodological cycling of weather data). This finding that stomatal conductance responded to atmospheric  $\text{CO}_2$  is consistent with both tree ring studies (Saurer et al., 2014) and flux tower measurements (Keenan et al., 2013).

The effect of  $\text{CO}_2$  fertilization, and associated response of stomatal conductance and net assimilation led to a multi-decadal increase in  $c_i/c_a$  for all model formulations (Figure 76A).

Field Code Changed

Field Code Changed

Field Code Changed

1 The  $c_i/c_a$  increased from 0.71 to 0.76, 0.67 to 0.71 and 0.66 to 0.68 for the *limited nitrogen*,  
 2 *unlimited nitrogen* and *no downregulation discrimination* formulations respectively from 1850-  
 3 2013. All simulations therefore suggested an *increase* in photosynthetic discrimination. This  
 4 increase in discrimination falls in between two hypotheses posed by Saurer et al., (2004)  
 5 regarding stomatal response to increased CO<sub>2</sub>: 1) reduction in stomatal conductance causes  $c_i$   
 6 to proportionally increase with  $c_a$  keeping  $c_i/c_a$  constant and 2) minimal stomatal conductance  
 7 response where  $c_i$  increases at the same rate as  $c_a$  (constant  $c_a - c_i$ ) causing  $c_i/c_a$  to increase. Our  
 8 simulation generally agrees with the observed trend in  $c_i/c_a$  as estimated from tree ring isotope  
 9 measurements from a network of European forests (Frank et al., 2015). When controlled for  
 10 trends in climate, Frank et al. (2015) found that  $c_i/c_a$  was approximately constant during the last  
 11 century. If the Niwot Ridge multi-decadal warming trends in temperature and humidity (Mitton  
 12 and Ferrenberg, 2012) were included in the CLM simulations the stomatal response may have  
 13 been stronger thereby holding  $c_i/c_a$  constant.

14 The simulated stomatal closure in response to CO<sub>2</sub> fertilization led to an increase in  
 15 iWUE and WUE of approximately 20% and 10% respectively (Figure 7F) from 1960-  
 16 2000. This *simulated increase in iWUE* is consistent with ~~the model and~~ observation-based  
 17 studies (Ainsworth and Long, 2005; Franks et al., 2013; Peñuelas et al., 2011) which indicate a  
 18 15-20% increase in iWUE for forests *during that time*. The *overall increase in WUE* ~~is~~  
 19 suggests that the vegetation at Niwot Ridge has some ability to maintain net ecosystem  
 20 productivity when confronted with low soil moisture, low humidity conditions. Ultimately,  
 21 whether Niwot Ridge maintains the current magnitude of carbon sink (Figure 3; Figure S12)  
 22 will depend upon the severity of drought conditions, as improvements in WUE, in general, are  
 23 only likely to negate weak to moderate levels of drought (Frank et al., 2013).

24 *The limited nitrogen formulation simulated larger values of  $A_n$  and  $g_s$ , and smaller iWUE*  
 25 *as compared to the unlimited nitrogen formulation (Figure 7). This is because the unlimited*  
 26 *nitrogen formulation was fully coupled (i.e. solved simultaneously) between  $A_n$  and  $g_s$  (Eq. 4).*  
 27 *The limited nitrogen formulation, however, was only partially coupled because  $A_n$  and  $g_s$  were*  
 28 *initially solved simultaneously through the potential  $A_n$  (Eq. 1), however, under N-limitation*  
 29  *$A_n$  becomes limited below its potential value (Eq. 9) through  $f_{dreg}$ . Therefore  $g_s$  is calculated*  
 30 *through the potential  $A_n$  (Eq. 4) and not the N-limited  $A_n$ .*

31 The simultaneous increase in both simulated photosynthetic discrimination and iWUE  
 32 conflicts with ~~previous literature observations~~ where increases in iWUE are typically linked

Field Code Changed

Commented [BR4]: Saurer uses traditional definition of  $c_i$ , should I use that or be consistent with CLM?

Field Code Changed

Field Code Changed

Field Code Changed

Formatted: Indent: First line: 0.4"

Formatted: Font: Italic

Formatted: Font: Italic

Formatted: Font: Italic, Subscript

Formatted: Subscript

Formatted: Font: Italic

Formatted: Font: Italic, Subscript

Formatted: Font: Italic

Formatted: Font: Italic

Formatted: Font: Italic

Formatted: Font: Not Italic

Formatted: Not Highlight

Formatted: Font: Italic, Not Highlight

Formatted: Font: Italic, Subscript, Not Highlight

Formatted: Font: Italic

Formatted: Font: Italic, Subscript

Formatted: Font: Italic

Formatted: Font: Italic, Subscript

Formatted: Font: Italic

Formatted: Font: Italic, Subscript

Formatted: English (United Kingdom), Highlight

1 with weakening discrimination (e.g. Saurer et al., 2004) using a linear model. ~~However, under~~  
2 ~~certain conditions iWUE and discrimination can vary independently because of variation in leaf~~  
3 ~~evaporative demand (VPD) and atmospheric CO<sub>2</sub> (Seibt et al., 2008).~~ In general, an increase  
4 in atmospheric CO<sub>2</sub> alone tends to increase iWUE because of reduced stomatal conductance,  
5 however, the impact upon discrimination is close to neutral because the increased supply of  
6 CO<sub>2</sub> external to the leaf is offset by reduced stomatal conductance (Saurer et al., 2004) The  
7 VPD likely plays an important role in determining the final trends for iWUE and discrimination,  
8 where an increasing VPD should further reduce stomatal conductance thereby promoting the  
9 well-established relationship (increasing iWUE, decreasing discrimination). In contrast, a weak  
10 or decreasing trend in VPD should promote the opposite relationship (increasing iWUE,  
11 increasing discrimination). ~~However, under certain conditions iWUE and discrimination can~~  
12 ~~vary independently because of variation in leaf evaporative demand (VPD) and atmospheric~~  
13 ~~CO<sub>2</sub> (Seibt et al., 2008).~~ The CLM model at present neglects mesophyll conductance  
14 (*g<sub>m</sub>*). When Seibt et al. (2008) included *g<sub>m</sub>* mesophyll conductance in a model that linked iWUE  
15 to discrimination they found there were certain conditions when iWUE and discrimination  
16 increased together. This is in part because mesophyll conductance, unlike stomatal  
17 conductance, does not respond as strongly to changes in VPD, yet has a significant impact upon  
18  $C_i/C_a$  and discrimination (Flexas et al., 2006). Harvard Forest is an example of a site that was  
19 observed to show ~~For example,~~ simultaneous increase in iWUE and discrimination over the last  
20 two decades derived from tree rings ~~were identified at Harvard Forest~~ (Belmecheri et al., 2014).  
21 In our model simulation ~~Here,~~ we do not consider multi-decadal trends in climate or mesophyll  
22 conductance, therefore increasing atmospheric CO<sub>2</sub> must be the primary driver for the  
23 ~~modeled/simulated~~ simultaneous increase in discrimination and iWUE at Niwot Ridge (Figure  
24 ~~7e~~). These trends in iWUE and discrimination ~~simulated at Niwot Ridge~~ have also been found  
25 in a fully-coupled, isotope enabled, global CESM simulation (Figure S32). Specifically, a  
26 random sample of land model grid cells representing conifer species in British Columbia (lat:  
27 52.3° N, lon: -122.5° W) and Quebec (lat: 49.5° N, lon: -70.0° W) all showed an increase in  
28 photosynthetic discrimination and a 10% increase in WUE from 1850-2005. These randomly  
29 chosen grid cells are likely better analogs to the site-level simulations described here because  
30 they represent boreal conifer forests, whereas the grid cells that are in the Niwot Ridge area  
31 were heterogeneous in land cover (e.g. tundra, grassland, forest) and a poor representation of  
32 conifer forest.

Field Code Changed

Field Code Changed

Formatted: Font: Italic

Formatted: Font: Italic, Subscript

Formatted: Font: Italic

Formatted: Font: Italic, Subscript

Formatted: Font: Italic

Formatted: Font: Italic, Subscript

Field Code Changed

The trends in the global simulation suggest that the site level trends are not isolated to the specific conditions of Niwot Ridge, but are a function of the model formulation. There is a relationship between iWUE and  $c_i^*/c_a$  (discrimination) as derived from equation (119) within the CLM model,

$$\frac{c_i^*}{c_a} \cong 1 - \frac{1.6}{c_a} iWUE. \quad (197)$$

The full derivation is provided in the supplement. Note that according to equation (19) increasing iWUE can be consistent with weakening discrimination (decreasing  $c_i^*/c_a$  ( $\sim \alpha_{psn}$ )) and therefore consistent with established understanding between trends in iWUE and discrimination. However, this ~~\_-trend imposed by iWUE~~ can be moderated/neutralized by increasing  $c_a$ . During the course of ~~our the Niwot Ridge~~ simulation (1850-2013) iWUE increased between 10-20% (Figure 76), however,  $c_a$  increased by 40% ~~\_-during that same time (1850-2013)-~~.

### 3.2.2 Magnitude of photosynthetic discrimination

The simulated photosynthetic discrimination (Fig. 87) was significantly larger than an estimate derived from observations and an isotopic mixing model (Bowling et al., 2014). For brevity we refer to the estimates based on the Bowling et al. (2014) method as ‘observed’ discrimination but highlight that they are derived from observations and not directly measured. On average, the simulated monthly growing season mean canopy discrimination was greater than observed values by 6.3, 6.1, and 5.1‰ for the *limited nitrogen*, *unlimited nitrogen*, and *no downregulation discrimination* formulations respectively. The model-observation mismatch in discrimination, despite model-observation agreement to biomass, carbon and latent heat flux tower observations (Figure 32) highlights the independent, and useful constraint isotopic observations provide for evaluating model performance. Specifically, the overestimation of discrimination may suggest the stomatal slope in the Ball-Berry model ( $m=9$  in Eq. 4) used for these simulations was too high. This is supported by Mao et al., (2016), who found a reduced stomatal slope ( $m=5.6$ ) was necessary for CLM 4.0 to match observed  $\delta^{13}\text{C}$  in an isotope labeling study of loblolly pine forest in Tennessee. The stomatal slope was also ~~found to be~~ important to match discrimination behavior in the ISOLSM model (Aranibar et al., 2006), a

Field Code Changed



predecessor to CLM. A global analysis of stomatal slope inferred from leaf gas exchange measurements found that evergreen coniferous species, such as those at Niwot Ridge, had near the lowest values compared to other PFTs (Lin et al., 2015). In addition, they found that low stomatal slope values were characteristic of species with low stemwood construction costs per water transpired (high WUE), low soil moisture availability, and cold temperatures.

Alternatively, discrimination may be overestimated because CLM does not consider the resistance to CO<sub>2</sub> diffusion into the leaf chloroplast, ~~the site within the leaf where carboxylation (photosynthesis) occurs.~~ The ability of CO<sub>2</sub> to diffuse across the chloroplast boundary layer, cell wall, and liquid interface is collectively known as the mesophyll conductance ( $g_m$ ) (Flexas et al., 2008). Multiple studies suggest that  $g_m$  is comparable in magnitude to  $g_s$ , and responds similarly to environmental conditions (Flexas et al., 2008). CLM does not account for  $g_m$ , and as a result assumes the intracellular CO<sub>2</sub> ( ~~$c_i$  within chloroplast~~) is the same as intercellular CO<sub>2</sub> (~~inside leaf stomata, outside chloroplast~~), but when it can be significantly lower (Di Marco et al., 1990; Sanchez-Rodriguez et al., 1999). The overestimation of  $c_i$  could have two important impacts upon our simulation. First, this may lead to unrealistically low values of  $V_{cmax}$  in order to compensate for the overestimation of  $c_i$ . In fact, we reduced the default value of  $V_{cmax}$  as much as 50% in our simulation to match the eddy covariance flux tower observations (see Section 3.3). Second, the overestimation of  $c_i$  should cause an overestimation of discrimination (Eq. 10), ~~consistent with which we have also observed in our simulations (Figure 8).~~ To determine whether the simulated discrimination bias is a model parameter calibration issue ( $g_s$ ) or from ~~a missing representation of excluding  $g_m$ , we recommend additional leaf gas exchange measurements be made at Niwot Ridge to better constrain the stomatal slope value. Furthermore, it would be instructive to include a mechanistic representation of mesophyll conductance within CLM.~~

The mixing model approach estimate of  $\Delta_{canopy}$  (17 ‰), combined with  $\delta_{atm}$  (-8.25 ‰) implies a  $\delta^{13}C$  of biomass between -26 to -25 ‰ (Figure 8). This range of values is only slightly more enriched than the observed ranges of  $\delta^{13}C$  of needle and root biomass (-27 to -26 ‰). The fact that the different approaches to measure discrimination differ by only 1 ‰, whereas CLM simulates a  $\Delta_{canopy}$  that is 5-6 ‰ greater than the mixing model discrimination, strongly suggests that the model has overestimated discrimination from 2006-2012. Therefore what appeared to be a successful match between the simulated and observed  $\delta^{13}C$  biomass, may in fact have been fortuitous, ~~ly reached through compensating during the simulation.~~ A multi-

Field Code Changed

Formatted: Normal, Indent: First line: 0"

Formatted: Subscript

Formatted: Subscript

Field Code Changed

Formatted: Font: Italic

Formatted: Font: Italic, Subscript

Formatted: Font: Italic

Formatted: Font: Italic, Subscript

Field Code Changed

Formatted: Subscript

Formatted: Font: Italic

Formatted: Font: Italic, Subscript

Formatted: Subscript

Formatted: Font: Italic

Field Code Changed

Formatted: Font: Italic

Formatted: Font: Italic

Formatted: Font: Italic

Formatted: Font: Italic, Subscript

Formatted: Font: Italic

Formatted: Font: Italic

Formatted: Font: Italic

Formatted: Font: Italic, Subscript

Formatted: Font: Italic

Formatted: Font: Italic, Subscript

Formatted: Font: Italic

Formatted: Font: Italic, Subscript

decadal time series of discrimination ~~estimates~~ inferred from  $\delta^{13}\text{C}$  of tree rings (Saurer et al., 2014; Frank et al., 2015) would be useful to investigate this mismatch as a function of time, but these data are not presently available.

~~If it is likely that~~ the overestimation of modeled discrimination originates from a lack of response of stomatal conductance to environmental conditions. ~~This~~ This could be a result of one or several of the following within the model: 1) ~~parameter calibration issue~~ the stomatal slope value is too high, 2) ~~boundary condition issue~~ the multi-decadal trends in climate (e.g. VPD) have not been included in the simulation 3) ~~neglecting  $g_m$~~  or 4) ~~model structural issue~~ the Ball-Berry representation of  ~~$g_{\text{stomatal conductance}}$~~  is not sensitive enough to changes in environmental conditions (e.g. ~~humidity~~ VPD, soil moisture). It has been shown that VPD may be an improved predictor of  $g_s$  (Katul et al., 2000; Leuning, 1995) and discrimination (Ballantyne et al., 2010, 2011) as compared to relative humidity, currently used in CLM 4.5. ~~It would be worthwhile to clearly identify in F~~ future work should consider which of ~~the these~~ free scenarios is responsible for overestimation of ~~the~~ discrimination.

### 3.2.3 Seasonal pattern of photosynthetic discrimination

The model formulations that did not explicitly consider the influence of nitrogen limitation upon discrimination (*unlimited nitrogen, no downregulation discrimination*) were most successful at reproducing the seasonality of discrimination (Figure [87](#); Figure [S43](#)). In general, the observed discrimination was stronger during the spring and fall and weaker during summer. This observed  $\Delta_{\text{canopy}}$  seasonal range (excluding November) varied from 16.5 to 18 ‰ using Reichstein partitioning (Figure [87](#)), and was more pronounced using Lasslop partitioning (16.5 to 23 ‰) (Figure [S43](#)). The nitrogen limited simulated  $\Delta_{\text{canopy}}$  had no seasonal trend whereas the *unlimited nitrogen* and *no downregulation discrimination* simulations both ranged from 21 to 23 ‰.

The main driver of the seasonality of discrimination was the net assimilation ( $A_n$ ) for the *unlimited nitrogen* formulation (Figure [98](#)). This was evident given the inversely proportional relationship between the simulated fractionation factor ( $\alpha_{\text{psn}}$ ) and  $A_n$ , consistent with equation ([119](#)). Stomatal conductance ( $g_s$ ) also influenced the seasonal pattern. The most direct evidence for this was during the period between days 175-200 (Figure [98](#)), where  $A_n$  descended from its highest value (favoring higher  $\alpha_{\text{psn}}$ ), and  $g_s$  abruptly ascended to its highest value (favoring higher  $\alpha_{\text{psn}}$ ). The  $\alpha_{\text{psn}}$  responded to this increase in  $g_s$  with an abrupt increase

Formatted: Font: Italic

Formatted: Font: Italic, Subscript

Field Code Changed

Field Code Changed

by approximately 0.003 (3 ‰). Similarly, the *limited nitrogen* simulation seasonal discrimination pattern was shaped by both  $A_n$  and  $g_s$ , although the magnitude for both was approximately 30% higher during the summer months as compared to the unlimited nitrogen simulation. This was because the calibrated  $V_{cmax}$  value for the *limited nitrogen* simulation was much higher than for the *unlimited nitrogen* simulation (section 3.3). The difference in  $\alpha_{psm}$  between the two model formulations coincided with the sharp increase in  $f_{dreg}$  between days 125 and 275, providing strong evidence that the downregulation mechanism within the *limited nitrogen* formulation led to increased discrimination during the summer. Therefore, it follows that the nitrogen downregulation mechanism was the root cause of the small range in simulated seasonal cycle discrimination for the *limited nitrogen* formulation, which was inconsistent with the observations.

#### 3.2.4 Environmental factors influencing seasonality of discrimination

The simulated  $\Delta_{canopy}$  was driven primarily by net assimilation ( $A_n$ ), followed by vapor pressure deficit (VPD) (Fig. 109). The correlation between VPD and  $\Delta_{canopy}$  was strongest for the *unlimited nitrogen* simulation, where the range in monthly average  $\Delta_{canopy}$  spanned values from 22 to 18 ‰ (Figure 109, middle row). This resembled the observed range in response based upon a fitted relationship from Bowling et al., (2014) that spanned from roughly 16 to 19 ‰ (left panels of Fig. 109), although with a consistent discrimination bias. The correlation between VPD and  $\Delta_{canopy}$ , however, does not demonstrate causality. If that were the case, given that  $g_s$  is a function of VPD ( $h_s$  term in Eq. 4) and discrimination is a function of  $g_s$  (Eq. 10; Eq. 118), a similar relationship should have existed between  $g_s$  and  $\Delta_{canopy}$ . This, in fact, was not the case. Overall, the influence of  $g_s$  (responding to VPD) (R-value = -0.50) was secondary to  $A_n$  (R-value = -0.77) in driving changes in discrimination (Figure 109). The model suggested that the range in seasonal discrimination (intra-annual variation) was driven by the magnitude of  $A_n$  based on the inverse relationship between  $A_n$  and  $\Delta_{canopy}$ , (equation 119) illustrated by the separation between months of low photosynthesis (October, May) vs. high photosynthesis (June, July, August). During times of relatively low photosynthesis  $A_n$  also drove the inter-annual variation in  $\Delta_{canopy}$ . On the other hand,  $g_s$  (VPD) was most influential in driving the inter-annual variation of discrimination during the summer months only, judging by the directly proportional relationship during the months of June, July and August. Strictly speaking,  $g_s$  is a function of  $h_s$  (leaf specific humidity) and not atmospheric VPD in CLM. However, the two

are closely related and the relationship between either variable (atmospheric VPD or simulated leaf humidity) to  $\Delta_{\text{canopy}}$  was similar (Figure S54).

The *limited nitrogen* formulation did not produce as wide a range in discrimination as compared to the observations (Figure 109, top row). Part of this result was attributed to the lack of response between  $A_n$  and  $\Delta_{\text{canopy}}$ . In this case, the discrimination did not decrease with increasing  $A_n$  because the signal was muted by the countering effect of  $f_{\text{dreg}}$ . The *limited nitrogen* formulation was, however, able to reproduce the same discrimination response to  $g_s$  as compared to the other model formulations. The tendency for the limited nitrogen model to simulate discrimination response to  $g_s$  and not to  $A_n$  may negatively impact its ability to simulate multi-decadal trends in discrimination. This may not be a major detriment to sites such as Niwot Ridge which have maintained a consistent level of carbon uptake during the last decade, and is likely more susceptible to environmental impact upon stomatal conductance. However, sites that have shown a significant increase in assimilation rate (e.g. Harvard Forest; (Keenan et al., 2013)) are less likely to be well represented by this model formulation.

Given the dependence of forest productivity at Niwot Ridge on snowmelt (Hu et al., 2010), it was surprising that the model simulated minimal soil moisture stress (Fig. 98e) and therefore minimal discrimination response to soil moisture. However, this finding was consistent with Bowling et al., (2014), who did not find an isotopic response to soil moisture. In addition, lack of response to change in soil moisture may not be indicative of poor performance of the isotopic sub-model performance, but rather an effect of the hydrology sub-model (Duarte et al. (in prep)). However, a comparison of observed soil moisture at various depths at Niwot Ridge generally agrees with the CLM simulated soil moisture (not shown), suggesting the lack of model response to soil moisture was not from biases in the hydrology model.

### 3.3 Discrimination formulations: implications for model development

The *limited* and *unlimited model* formulations tested in this study represented two approaches to account for nitrogen limitation within ecosystem models. The *limited nitrogen* formulation reduced photosynthesis, *after the main photosynthesis calculation*, so that the carbon allocated to growth was accommodated by available nitrogen. This *allocation downscaling* approach is common to a subset of models, for example, CLM (Thornton et al., 2007), DAYCENT (Parton et al., 2010) and ED2.1 (Medvigy et al., 2009). Another class of

Field Code Changed

Field Code Changed

Field Code Changed

Field Code Changed

models limits photosynthesis based upon foliar nitrogen content and adjusts the photosynthetic capacity through nitrogen availability in the leaf through  $V_{\text{cmax}}$  (e.g. CABLE, GDAY, LPJ-GUESS, OCN, SDVGM, TECO, see Zaehle et al., 2014). These *foliar nitrogen* models are similar to the *unlimited nitrogen* formulation of CLM because the scaling of photosynthesis was taken into account in the  $V_{\text{cmax}}$  scaling methodology (see discussion in section 2.1.2 and 2.4), *prior to the photosynthesis calculation*. In general, there were no categorical differences in behavior between these two classes of models during CO<sub>2</sub> manipulation experiments held at Duke forest and ORNL (Zaehle et al., 2014). CLM 4.0 was one of the few models in that study to consistently underestimate the NPP response to an increase of atmospheric CO<sub>2</sub> due to nitrogen limitation, however this finding was attributed to a lower initial supply of nitrogen. Also within this experiment, it was found that models that had no or partial coupling (CLM 4.0, DAYCENT) between  $A_n$  and  $g_s$ , generally predicted lower than observed WUE response to increases in CO<sub>2</sub> (De Kauwe et al., 2013). Similar to CLM 4.0, the *limited nitrogen* formulation of CLM 4.5 in this manuscript is partially coupled (see Section 3.2.1). The unlimited nitrogen formulation of CLM 4.5, on the other hand, is fully coupled and similar to De Kauwe et al., (2013) outperformed the partially coupled version of CLM.

The *unlimited nitrogen* formulation described in our study is a simplified foliar nitrogen model, in that, all of the information about nitrogen limitation is incorporated within the  $V_{\text{cmax}}$  downscaling approach. A more versatile approach would link a dynamic nitrogen cycle directly with the calculation of  $V_{\text{cmax}}$ . This capability ~~was recently is currently being~~ developed within CLM (Ghimire et al., 2016) and is scheduled to be included in the next CLM release (Ghimire et al., in review) and future work should test its functionality.

The performance of the *unlimited nitrogen* formulation was nearly identical to the *no downregulation discrimination* formulation in terms of isotopic behavior despite the mechanistic differences. The *no downregulation discrimination* formulation included nitrogen limitation within the bulk carbon behavior but ignored the impact of  $f_{\text{dreg}}$  upon discrimination behavior. The relative high simulation skill with this formulation implied that the ‘potential’ GPP linked to  $A_n$ , was a more effective predictor of discrimination behavior than the ‘downscaled’ GPP, which is linked to  $A_n * (1 - f_{\text{dreg}})$  (equation 119). There are several potential explanations for an unrealistically large value of  $f_{\text{dreg}}$ . First this could indicate that the  $V_{\text{cmax}}$  parameter was too large, thereby requiring a large  $f_{\text{dreg}}$  to compensate. As noted in Section (3.1) the default temperate evergreen  $V_{\text{cmax}25}$  was  $\sim 62 \mu\text{mol m}^{-2} \text{s}^{-1}$ , much larger than what was

Field Code Changed

Formatted: Font: Italic

Formatted: Font: Italic, Subscript

Formatted: Font: Italic

Formatted: Font: Italic, Subscript

Formatted: Subscript

Formatted: Font: Italic

Formatted: Highlight

found based on literature reviews (Monson et al., 2005; Tomaszewski and Sievering, 2007) . We found to match the observed GPP we had to impose  $f_{dreg}$  that had the same effect as reducing  $V_{cmax}$  (Figure S24) to values of 51 and 34  $\mu\text{mol m}^{-2} \text{s}^{-1}$  for the *limited nitrogen* and *unlimited nitrogen* formulations respectively. Alternatively, it could be that there are physiological processes that are acting to reduce nitrogen limitation (e.g. nitrogen storage pools or transient carbon storage as non-structural carbohydrates), or that the current measurement techniques are underestimating GPP due to biases within the flux partitioning methods.

### 3.4 Disequilibrium, possible explanations of mismatch

Carbon cycle models (e.g. Fung et al., 1997) indicate that the steady decrease of  $\delta_{\text{atm}}$  (Suess effect, Fig. 24) should lead to a positive disequilibrium between land surface processes ( $\delta^{13}\text{C}$  difference between GPP and ER, Eq. 142). This is because the  $\delta_{\text{GPP}}$  reflects the most recent ( $\delta^{13}\text{C}$  depleted) state of the atmosphere, whereas the  $\delta_{\text{ER}}$  reflects carbon (e.g. soil carbon) assimilated from an older ( $\delta^{13}\text{C}$  enriched) atmosphere. This positive disequilibrium pattern promoted by the Suess effect was consistent with all CLM formulations for this study with an annual average disequilibrium of 0.8 ‰. In contrast, a negative disequilibrium (-0.6 ‰) was identified at Niwot Ridge based upon observations (Bowling et al. 2014) as well as in other forests (Flanagan et al., 2012; Wehr and Saleska, 2015; Wingate et al., 2010). Bowling et al. (2014) hypothesized several reasons for this: 1) a strong seasonal stomatal response to atmospheric humidity, 2) decreased photosynthetic discrimination associated with  $\text{CO}_2$  fertilization, 3) decreased photosynthetic discrimination associated with multi-decadal warming and increased VPD, and 4) post-photosynthetic discrimination. We evaluated the first three hypotheses within the context of ~~our~~the CLM simulations.

The model results suggest a seasonal variation of discrimination that is a function of both VPD and  $A_n$ . The simulated seasonal range in discrimination (Figure 87; Figure S43) varied by approximately 2 ‰, and this range in seasonal discrimination could contribute to a negative disequilibrium provided specific timing of assimilation, assimilate storage and respiration not currently considered in the model. For example, if a significant portion of photosynthetic assimilation was stored during the spring with relatively high discrimination, and then respired during the summer, the net effect would deplete the  $\delta_{\text{ER}}$  and thereby promote negative disequilibrium during the summer months when discrimination is lower. Theoretically, this could be achieved by explicitly including carbohydrate storage pools within CLM. Isotopic tracer studies have shown assimilated carbon can exist for weeks to months within the

Field Code Changed

Field Code Changed

1 vegetation and soil before it is finally respired (Epron et al., 2012; Hogberg et al., 2008).

2 Although carbon storage pools are included in CLM, their allocation is almost always  
3 instantaneous for evergreen systems and could not provide the isotopic effect described above.

4 The CO<sub>2</sub> fertilization effect tends to favor photosynthesis in plants and has been shown to  
5 simultaneously increase WUE and decrease stomatal conductance as inferred from  $\delta^{13}\text{C}$  in tree  
6 rings (Frank et al., 2015; Flanagan et al., 2012; Wingate et al., 2010). In general a decrease in  
7 stomatal conductance and increase in WUE is associated with a decrease in C3 discrimination  
8 (Farquhar et al., 1982), which opposes the disequilibrium trend imposed by the Suess effect.

9 The model simulation agrees with both these trends in WUE and stomatal conductance, yet  
10 simulates an *increase* in discrimination (Figure 65; Figure 76), which reinforces the Suess effect  
11 pattern upon disequilibrium. Although this appears to be a mismatch between forest processes  
12 and model performance the model is operating within the limits of the discrimination  
13 parameterization (Eq. 17) in which the magnitude of photosynthetic discrimination is inversely  
14 proportional to the iWUE, but is also proportional to atmospheric CO<sub>2</sub> (see section 3.2.1).

15 A multi-decadal decrease in photosynthetic discrimination may also result from change in  
16 climate. Meteorological measurements at Niwot Ridge during the last several decades  
17 generally support conditions of higher VPD based upon a warming trend from an average  
18 annual temperature of 1.1 °C in the 1980's to 2.7 °C in the 2000's (Mitton and Ferrenberg,  
19 2012) and no overall trend in precipitation. It is possible that a multi-decadal trend in increasing  
20 VPD contributed to multi-decadal weakening in photosynthetic discrimination given the  
21 observed (Bowling et al., 2014) and modelled (Figure 109) correlation between  $\Delta_{\text{canopy}}$  and  
22 VPD. The model meteorology only included the years 1998-2013 and did not include the rapid  
23 warming after the 1980's. It is unclear whether, if the full period of warming were to be  
24 included in the simulation, the simulated discrimination response to VPD would be enough to  
25 counter the Suess effect and lead to negative disequilibrium. Still, there is evidence that the  
26 model is overestimating contemporary discrimination (Section 3.4) and the exclusion of the full  
27 multi-decadal shift in VPD could be a significant reason why.

28 Finally, post-photosynthetic discrimination processes are likely to impact the magnitude  
29 and sign of the isotopic disequilibrium (Bowling et al., 2008; Brüggemann et al., 2011) at  
30 multiple temporal scales. None of these isotopic processes are currently modelled within CLM  
31 4.5, so at present the model cannot be used to examine them.

Field Code Changed

Field Code Changed

Field Code Changed

Field Code Changed

## 4 Conclusions

This study provides a rigorous test of the representation of C isotope discrimination within the highly mechanistic terrestrial carbon model CLM. ~~Special attention was paid to provide an accurate set of boundary conditions to isolate the isotopic performance including 1) customized atmospheric  $\text{CO}_2$  and  $\delta_{\text{atm}}$  time series, 2) customized model initialization procedure, and 3) empirical  $V_{\text{cmax}}$  calibration procedure. Once the model satisfactorily represented observed carbon exchange, water exchange, and biomass growth, it was successful at simulating several aspects of isotope behavior.~~

CLM was able to accurately simulate  $\delta^{13}\text{C}$  in leaf and stem biomass and the seasonal cycle in  $\Delta_{\text{canopy}}$ . ~~but only when. This performance could only be achieved, however, if  $V_{\text{cmax}}$  was calibrated in such a way to mimic the functionality of a foliar nitrogen model by accounting for nitrogen limitation prior to photosynthesis. With the traditional *nitrogen limited* approach, in which the nitrogen limitation occurs after photosynthesis and the  $c_i/c_a$  is influenced by this limitation but the stomatal conductance is not, the model tended to overestimate the magnitude of photosynthetic discrimination, and eliminated the observed seasonal weakening of  $\Delta_{\text{canopy}}$ . Although the overestimation of photosynthetic discrimination could likely be corrected with adjustments to the stomatal conductance parameterization, the seasonal trend was inherent to the model. Thus our results suggest that shifting nitrogen controls either before photosynthesis through a reduction in  $V_{\text{cmax}}$ , or entirely after the photosynthetic process such that nitrogen constraints have no effect on discrimination, are more consistent with the isotopic observations than the current model formulation.~~

Although the *unlimited nitrogen* formulation was able to match observed  $\delta^{13}\text{C}$  of biomass and seasonal patterns in discrimination, it still overestimated the contemporary magnitude of discrimination (2006-2012). Future work should identify whether this overestimation was a result of parameterization (stomatal slope), exclusion of multi-decadal shifts in  $\text{VPD}_s$ , ~~or~~ limitations in the representation of stomatal conductance (Ball-Berry model) or absence of the representation of mesophyll conductance.

The model attributed most of the range in seasonal discrimination to variation in net assimilation rate ( $A_n$ ) followed by variation in VPD, with little to no impact from soil moisture. The model suggested that  $A_n$  drove the seasonal range in discrimination (across-month variation) whereas VPD drove the inter-annual variation during the summer months. This



finding suggests that to simulate multi-decadal trends in photosynthetic discrimination, response to assimilation rate and VPD must be well represented within the model.

The model simulated a positive disequilibrium that was driven by both the Suess effect, and increased photosynthetic discrimination from CO<sub>2</sub> fertilization. It is possible that the negative disequilibrium that was inferred from observations (Bowling et al., 2014) was driven from the impacts of climate change and/or post-photosynthetic discrimination – not considered in this version of the model. ~~Future work should quantify the impact of this multi-decadal warming and post-photosynthetic discrimination processes upon disequilibrium.~~

The model simulated a consistent increase in water-use efficiency as a response to CO<sub>2</sub> fertilization and decrease in stomatal conductance. The model simulated an increase in WUE despite an increase in discrimination, however C3 plants typically express the opposite trends (increase in WUE, decrease in discrimination). Although CLM includes parameterization that promotes an increase in WUE with a decrease in discrimination, this trend was likely ~~moderated/neutralized by other environmental variables (e.g. increase in  $c_a$ ).~~

Initial indications are that  $\delta^{13}\text{C}$  isotope data can bring additional constraint to model parameterization beyond what traditional flux tower measurements of carbon, water exchange, and biomass measurements. The isotope measurements suggested a stomatal conductance value generally lower than what was consistent with the flux tower measurements. Unexpectedly, the isotopes also provided guidance upon model formulation related to nitrogen limitation. The success of our empirical approach to account for nutrient limitation within the  $V_{cmax}$  parameterization, suggests that additional testing of foliar nitrogen models are worthwhile.

## Acknowledgements

This research was supported by the U.S. Department of Energy, Office of Science, Office of Biological and Environmental Research, Terrestrial Ecosystem Science Program under Award Number DE-SC0010625. Thank you to Sean Burns and Peter Blanken for sharing flux tower and meteorological data from Niwot Ridge. Thank you to those at NOAA who provided the atmospheric flask data from Niwot Ridge including Bruce Vaughn, Ed Dlugokencky, the INSTAAR Stable Isotope Lab and NOAA GMD. A special thanks to Keith Lindsay at NCAR

1 for providing global CESM output to help improve the discussion of model behavior. We are  
2 grateful to Ralph Keeling and two anonymous reviewers who provided helpful comments.- The  
3 support and resources from the Center for High Performance Computing at the University of  
4 Utah are gratefully acknowledged.

5

## References

- Ainsworth, E. A. and Long, S. P.: What have we learned from 15 years of free-air CO<sub>2</sub> enrichment (FACE)? A meta-analytic review of the responses of photosynthesis, canopy properties and plant production to rising CO<sub>2</sub>, *New Phytol.*, 165(2), 351–372, doi:10.1111/j.1469-8137.2004.01224.x, 2005.
- Andrews, S. F., Flanagan, L. B., Sharp, E. J. and Cai, T.: Variation in water potential, hydraulic characteristics and water source use in montane Douglas-fir and lodgepole pine trees in southwestern Alberta and consequences for seasonal changes in photosynthetic capacity, *Tree Physiol.*, 32, 146–160, doi:10.1093/treephys/tpr136, 2012.
- Aranibar, J. N., Berry, J. A., Riley, W. J., Pataki, D. E., Law, B. E. and Ehleringer, J. R.: Combining meteorology, eddy fluxes, isotope measurements, and modeling to understand environmental controls of carbon isotope discrimination at the canopy scale, *Glob. Change Biol.*, 12(4), 710–730, 2006.
- Arora, V. K., Boer, G. J., Friedlingstein, P., Eby, M., Jones, C. D., Christian, J. R., Bonan, G., Bopp, L., Brovkin, V., Cadule, P., Hajima, T., Ilyina, T., Lindsay, K., Tjiputra, J. F. and Wu, T.: Carbon-Concentration and Carbon-Climate Feedbacks in CMIP5 Earth System Models, *J. Clim.*, 26(15), 5289–5314, doi:10.1175/jcli-d-12-00494.1, 2013.
- Ballantyne, A. P., Miller, J. B. and Tans, P. P.: Apparent seasonal cycle in isotopic discrimination of carbon in the atmosphere and biosphere due to vapor pressure deficit, *Glob. Biogeochem. Cycles*, 24, GB3018, doi:10.1029/2009GB003623, 2010.
- Ballantyne, A. P., Miller, J. B., Baker, I. T., Tans, P. P. and White, J. W. C.: Novel applications of carbon isotopes in atmospheric CO<sub>2</sub>: What can atmospheric measurements teach us about processes in the biosphere?, *Biogeosciences*, 8(10), 3093–3106, 2011.
- Bauerle, W. L., Oren, R., Way, D. A., Qian, S. S., Stoy, P. C., Thornton, P. E., Bowden, J. D., Hoffman, F. M. and Reynolds, R. F.: Photoperiodic regulation of the seasonal pattern of photosynthetic capacity and the implications for carbon cycling, *Proc. Natl. Acad. Sci. U. S. A.*, 109(22), 8612–8617, 2012.
- Belmecheri, S., Maxwell, R. S., Taylor, A. H., Davis, K. J., Freeman, K. H. and Munger, W. J.: Tree-ring  $\delta^{13}\text{C}$  tracks flux tower ecosystem productivity estimates in a NE temperate forest, *Environ. Res. Lett.*, 9(7), 74011, doi:10.1088/1748-9326/9/7/074011, 2014.
- Boisvenue, C. and Running, S. W.: Simulations show decreasing carbon stocks and potential for carbon emissions in Rocky Mountain forests over the next century, *Ecol. Appl.*, 20(5), 1302–1319, 2010.
- Bowling, D. R., Pataki, D. E. and Randerson, J. T.: Carbon isotopes in terrestrial ecosystem pools and CO<sub>2</sub> fluxes, *New Phytol.*, 178, 24–40, doi: 10.1111/j.1469-8137.2007.02342.x, 2008.
- Bowling, D. R., Ballantyne, A. P., Miller, J. B., Burns, S. P., Conway, T. J., Menzer, O., Stephens, B. B. and Vaughn, B. H.: Ecological processes dominate the  $^{13}\text{C}$  land disequilibrium in a Rocky Mountain subalpine forest, *Glob. Biogeochem. Cycles*, 28(4), 2013GB004686, doi:10.1002/2013GB004686, 2014a.

Formatted: Bibliography, Widow/Orphan control, Adjust space between Latin and Asian text, Adjust space between Asian text and numbers

Field Code Changed

[Bowling, D. R., Ballantyne, A. P., Miller, J. B., Burns, S. P., Conway, T. J., Menzer, O., Stephens, B. B. and Vaughn, B. H.: Ecological processes dominate the  \$^{13}\text{C}\$  land disequilibrium in a Rocky Mountain subalpine forest, \*Glob. Biogeochem. Cycles\*, 28\(4\), 2013GB004686, doi:10.1002/2013GB004686, 2014b.](#)

[Bradford, M. A., Fierer, N. and Reynolds, J. F.: Soil carbon stocks in experimental mesocosms are dependent on the rate of labile carbon, nitrogen and phosphorus inputs to soils, \*Funct. Ecol.\*, 22\(6\), 964–974, doi:10.1111/j.1365-2435.2008.01404.x, 2008.](#)

[Braswell, B. H., Sacks, W. J., Linder, E. and Schimel, D. S.: Estimating diurnal to annual ecosystem parameters by synthesis of a carbon flux model with eddy covariance net ecosystem exchange observations, \*Glob. Change Biol.\*, 11, 335–355, doi:10.1111/j.1365-2486.2005.00897.x, 2005.](#)

[Brüggemann, N., Gessler, A., Kayler, Z., Keel, S. G., Badeck, F., Barthel, M., Boeckx, P., Buchmann, N., Brugnoli, E., Esperschütz, J., Gavrichkova, O., Ghashghaie, J., Gomez-Casanovas, N., Keitel, C., Knohl, A., Kuptz, D., Palacio, S., Salmon, Y., Uchida, Y. and Bahn, M.: Carbon allocation and carbon isotope fluxes in the plant-soil-atmosphere continuum: a review, \*Biogeosciences\*, 8\(11\), 3457–3489, doi:10.5194/bg-8-3457-2011, 2011a.](#)

[Brüggemann, N., Gessler, A., Kayler, Z., Keel, S. G., Badeck, F., Barthel, M., Boeckx, P., Buchmann, N., Brugnoli, E., Esperschütz, J., Gavrichkova, O., Ghashghaie, J., Gomez-Casanovas, N., Keitel, C., Knohl, A., Kuptz, D., Palacio, S., Salmon, Y., Uchida, Y. and Bahn, M.: Carbon allocation and carbon isotope fluxes in the plant-soil-atmosphere continuum: A review, \*Biogeosciences\*, 8\(11\), 3457–3489, 2011b.](#)

[Collatz, G. J., Ball, J. T., Grivet, C. and Berry, J. A.: Regulation of stomatal conductances and transpiration a physiological model of canopy processes, \*Agric. For. Meteorol.\*, 54, 107–136, 1991.](#)

[De Kauwe, M. G., Medlyn, B. E., Zaehle, S., Walker, A. P., Dietze, M. C., Hickler, T., Jain, A. K., Luo, Y., Parton, W. J., Prentice, I. C., Smith, B., Thornton, P. E., Wang, S., Wang, Y.-P., Wärlind, D., Weng, E., Crous, K. Y., Ellsworth, D. S., Hanson, P. J., Seok Kim, H., Warren, J. M., Oren, R. and Norby, R. J.: Forest water use and water use efficiency at elevated  \$\text{CO}\_2\$ : a model-data intercomparison at two contrasting temperate forest FACE sites, \*Glob. Change Biol.\*, 19\(6\), 1759–1779, doi:10.1111/gcb.12164, 2013.](#)

[Desai, A. R., Moore, D. J. P., Ahue, W. K. M., Wilkes, P. T. V., De Wekker, S. F. J., Brooks, B. G., Campos, T. L., Stephens, B. B., Monson, R. K., Burns, S. P., Quaife, T., Aulenbach, S. M. and Schimel, D. S.: Seasonal pattern of regional carbon balance in the central Rocky Mountains from surface and airborne measurements, \*J. Geophys. Res.\*, 116, G04009\(4\), doi:10.1029/2011JG001655, 2011.](#)

[Di Marco, G., Manes, F., Tricoli, D. and Vitale, E.: Fluorescence Parameters Measured Concurrently with Net Photosynthesis to Investigate Chloroplastic  \$\text{CO}\_2\$  Concentration in Leaves of \*Quercus ilex\* L., \*J. Plant Physiol.\*, 136\(5\), 538–543, doi:10.1016/S0176-1617\(11\)80210-5, 1990.](#)

[Dlugokencky, E. J., Lang, P. M., Masarie, K. A., Crotwell, A. M. and Crotwell, M. J.: Atmospheric Carbon Dioxide Dry Air Mole Fractions from the NOAA ESRL Carbon Cycle](#)

Cooperative Global Air Sampling network, 1968-2014. Version: 2015-08-03. Path: [ftp://aftp.cmdl.noaa.gov/data/trace\\_gases/co2/flask/surface/](ftp://aftp.cmdl.noaa.gov/data/trace_gases/co2/flask/surface/), 2015.

Ehleringer, J. R., Buchmann, N. and Flanagan, L. B.: Carbon isotope ratios in belowground carbon cycle processes, *Ecol. Appl.*, 10(2), 412–422, 2000.

Epron, D., Bahn, M., Derrien, D., Lattanzi, F. A., Pumpanen, J., Gessler, A., Högberg, P., Maillard, P., Dannoura, M., Gérant, D. and Buchmann, N.: Pulse-labelling trees to study carbon allocation dynamics: a review of methods, current knowledge and future prospects, *Tree Physiol.*, 32(6), 776–798, doi:10.1093/treephys/tps057, 2012.

Farquhar, G. D., von Caemmerer, S. and Berry, J. A.: A Biochemical Model of Photosynthetic CO<sub>2</sub> Assimilation in Leaves of C<sub>3</sub> Species, *Planta*, 149, 78–90, 1980.

Farquhar, G. D., O’Leary, M. H. and Berry, J. A.: On the relationship between carbon isotope discrimination and the intercellular carbon dioxide concentration in leaves, *Aust. J. Plant Physiol.*, 9(2), 121–137, 1982.

Farquhar, G. D., Ehleringer, J. R. and Hubick, K. T.: Carbon isotope discrimination and photosynthesis, *Annu. Rev. Plant Physiol. Plant Mol. Biol.*, 40, 503–537, 1989.

Flanagan, L. B., Cai, T., Black, T. A., Barr, A. G., McCaughey, J. H. and Margolis, H. A.: Measuring and modeling ecosystem photosynthesis and the carbon isotope composition of ecosystem-respired CO<sub>2</sub> in three boreal coniferous forests, *Agric. For. Meteorol.*, 153, 165–176, 2012.

Flexas, J., Ribas-Carbó, M., Hanson, D. T., Bota, J., Otto, B., Cifre, J., McDowell, N., Medrano, H. and Kaldenhoff, R.: Tobacco aquaporin NtAQP1 is involved in mesophyll conductance to CO<sub>2</sub> in vivo, *Plant J.*, 48(3), 427–439, doi:10.1111/j.1365-3113.2006.02879.x, 2006.

Flexas, J., Ribas-Carbo, M., Diaz-Espej, A., Galmes, J. and Medrano, H.: Mesophyll conductance to CO<sub>2</sub>: current knowledge and future prospects, *Plant Cell Environ.*, 31(5), 602–621, 2008.

Francey, R. J., Allison, C. E., Etheridge, D. M., Trudinger, C. M., Enting, I. G., Leuenberger, M., Langenfelds, R. L., Michel, E. and Steele, L. P.: A 1000-year high precision record of δ<sup>13</sup>C in atmospheric CO<sub>2</sub>, *Tellus*, 51B, 170–193, 1999.

Frank, D. C., Poulter, B., Saurer, M., Esper, J., Huntingford, C., Helle, G., Treydte, K., Zimmermann, N. E., Schleser, G. H., Ahlström, A., Ciais, P., Friedlingstein, P., Levis, S., Lomas, M., Sitch, S., Viovy, N., Andreu-Hayles, L., Bednarz, Z., Berninger, F., Boettger, T., D’Alessandro, C. M., Daux, V., Filot, M., Grabner, M., Gutierrez, E., Haupt, M., Hiltunen, E., Jungner, H., Kalela-Brundin, M., Krapiec, M., Leuenberger, M., Loader, N. J., Marah, H., Masson-Delmotte, V., Pazdur, A., Pawelczyk, S., Pierre, M., Planells, O., Pukienė, R., Reynolds-Henne, C. E., Rinne, K. T., Saracino, A., Sonninen, E., Stievenard, M., Switsur, V., R., Szczepanek, M., Szychowska-Krapiec, E., Todaro, L., Waterhouse, J. S. and Weigl, M.: Water-use efficiency and transpiration across European forests during the Anthropocene, *Nat. Clim. Change*, 5(6), 579–583, doi:10.1038/nclimate2614, 2015.

Franks, P. J., Adams, M. A., Amthor, J. S., Barbour, M. M., Berry, J. A., Ellsworth, D. S., Farquhar, G. D., Ghannoum, O., Lloyd, J., McDowell, N., Norby, R. J., Tissue, D. T. and von

1 [Caemmerer, S.: Sensitivity of plants to changing atmospheric CO<sub>2</sub> concentration: From the](#)  
2 [geological past to the next century, \*New Phytol.\*, 197\(4\), 1077–1094, 2013.](#)

3 [Friedlingstein, P., Cox, P. M., Betts, R. A., Bopp, L., von Bloh, W., Brovkin, V., Cadule, P.,](#)  
4 [Doney, S. C., Eby, M., Fung, I. Y., Bala, G., John, J., Jones, C. D., Joos, F., Kato, T., Kawamiya,](#)  
5 [M., Knorr, W., Lindsay, K., Matthews, H. D., Raddatz, T., Rayner, P., Reick, C., Roeckner, E.,](#)  
6 [Schnitzler, K.-G., Schnur, R., Strassmann, K., Weaver, A. J., Yoshikawa, C. and Zeng, N.:](#)   
7 [Climate-carbon cycle feedback analysis: Results from the C4MIP model intercomparison, \*J.\*](#)  
8 [\*Clim.\*, 19, 3337–3353, 2006.](#)

9 [Fung, I. Y., Field, C. B., Berry, J. A., Thompson, M. V., Randerson, J. T., Malmstrom, C. M.,](#)  
10 [Vitousek, P. M., Collatz, G. J., Sellers, P. J., Randall, D. A., Denning, A. S., Badeck, F. and](#)  
11 [John, J.: Carbon 13 exchanges between the atmosphere and biosphere, \*Glob. Biogeochem.\*](#)  
12 [\*Cycles\*, 11\(4\), 507–533, 1997.](#)

13 [Ghimire, B., Riley, W. J., Koven, C. D., Mu, M. and Randerson, J. T.: Representing leaf and](#)  
14 [root physiological traits in CLM improves global carbon and nitrogen cycling predictions, \*J.\*](#)  
15 [\*Adv. Model. Earth Syst.\*, n/a-n/a, doi:10.1002/2015MS000538, 2016.](#)

16 [Greenland, D.: The Climate of Niwot Ridge, Front Range, Colorado, U.S.A., \*Arct. Alp. Res.\*,](#)  
17 [21\(4\), 380–391, 1989.](#)

18 [Hogberg, P., Hogberg, M. N., Gottlicher, S. G., Betson, N. R., Keel, S. G., Metcalfe, D. B.,](#)  
19 [Campbell, C., Schindlbacher, A., Hurry, V., Lundmark, T., Linder, S. and Nasholm, T.: High](#)  
20 [temporal resolution tracing of photosynthate carbon from the tree canopy to forest soil](#)  
21 [microorganisms, \*New Phytol.\*, 177\(1\), 220–228, 2008.](#)

22 [Hu, J., Moore, D. J. P., Burns, S. P. and Monson, R. K.: Longer growing seasons lead to less](#)  
23 [carbon sequestration by a subalpine forest, \*Glob. Change Biol.\*, 16\(2\), 771–783,](#)  
24 [doi:10.1111/j.1365-2486.2009.01967.x, 2010.](#)

25 [Katul, G. G., Ellsworth, D. S. and Lai, C.-T.: Modelling assimilation and intercellular CO<sub>2</sub>](#)  
26 [from measured conductance: a synthesis of approaches, \*Plant Cell Environ.\*, 23\(12\), 1313–](#)  
27 [1328, doi:10.1046/j.1365-3040.2000.00641.x, 2000.](#)

28 [Keenan, T. F., Hollinger, D. Y., Bohrer, G., Dragoni, D., Munger, J. W., Schmid, H. P. and](#)  
29 [Richardson, A. D.: Increase in forest water-use efficiency as atmospheric carbon dioxide](#)  
30 [concentrations rise, \*Nature\*, 499\(7458\), 324–327, doi:10.1038/nature12291, 2013.](#)

31 [Kolari, P., Lappalainen, H. K., HäNninen, H. and Hari, P.: Relationship between temperature](#)  
32 [and the seasonal course of photosynthesis in Scots pine at northern timberline and in southern](#)  
33 [boreal zone, \*Tellus B\*, 59\(3\), 542–552, doi:10.1111/j.1600-0889.2007.00262.x, 2007.](#)

34 [Lasslop, G., Reichstein, M., Papale, D., Richardson, A., Arneth, A., Barr, A., Stoy, P. and](#)  
35 [Wohlfahrt, G.: Separation of net ecosystem exchange into assimilation and respiration using a](#)  
36 [light response curve approach: critical issues and global evaluation, \*Glob. Change Biol.\*, 16,](#)  
37 [187–208, 2010.](#)

38 [Le Quéré, C., Moriarty, R., Andrew, R. M., Peters, G. P., Ciais, P., Friedlingstein, P., Jones, S.](#)  
39 [D., Sitch, S., Tans, P., Arneth, A., Boden, T. A., Bopp, L., Bozec, Y., Canadell, J. G., Chini, L.,](#)  
40 [P., Chevallier, F., Cosca, C. E., Harris, I., Hoppema, M., Houghton, R. A., House, J. I., Jain, A.](#)

1 [K., Johannessen, T., Kato, E., Keeling, R. F., Kitidis, V., Klein Goldewijk, K., Koven, C.,](#)  
2 [Landa, C. S., Landschützer, P., Lenton, A., Lima, I. D., Marland, G., Mathis, J. T., Metzl, N.,](#)  
3 [Nojiri, Y., Olsen, A., Ono, T., Peng, S., Peters, W., Pfeil, B., Poulter, B., Raupach, M. R.,](#)  
4 [Regnier, P., Rödenbeck, C., Saito, S., Salisbury, J. E., Schuster, U., Schwinger, J., Séférian, R.,](#)  
5 [Segschneider, J., Steinhoff, T., Stocker, B. D., Sutton, A. J., Takahashi, T., Tilbrook, B., van](#)  
6 [der Werf, G. R., Viovy, N., Wang, Y.-P., Wanninkhof, R., Wiltshire, A. and Zeng, N.: Global](#)  
7 [carbon budget 2014, Earth Syst. Sci. Data, 7\(1\), 47–85, doi:10.5194/essd-7-47-2015, 2015.](#)

8 [Leuning, R.: A critical appraisal of a combined stomatal-photosynthesis model for C3 plants,](#)  
9 [Plant Cell Environ., 18\(4\), 339–355, doi:10.1111/j.1365-3040.1995.tb00370.x, 1995.](#)

10 [Lin, Y.-S., Medlyn, B. E., Duursma, R. A., Prentice, I. C., Wang, H., Baig, S., Eamus, D., de](#)  
11 [Dios, V. R., Mitchell, P., Ellsworth, D. S., de Beeck, M. O., Wallin, G., Uddling, J., Tarvainen,](#)  
12 [L., Linderson, M.-L., Cernusak, L. A., Nippert, J. B., Ocheltree, T. W., Tissue, D. T., Martin-](#)  
13 [StPaul, N. K., Rogers, A., Warren, J. M., De Angelis, P., Hikosaka, K., Han, Q., Onoda, Y.,](#)  
14 [Gimeno, T. E., Barton, C. V. M., Bennie, J., Bonal, D., Bosc, A., Löw, M., Macinins-Ng, C.,](#)  
15 [Rey, A., Rowland, L., Setterfield, S. A., Tausz-Posch, S., Zaragoza-Castells, J., Broadmeadow,](#)  
16 [M. S. J., Drake, J. E., Freeman, M., Ghannoum, O., Hutley, L. B., Kelly, J. W., Kikuzawa, K.,](#)  
17 [Kolari, P., Koyama, K., Limousin, J.-M., Meir, P., Lola da Costa, A. C., Mikkelsen, T. N.,](#)  
18 [Salinas, N., Sun, W. and Wingate, L.: Optimal stomatal behaviour around the world, Nat. Clim.](#)  
19 [Change, 5\(5\), 459–464, doi:10.1038/nclimate2550, 2015.](#)

20 [Mao, J., Ricciuto, D. M., Thornton, P. E., Warren, J. M., King, A. W., Shi, X., Iversen, C. M.](#)  
21 [and Norby, R. J.: Evaluating the Community Land Model in a pine stand with shading](#)  
22 [manipulations and  \$\delta^{13}\text{C}\$  labeling,](#)  
23 [Biogeosciences, 13\(3\), 641–657, doi:10.5194/bg-13-641-2016, 2016.](#)

24 [Martinelli, L. A., Almeida, S., Brown, I. F., Moreira, M. Z., Victoria, R. L., Sternberg, L. S. L.,](#)  
25 [Ferreira, C. A. C. and Thomas, W. W.: Stable carbon isotope ratio of tree leaves, boles and fine](#)  
26 [litter in a tropical forest in Rondonia, Brazil, Oecologia, 114\(2\), 170–179, 1998.](#)

27 [McDowell, N. G., Allen, C. D. and Marshall, L.: Growth, carbon-isotope discrimination, and](#)  
28 [drought-associated mortality across a Pinus ponderosa elevational transect, Glob. Change Biol.,](#)  
29 [16\(1\), 399–415, 2010.](#)

30 [Medvigy, D., Wofsy, S. C., Munger, J. W., Hollinger, D. Y. and Moorcroft, P., R.: Mechanistic](#)  
31 [scaling of ecosystem function and dynamics in space and time: Ecosystem Demography model](#)  
32 [version 2, J. Geophys. Res.-Biogeosciences, 114, G01002, doi:10.1029/2008JG000812, 2009.](#)

33 [Mitton, J. . and Ferrenberg, S. M.: Mountain pine beetle develops an unprecedented summer](#)  
34 [generation in response to climate warming, Am. Nat., 179\(5\), 1–9, 2012.](#)

35 [Monson, R. K., Turnipseed, A. A., Sparks, J. P., Harley, P. C., Scott-Denton, L. E., Sparks, K.](#)  
36 [and Huxman, T. E.: Carbon sequestration in a high-elevation, subalpine forest, Glob. Change](#)  
37 [Biol., 8, 459–478, 2002.](#)

38 [Monson, R. K., Sparks, J. P., Rosentiel, T. N., Scott-Denton, L. E., Huxman, T. E., Harley, P.](#)  
39 [C., Turnipseed, A. A., Burns, S. P., Backlund, B. and Hu, J.: Climatic influences on net](#)  
40 [ecosystem CO<sub>2</sub> exchange during the transition from wintertime carbon source to springtime](#)  
41 [carbon sink in a high-elevation, subalpine forest, Oecologia, 146, 130-147-5-169–2, 2005.](#)

1 [Oleson et al.: Technical Description of version 4.5 of the Community Land Model \(CLM\).](#)  
2 [\[online\]](#) Available from:  
3 [http://www.cesm.ucar.edu/models/cesm1.2/clm/CLM45\\_Tech\\_Note.pdf](http://www.cesm.ucar.edu/models/cesm1.2/clm/CLM45_Tech_Note.pdf), 2013.

4 [Parton, W. J., Hanson, P. J., Swanston, C., Torn, M., Trumbore, S. E., Riley, W. and Kelly, R.: ForCent model development and testing using the Enriched Background Isotope Study experiment, J. Geophys. Res. Biogeosciences, 115\(G4\), G04001, doi:10.1029/2009JG001193, 2010.](#)

8 [Peñuelas, J., Canadell, J. G. and Ogaya, R.: Increased water-use efficiency during the 20th century did not translate into enhanced tree growth, Glob. Ecol. Biogeogr., 20\(4\), 597–608, doi:10.1111/j.1466-8238.2010.00608.x, 2011.](#)

11 [Reichstein, M., Falge, E., Baldocchi, D., Papale, D., Aubinet, M., Berbigier, P., Bernhofer, C., Buchmann, N., Gilmanov, T., Granier, A., Grunwald, T., Havrankova, K., Ilvesniemi, H., Janous, D., Knohl, A., Laurila, T., Lohila, A., Loustau, D., Matteucci, G., Meyers, T., Miglietta, F., Ourcival, J. M., Pumpanen, J., Rambal, S., Rotenberg, E., Sanz, M., Tenhunen, J., Seufert, G., Vaccari, F., Vesala, T., Yakir, D. and Valentini, R.: On the separation of net ecosystem exchange into assimilation and ecosystem respiration: review and improved algorithm, Glob. Change Biol., 11\(9\), 1424–1439, 2005.](#)

18 [Ricciuto, D. M., Davis, K. J. and Keller, K.: A Bayesian calibration of a simple carbon cycle model: The role of observations in estimating and reducing uncertainty, Glob. Biogeochem. Cycles, 22, GB2030, doi:10.1029/2006GB002908, 2008.](#)

21 [Ricciuto, D. M., King, A. W., Dragoni, D. and Post, W. M.: Parameter and prediction uncertainty in an optimized terrestrial carbon cycle model: Effects of constraining variables and data record length, J. Geophys. Res. Biogeosciences, 116\(G1\), G01033, doi:10.1029/2010JG001400, 2011.](#)

25 [Richardson, A. D., Williams, M., Hollinger, D. Y., Moore, D. J. P., Dail, D. B., Davidson, E. A., Scott, N. A., Evans, R. S., Hughes, H., Lee, J. T., Rodrigues, C. and Savage, K.: Estimating parameters of a forest ecosystem C model with measurements of stocks and fluxes as joint constraints, Oecologia, 164\(1\), 25–40, 2010.](#)

29 [Roden, J. S. and Ehleringer, J. R.: Summer precipitation influences the stable oxygen and carbon isotopic composition of tree-ring cellulose in \*Pinus ponderosa\*, Tree Physiol., 27\(4\), 491–501, 2007.](#)

32 [Rubino, M., Etheridge, D. M., Trudinger, C. M., Allison, C. E., Battle, M. O., Langenfelds, R. L., Steele, L. P., Curran, M., Bender, M., White, J. W. C., Jenk, T. M., Blunier, T. and Francey, R. J.: A revised 1000 year atmospheric  \$\delta^{13}\text{C}\$ -CO<sub>2</sub> record from Law Dome and South Pole, Antarctica, J. Geophys. Res. Atmospheres, 118\(15\), 8482–8499, doi:10.1002/jgrd.50668, 2013.](#)

36 [Sánchez-Rodríguez, J., Pérez, P. and Martínez-Carrasco, R.: Photosynthesis, carbohydrate levels and chlorophyll fluorescence-estimated intercellular CO<sub>2</sub> in water-stressed \*Casuarina equisetifolia\* Forst. & Forst., Plant Cell Environ., 22\(7\), 867–873, doi:10.1046/j.1365-3040.1999.00447.x, 1999.](#)



1 [Saurer, M., Siegwolf, R. T. W. and Schweingruber, F. H.: Carbon isotope discrimination](#)  
2 [indicates improving water-use efficiency of trees in northern Eurasia over the last 100 years.](#)  
3 [Glob. Change Biol., 10\(12\), 2109–2120, doi:10.1111/j.1365-2486.2004.00869.x, 2004.](#)

4 [Saurer, M., Spahni, R., Frank, D. C., Joos, F., Leuenberger, M., Loader, N. J., McCarroll, D.,](#)  
5 [Gagen, M., Poulter, B., Siegwolf, R. T. W., Andreu-Hayles, L., Boettger, T., Dorado Liñán, I.,](#)  
6 [Fairchild, I. J., Friedrich, M., Gutierrez, E., Haupt, M., Hiltunen, E., Heinrich, I., Helle, G.,](#)  
7 [Grubb, H., Jalkanen, R., Levanič, T., Linderholm, H. W., Robertson, I., Sonninen, E., Treydte,](#)  
8 [K., Waterhouse, J. S., Woodley, E. J., Wynn, P. M. and Young, G. H. F.: Spatial variability and](#)  
9 [temporal trends in water-use efficiency of European forests, Glob. Change Biol., 20\(12\), 3700–](#)  
10 [3712, doi:10.1111/gcb.12717, 2014.](#)

11 [Schaeffer, S. M., Miller, J. B., Vaughn, B. H., White, J. W. C. and Bowling, D. R.: Long-term](#)  
12 [field performance of a tunable diode laser absorption spectrometer for analysis of carbon](#)  
13 [isotopes of CO<sub>2</sub> in forest air, Atmospheric Chem. Phys., 8, 5263–5277, 2008.](#)

14 [Schimel, D. T., Kittel, G. F., Running, S., Monson, R., Turnispeed, A. and Anderson, D.:](#)  
15 [Carbon sequestration studied in western U.S. mountains, Eos Trans AGU, 83\(40\), 445–449,](#)  
16 [2002.](#)

17 [Scott-Denton, L. E., Sparks, K. L. and Monson, R. K.: Spatial and temporal controls of soil](#)  
18 [respiration rate in a high-elevation, subalpine forest, Soil Biol. Biochem., 35, 525–534, 2003.](#)

19 [Sellers, P. J., Randall, D. A., Collatz, G. J., Berry, J. A., Field, C. B., Dazlich, D. A., Zhang, C.,](#)  
20 [Collelo, G. D. and Bounoua, L.: A revised land surface parameterization \(SiB2\) for atmospheric](#)  
21 [GCMs. Part I: Model formulation, J. Clim., 9\(4\), 676–705, 1996.](#)

22 [Thornton, P. E. and Rosenbloom, N. A.: Ecosystem model spin-up: Estimating steady state](#)  
23 [conditions in a coupled terrestrial carbon and nitrogen cycle model, Ecol. Model., 189\(1–2\),](#)  
24 [25–48, doi:10.1016/j.ecolmodel.2005.04.008, 2005.](#)

25 [Thornton, P. E., Law, B. E., Gholz, H. L., Clark, K. L., Falge, E., Ellsworth, D. S., Golstein, A.](#)  
26 [H., Monson, R. K., Hollinger, D., Falk, M., Chen, J. and Sparks, J. P.: Modeling and measuring](#)  
27 [the effects of disturbance history and climate on carbon and water budgets in evergreen](#)  
28 [needleleaf forests, Agric. For. Meteorol., 113\(1–4\), 185–222, 2002.](#)

29 [Thornton, P. E., Lamarque, J.-F., Rosenbloom, N. A. and Mahowald, N. M.: Influence of](#)  
30 [carbon-nitrogen cycle coupling on land model response to CO<sub>2</sub> fertilization and climate](#)  
31 [variability, Glob. Biogeochem. Cycles, 21, GB4018, doi:10.1029/2006GB002868, 2007.](#)

32 [Troler, M., White, J. W. C., Tans, P. P., Masarie, K. A. and Gemery, P. A.: Monitoring the](#)  
33 [isotopic composition of atmospheric CO<sub>2</sub>: Measurements from the NOAA Global Air](#)  
34 [Sampling Network, J. Geophys. Res.-Atmospheres, 101\(D20\), 25,897–25,916, 1996.](#)

35 [van der Velde, I. R., Miller, J. B., Schaefer, K., Masarie, K. A., Denning, S., White, J. W. C.,](#)  
36 [Tans, P. P., Krol, M. C. and Peters, W.: Biosphere model simulations of interannual variability](#)  
37 [in terrestrial 13C/12C exchange, Glob. Biogeochem. Cycles, 27\(3\), 637–649,](#)  
38 [doi:10.1002/gbc.20048, 2013.](#)

Wehr, R. and Saleska, S. R.: An improved isotopic method for partitioning net ecosystem-atmosphere CO<sub>2</sub> exchange, *Agric. For. Meteorol.*, 214–215, 515–531, doi:10.1016/j.agrformet.2015.09.009, 2015.

White, J. W. C., Vaughn, B. H., Michel, S. E., University of Colorado and Institute of Arctic and Alpine Research (INSTAAR): Stable Isotopic Composition of Atmospheric Carbon Dioxide (13C and 18O) from the NOAA ESRL Carbon Cycle Cooperative Global Air Sampling Network, 1990–2014, Version: 2015-10-26, Path: ftp://aftp.cmdl.noaa.gov/data/trace\_gases/co2c13/flask/, 2015.

White et al.: Parameterization and Sensitivity Analysis of the Biome-BGC Terrestrial Ecosystem Model: Net Primary Production Controls, [online] Available from: http://secure.ntsg.umt.edu/publications/2000/WTRN00/White\_2000.pdf, 2000.

Wingate, L., Ogee, J., Burlett, R., Bosc, A., Devaux, M., Grace, J., Loustau, D. and Gessler, A.: Photosynthetic carbon isotope discrimination and its relationship to the carbon isotope signals of stem, soil and ecosystem respiration, *New Phytol.*, 188(2), 576–589, 2010.

Zaehle, S., Medlyn, B. E., De Kauwe, M. G., Walker, A. P., Dietze, M. C., Hickler, T., Luo, Y., Wang, Y.-P., El-Masri, B., Thornton, P., Jain, A., Wang, S., Warlind, D., Weng, E., Parton, W., Iversen, C. M., Gallet-Budynnek, A., McCarthy, H., Finzi, A., Hanson, P. J., Prentice, I. C., Oren, R. and Norby, R. J.: Evaluation of 11 terrestrial carbon–nitrogen cycle models against observations from two temperate Free-Air CO<sub>2</sub> Enrichment studies, *New Phytol.*, 202(3), 803–822, doi:10.1111/nph.12697, 2014.

Zarter, C. R., Demmig-Adams, B., Ebbert, V., Adamska, I. and Adams, W. W.: Photosynthetic capacity and light harvesting efficiency during the winter-to-spring transition in subalpine conifers, *New Phytol.*, 172(2), 283–292, doi:10.1111/j.1469-8137.2006.01816.x, 2006.

Zeng, X.: Global Vegetation Root Distribution for Land Modeling, *J. Hydrometeorol.*, 2(5), 525–530, doi:10.1175/1525-7541(2001)002<0525:GVRDFL>2.0.CO;2, 2001.

Zeng, X. and Decker, M.: Improving the Numerical Solution of Soil Moisture–Based Richards Equation for Land Models with a Deep or Shallow Water Table, *J. Hydrometeorol.*, 10(1), 308–319, doi:10.1175/2008JHM1011.1, 2009.

Ainsworth, E. A. and Long, S. P.: What have we learned from 15 years of free air CO<sub>2</sub> enrichment (FACE)? A meta analytic review of the responses of photosynthesis, canopy properties and plant production to rising CO<sub>2</sub>, *New Phytol.*, 165(2), 351–372, doi:10.1111/j.1469-8137.2004.01224.x, 2005.

Andrews, S. F., Flanagan, L. B., Sharp, E. J. and Cai, T.: Variation in water potential, hydraulic characteristics and water source use in montane Douglas fir and lodgepole pine trees in southwestern Alberta and consequences for seasonal changes in photosynthetic capacity, *Tree Physiol.*, 32, 146–160, doi:10.1093/treephys/tpr136, 2012.

Aranibar, J. N., Berry, J. A., Riley, W. J., Pataki, D. E., Law, B. E. and Ehleringer, J. R.: Combining meteorology, eddy fluxes, isotope measurements, and modeling to understand environmental controls of carbon isotope discrimination at the canopy scale, *Glob. Change Biol.*, 12(4), 710–730, 2006.

**Formatted:** Bibliography, Widow/Orphan control, Adjust space between Latin and Asian text, Adjust space between Asian text and numbers

Arora, V. K., Boer, G. J., Friedlingstein, P., Eby, M., Jones, C. D., Christian, J. R., Bonan, G., Bopp, L., Brovkin, V., Cadule, P., Hajima, T., Ilyina, T., Lindsay, K., Tziputra, J. F. and Wu, T.: Carbon Concentration and Carbon Climate Feedbacks in CMIP5 Earth System Models, *J. Clim.*, 26(15), 5289–5314, doi:10.1175/jcli-d-12-00494.1, 2013.

Ballantyne, A. P., Miller, J. B. and Tans, P. P.: Apparent seasonal cycle in isotopic discrimination of carbon in the atmosphere and biosphere due to vapor pressure deficit, *Glob. Biogeochem. Cycles*, 24, GB3018, doi:10.1029/2009GB003623, 2010.

Ballantyne, A. P., Miller, J. B., Baker, I. T., Tans, P. P. and White, J. W. C.: Novel applications of carbon isotopes in atmospheric CO<sub>2</sub>: What can atmospheric measurements teach us about processes in the biosphere?, *Biogeosciences*, 8(10), 3093–3106, 2011.

Bauerle, W. L., Oren, R., Way, D. A., Qian, S. S., Stoy, P. C., Thornton, P. E., Bowden, J. D., Hoffman, F. M. and Reynolds, R. F.: Photoperiodic regulation of the seasonal pattern of photosynthetic capacity and the implications for carbon cycling, *Proc. Natl. Acad. Sci. U. S. A.*, 109(22), 8612–8617, 2012.

Belmecheri, S., Maxwell, R. S., Taylor, A. H., Davis, K. J., Freeman, K. H. and Munger, W. J.: Tree ring  $\delta^{13}\text{C}$  tracks flux tower ecosystem productivity estimates in a NE temperate forest, *Environ. Res. Lett.*, 9(7), 74011, doi:10.1088/1748-9326/9/7/074011, 2014.

Boisvenue, C. and Running, S. W.: Simulations show decreasing carbon stocks and potential for carbon emissions in Rocky Mountain forests over the next century, *Ecol. Appl.*, 20(5), 1302–1319, 2010.

Bowling, D. R., Pataki, D. E. and Randerson, J. T.: Carbon isotopes in terrestrial ecosystem pools and CO<sub>2</sub> fluxes, *New Phytol.*, 178, 24–40, doi: 10.1111/j.1469-8137.2007.02342.x, 2008.

Bowling, D. R., Ballantyne, A. P., Miller, J. B., Burns, S. P., Conway, T. J., Menzer, O., Stephens, B. B. and Vaughn, B. H.: Ecological processes dominate the  $^{13}\text{C}$  land disequilibrium in a Rocky Mountain subalpine forest, *Glob. Biogeochem. Cycles*, 28(4), 2013GB004686, doi:10.1002/2013GB004686, 2014a.

Bowling, D. R., Ballantyne, A. P., Miller, J. B., Burns, S. P., Conway, T. J., Menzer, O., Stephens, B. B. and Vaughn, B. H.: Ecological processes dominate the  $^{13}\text{C}$  land disequilibrium in a Rocky Mountain subalpine forest, *Glob. Biogeochem. Cycles*, 28(4), 2013GB004686, doi:10.1002/2013GB004686, 2014b.

Bradford, M. A., Fierer, N. and Reynolds, J. F.: Soil carbon stocks in experimental mesocosms are dependent on the rate of labile carbon, nitrogen and phosphorus inputs to soils, *Funct. Ecol.*, 22(6), 964–974, doi:10.1111/j.1365-2435.2008.01404.x, 2008.

Braswell, B. H., Sacks, W. J., Linder, E. and Schimel, D. S.: Estimating diurnal to annual ecosystem parameters by synthesis of a carbon flux model with eddy covariance net ecosystem exchange observations, *Glob. Change Biol.*, 11, 335–355, doi:10.1111/j.1365-2486.2005.00897.x, 2005.

Brüggemann, N., Gessler, A., Kayler, Z., Keel, S. G., Badeck, F., Barthel, M., Boeckx, P., Buchmann, N., Brugnoli, E., Esperschütz, J., Gavrichkova, O., Ghashghaie, J., Gomez

Casanovas, N., Keitel, C., Knohl, A., Kuptz, D., Palacio, S., Salmon, Y., Uchida, Y. and Bahn, M.: Carbon allocation and carbon isotope fluxes in the plant soil atmosphere continuum: a review, *Biogeosciences*, 8(11), 3457–3489, doi:10.5194/bg-8-3457-2011, 2011a.

Brüggemann, N., Gessler, A., Kayler, Z., Keel, S. G., Badeck, F., Barthel, M., Boeckx, P., Buchmann, N., Brugnoli, E., Esperschütz, J., Gavrichkova, O., Ghashghaie, J., Gomez-Casanovas, N., Keitel, C., Knohl, A., Kuptz, D., Palacio, S., Salmon, Y., Uchida, Y. and Bahn, M.: Carbon allocation and carbon isotope fluxes in the plant soil atmosphere continuum: A review, *Biogeosciences*, 8(11), 3457–3489, 2011b.

Collatz, G. J., Ball, J. T., Griwet, C. and Berry, J. A.: Regulation of stomatal conductances and transpiration a physiological model of canopy processes, *Agric. For. Meteorol.*, 54, 107–136, 1991.

Desai, A. R., Moore, D. J. P., Ahue, W. K. M., Wilkes, P. T. V., De Wekker, S. F. J., Brooks, B. G., Campos, T. L., Stephens, B. B., Monson, R. K., Burns, S. P., Quaife, T., Aulenbach, S. M. and Schimel, D. S.: Seasonal pattern of regional carbon balance in the central Rocky Mountains from surface and airborne measurements, *J. Geophys. Res.*, 116, G04009(4), doi:10.1029/2011JG001655, 2011.

Di Marco, G., Manes, F., Tricoli, D. and Vitale, E.: Fluorescence Parameters Measured Concurrently with Net Photosynthesis to Investigate Chloroplastic CO<sub>2</sub> Concentration in Leaves of *Quercus ilex* L., *J. Plant Physiol.*, 136(5), 538–543, doi:10.1016/S0176-1617(11)80210-5, 1990.

Dlugokencky, E. J., Lang, P. M., Masarie, K. A., Crotwell, A. M. and Crotwell, M. J.: Atmospheric Carbon Dioxide Dry Air Mole Fractions from the NOAA ESRL Carbon Cycle Cooperative Global Air Sampling network, 1968–2014, Version: 2015-08-03, Path: [ftp://afgp.emdl.noaa.gov/data/trace\\_gases/co2/flask/surface/](ftp://afgp.emdl.noaa.gov/data/trace_gases/co2/flask/surface/), 2015.

Ehleringer, J. R., Buchmann, N. and Flanagan, L. B.: Carbon isotope ratios in belowground carbon cycle processes, *Ecol. Appl.*, 10(2), 412–422, 2000.

Epron, D., Bahn, M., Derrien, D., Lattanzi, F. A., Pumpanen, J., Gessler, A., Höglberg, P., Maillard, P., Dannoura, M., Gérant, D. and Buchmann, N.: Pulse labelling trees to study carbon allocation dynamics: a review of methods, current knowledge and future prospects, *Tree Physiol.*, 32(6), 776–798, doi:10.1093/treephys/tps057, 2012.

Farquhar, G. D., von Caemmerer, S. and Berry, J. A.: A Biochemical Model of Photosynthetic CO<sub>2</sub> Assimilation in Leaves of C<sub>3</sub> Species, *Planta*, 149, 78–90, 1980.

Farquhar, G. D., O'Leary, M. H. and Berry, J. A.: On the relationship between carbon isotope discrimination and the intercellular carbon dioxide concentration in leaves, *Aust. J. Plant Physiol.*, 9(2), 121–137, 1982.

Farquhar, G. D., Ehleringer, J. R. and Hubick, K. T.: Carbon isotope discrimination and photosynthesis, *Annu. Rev. Plant Physiol. Plant Mol. Biol.*, 40, 503–537, 1989.

Flanagan, L. B., Cai, T., Black, T. A., Barr, A. G., McCaughey, J. H. and Margolis, H. A.: Measuring and modeling ecosystem photosynthesis and the carbon isotope composition of

ecosystem-respired CO<sub>2</sub> in three boreal coniferous forests. *Agric. For. Meteorol.*, 153, 165–176, 2012.

Flexas, J., Ribas Carbo, M., Diaz Espej, A., Galmes, J. and Medrano, H.: Mesophyll conductance to CO<sub>2</sub>: current knowledge and future prospects, *Plant Cell Environ.*, 31(5), 602–621, 2008.

Francey, R. J., Allison, C. E., Etheridge, D. M., Trudinger, C. M., Enting, I. G., Leuenberger, M., Langenfelds, R. L., Michel, E. and Steele, L. P.: A 1000-year high precision record of δ<sup>13</sup>C in atmospheric CO<sub>2</sub>, *Tellus*, 51B, 170–193, 1999.

Frank, D. C., Poulter, B., Saurer, M., Esper, J., Huntingford, C., Helle, G., Treydte, K., Zimmermann, N. E., Schleser, G. H., Ahlström, A., Ciais, P., Friedlingstein, P., Levis, S., Lomas, M., Sitch, S., Viovy, N., Andreu-Hayles, L., Bednarz, Z., Berninger, F., Boettger, T., D'Alessandro, C. M., Daux, V., Filot, M., Grabner, M., Gutierrez, E., Haupt, M., Hilasvuori, E., Jungner, H., Kalela-Brundin, M., Krapiec, M., Leuenberger, M., Loader, N. J., Marah, H., Masson-Delmotte, V., Pazdur, A., Pawelezyk, S., Pierre, M., Planells, O., Pukiene, R., Reynolds-Henne, C. E., Rinne, K. T., Saracino, A., Sonninen, E., Stievenard, M., Switsur, V., Szczepanek, M., Szychowska-Krapiec, E., Todaro, L., Waterhouse, J. S. and Weigl, M.: Water use efficiency and transpiration across European forests during the Anthropocene, *Nat. Clim. Change*, 5(6), 579–583, doi:10.1038/nclimate2614, 2015.

Franks, P. J., Adams, M. A., Amthor, J. S., Barbour, M. M., Berry, J. A., Ellsworth, D. S., Farquhar, G. D., Ghanoun, O., Lloyd, J., McDowell, N., Norby, R. J., Tissue, D. T. and von Caemmerer, S.: Sensitivity of plants to changing atmospheric CO<sub>2</sub> concentration: From the geological past to the next century, *New Phytol.*, 197(4), 1077–1094, 2013.

Friedlingstein, P., Cox, P. M., Betts, R. A., Bopp, L., von Bloh, W., Brovkin, V., Cadule, P., Doney, S. C., Eby, M., Fung, I. Y., Bala, G., John, J., Jones, C. D., Joos, F., Kato, T., Kawamiya, M., Knorr, W., Lindsay, K., Matthews, H. D., Raddatz, T., Rayner, P., Reick, C., Roeckner, E., Schnitzler, K. G., Schnur, R., Strassmann, K., Weaver, A. J., Yoshikawa, C. and Zeng, N.: Climate-carbon cycle feedback analysis: Results from the C4MIP model intercomparison, *J. Clim.*, 19, 3337–3353, 2006.

Fung, I. Y., Field, C. B., Berry, J. A., Thompson, M. V., Randerson, J. T., Malmstrom, C. M., Vitousek, P. M., Collatz, G. J., Sellers, P. J., Randall, D. A., Denning, A. S., Badeck, F. and John, J.: Carbon-13 exchanges between the atmosphere and biosphere, *Glob. Biogeochem. Cycles*, 11(4), 507–533, 1997.

Greenland, D.: The Climate of Niwot Ridge, Front Range, Colorado, U.S.A., *Arct. Alp. Res.*, 21(4), 380–391, 1989.

Hogberg, P., Hogberg, M. N., Gottlicher, S. G., Betson, N. R., Keel, S. G., Metcalfe, D. B., Campbell, C., Schindlbacher, A., Hurry, V., Lundmark, T., Linder, S. and Nasholm, T.: High temporal resolution tracing of photosynthate carbon from the tree canopy to forest soil microorganisms, *New Phytol.*, 177(1), 220–228, 2008.

Hu, J., Moore, D. J. P., Burns, S. P. and Monson, R. K.: Longer growing seasons lead to less carbon sequestration by a subalpine forest, *Glob. Change Biol.*, 16(2), 771–783, doi:10.1111/j.1365-2486.2009.01967.x, 2010.

Katul, G. G., Ellsworth, D. S. and Lai, C. T.: Modelling assimilation and intercellular CO<sub>2</sub> from measured conductance: a synthesis of approaches, *Plant Cell Environ.*, 23(12), 1313–1328, doi:10.1046/j.1365-3040.2000.00641.x, 2000.

Keenan, T. F., Hollinger, D. Y., Bohrer, G., Dragoni, D., Munger, J. W., Schmid, H. P. and Richardson, A. D.: Increase in forest water use efficiency as atmospheric carbon dioxide concentrations rise, *Nature*, 499(7458), 324–327, doi:10.1038/nature12291, 2013.

Kolari, P., Lappalainen, H. K., HäNninen, H. and Hari, P.: Relationship between temperature and the seasonal course of photosynthesis in Scots pine at northern timberline and in southern boreal zone, *Tellus B*, 59(3), 542–552, doi:10.1111/j.1600-0889.2007.00262.x, 2007.

Lasslop, G., Reichstein, M., Papale, D., Richardson, A., Arneth, A., Barr, A., Stoy, P. and Wohlfahrt, G.: Separation of net ecosystem exchange into assimilation and respiration using a light response curve approach: critical issues and global evaluation, *Glob. Change Biol.*, 16, 187–208, 2010.

Le Quéré, C., Moriarty, R., Andrew, R. M., Peters, G. P., Ciais, P., Friedlingstein, P., Jones, S. D., Sitch, S., Tans, P., Arneth, A., Boden, T. A., Bopp, L., Bozec, Y., Canadell, J. G., Chini, L. P., Chevallier, F., Cosen, C. E., Harris, I., Hoppema, M., Houghton, R. A., House, J. I., Jain, A. K., Johannessen, T., Kato, E., Keeling, R. F., Kitidis, V., Klein Goldewijk, K., Koven, C., Landa, C. S., Landschützer, P., Lenton, A., Lima, I. D., Marland, G., Mathis, J. T., Metzl, N., Nojiri, Y., Olsen, A., Ono, T., Peng, S., Peters, W., Pfeil, B., Poulter, B., Raupach, M. R., Regnier, P., Rödenbeck, C., Saito, S., Salisbury, J. E., Schuster, U., Schwinger, J., Séférian, R., Segsneider, J., Steinhoff, T., Stocker, B. D., Sutton, A. J., Takahashi, T., Tilbrook, B., van der Werf, G. R., Viovy, N., Wang, Y. P., Wanninkhof, R., Wiltshire, A. and Zeng, N.: Global carbon budget 2014, *Earth Syst. Sci. Data*, 7(1), 47–85, doi:10.5194/essd-7-47-2015, 2015.

Leuning, R.: A critical appraisal of a combined stomatal photosynthesis model for C<sub>3</sub> plants, *Plant Cell Environ.*, 18(4), 339–355, doi:10.1111/j.1365-3040.1995.tb00370.x, 1995.

Lin, Y. S., Medlyn, B. E., Duursma, R. A., Prentice, I. C., Wang, H., Baig, S., Eamus, D., de Dios, V. R., Mitchell, P., Ellsworth, D. S., de Beeck, M. O., Wallin, G., Uddling, J., Tarvainen, L., Linderson, M. L., Cernusak, L. A., Nippert, J. B., Oecheltree, T. W., Tissue, D. T., Martin-StPaul, N. K., Rogers, A., Warren, J. M., De Angelis, P., Hikosaka, K., Han, Q., Onoda, Y., Gimeno, T. E., Barton, C. V. M., Bennie, J., Bonal, D., Bose, A., Löw, M., Macinins Ng, C., Rey, A., Rowland, L., Setterfield, S. A., Tausz-Pösch, S., Zaragoza-Castells, J., Broadmeadow, M. S. J., Drake, J. E., Freeman, M., Ghannoum, O., Hutley, L. B., Kelly, J. W., Kikuzawa, K., Kolari, P., Koyama, K., Limousin, J. M., Meir, P., Lola da Costa, A. C., Mikkelsen, T. N., Salinas, N., Sun, W. and Wingate, L.: Optimal stomatal behaviour around the world, *Nat. Clim. Change*, 5(5), 459–464, doi:10.1038/nclimate2550, 2015.

Mao, J., Ricciuto, D. M., Thornton, P. E., Warren, J. M., King, A. W., Shi, X., Iversen, C. M. and Norby, R. J.: Evaluating the Community Land Model in a pine stand with shading manipulations and <sup>13</sup>C labeling, *Biogeosciences*, 13(3), 641–657, doi:10.5194/bg-13-641-2016, 2016.

Martinelli, L. A., Almeida, S., Brown, I. F., Moreira, M. Z., Victoria, R. L., Sternberg, L. S. L., Ferreira, C. A. C. and Thomas, W. W.: Stable carbon isotope ratio of tree leaves, boles and fine litter in a tropical forest in Rondonia, Brazil, *Oecologia*, 114(2), 170–179, 1998.

McDowell, N. G., Allen, C. D. and Marshall, L.: Growth, carbon isotope discrimination, and drought-associated mortality across a *Pinus ponderosa* elevational transect, *Glob. Change Biol.*, 16(4), 399–415, 2010.

Medvigy, D., Wofsy, S. C., Munger, J. W., Hollinger, D. Y. and Moorcroft, P., R.: Mechanistic scaling of ecosystem function and dynamics in space and time: Ecosystem Demography model version 2, *J. Geophys. Res. Biogeosciences*, 114, G01002, doi:10.1029/2008JG000812, 2009.

Mitton, J., and Ferrenberg, S. M.: Mountain pine beetle develops an unprecedented summer generation in response to climate warming, *Am. Nat.*, 179(5), 1–9, 2012.

Monson, R. K., Turnipseed, A. A., Sparks, J. P., Harley, P. C., Scott-Denton, L. E., Sparks, K. and Huxman, T. E.: Carbon sequestration in a high-elevation, subalpine forest, *Glob. Change Biol.*, 8, 459–478, 2002.

Monson, R. K., Sparks, J. P., Rosentiel, T. N., Scott-Denton, L. E., Huxman, T. E., Harley, P. C., Turnipseed, A. A., Burns, S. P., Backlund, B. and Hu, J.: Climatic influences on net ecosystem CO<sub>2</sub> exchange during the transition from wintertime carbon source to springtime carbon sink in a high-elevation, subalpine forest, *Oecologia*, 146, 130–147–5–169–2, 2005.

Oleson et al.: Technical Description of version 4.5 of the Community Land Model (CLM), [online] Available from: [http://www.cesm.ucar.edu/models/cesm1.2/clm/CLM45\\_Tech\\_Note.pdf](http://www.cesm.ucar.edu/models/cesm1.2/clm/CLM45_Tech_Note.pdf), 2013.

Parton, W. J., Hanson, P. J., Swanston, C., Torn, M., Trumbore, S. E., Riley, W. and Kelly, R.: ForCent model development and testing using the Enriched Background Isotope Study experiment, *J. Geophys. Res. Biogeosciences*, 115(G4), G04001, doi:10.1029/2009JG001193, 2010.

Peñuelas, J., Canadell, J. G. and Ogaya, R.: Increased water-use efficiency during the 20th century did not translate into enhanced tree growth, *Glob. Ecol. Biogeogr.*, 20(4), 597–608, doi:10.1111/j.1466-8238.2010.00608.x, 2011.

Reichstein, M., Falge, E., Baldocchi, D., Papale, D., Aubinet, M., Berbigier, P., Bernhofer, C., Buchmann, N., Gilmanov, T., Granier, A., Grunwald, T., Havrankova, K., Ilvesniemi, H., Janous, D., Knohl, A., Laurila, T., Lohila, A., Loustau, D., Matteucci, G., Meyers, T., Miglietta, F., Ourival, J. M., Pumpanen, J., Rambal, S., Rotenberg, E., Sanz, M., Tenhunen, J., Seufert, G., Vaccari, F., Vesala, T., Yakir, D. and Valentini, R.: On the separation of net ecosystem exchange into assimilation and ecosystem respiration: review and improved algorithm, *Glob. Change Biol.*, 11(9), 1424–1439, 2005.

Ricciuto, D. M., Davis, K. J. and Keller, K.: A Bayesian calibration of a simple carbon cycle model: The role of observations in estimating and reducing uncertainty, *Glob. Biogeochem. Cycles*, 22, GB2030, doi:10.1029/2006GB002908, 2008.

Ricciuto, D. M., King, A. W., Dragoni, D. and Post, W. M.: Parameter and prediction uncertainty in an optimized terrestrial carbon cycle model: Effects of constraining variables and data record length, *J. Geophys. Res. Biogeosciences*, 116(G1), G01033, doi:10.1029/2010JG001400, 2011.



1 [Richardson, A. D., Williams, M., Hollinger, D. Y., Moore, D. J. P., Dail, D. B., Davidson, E.](#)  
 2 [A., Scott, N. A., Evans, R. S., Hughes, H., Lee, J. T., Rodrigues, C. and Savage, K.: Estimating](#)  
 3 [parameters of a forest ecosystem C model with measurements of stocks and fluxes as joint](#)  
 4 [constraints, \*Oecologia\*, 164\(1\), 25–40, 2010.](#)

5 [Roden, J. S. and Ehleringer, J. R.: Summer precipitation influences the stable oxygen and](#)  
 6 [carbon isotopic composition of tree ring cellulose in \*Pinus ponderosa\*, \*Tree Physiol.\*, 27\(4\),](#)  
 7 [491–501, 2007.](#)

8 [Rubino, M., Etheridge, D. M., Trudinger, C. M., Allison, C. E., Battle, M. O., Langenfelds, R.](#)  
 9 [L., Steele, L. P., Curran, M., Bender, M., White, J. W. C., Jenk, T. M., Blunier, T. and Francey,](#)  
 10 [R. J.: A revised 1000 year atmospheric  \$\delta^{13}\text{C}\$ -CO<sub>2</sub> record from Law Dome and South Pole,](#)  
 11 [Antarctica, \*J. Geophys. Res. Atmospheres\*, 118\(15\), 8482–8499, doi:10.1002/jgrd.50668, 2013.](#)

12 [Sánchez Rodríguez, J., Pérez, P. and Martínez Carrasco, R.: Photosynthesis, carbohydrate](#)  
 13 [levels and chlorophyll fluorescence estimated intercellular CO<sub>2</sub> in water stressed \*Casuarina\*](#)  
 14 [equisetifolia Forst. & Forst., \*Plant Cell Environ.\*, 22\(7\), 867–873, doi:10.1046/j.1365-](#)  
 15 [3040.1999.00447.x, 1999.](#)

16 [Saurer, M., Siegwolf, R. T. W. and Schweingruber, F. H.: Carbon isotope discrimination](#)  
 17 [indicates improving water use efficiency of trees in northern Eurasia over the last 100 years,](#)  
 18 [Glob. Change Biol., 10\(12\), 2109–2120, doi:10.1111/j.1365-2486.2004.00869.x, 2004.](#)

19 [Saurer, M., Spahni, R., Frank, D. C., Joos, F., Leuenberger, M., Loader, N. J., McCarroll, D.,](#)  
 20 [Gagen, M., Poulter, B., Siegwolf, R. T. W., Andreu-Hayles, L., Boettger, T., Dorado-Liñán, I.,](#)  
 21 [Fairchild, I. J., Friedrich, M., Gutierrez, E., Haupt, M., Hiltavuori, E., Heinrich, I., Helle, G.,](#)  
 22 [Grudd, H., Jalkanen, R., Levanič, T., Linderholm, H. W., Robertson, I., Sonninen, E., Treydte,](#)  
 23 [K., Waterhouse, J. S., Woodley, E. J., Wynn, P. M. and Young, G. H. F.: Spatial variability and](#)  
 24 [temporal trends in water use efficiency of European forests, Glob. Change Biol., 20\(12\), 3700–](#)  
 25 [3712, doi:10.1111/gcb.12717, 2014.](#)

26 [Schaeffer, S. M., Miller, J. B., Vaughn, B. H., White, J. W. C. and Bowling, D. R.: Long term](#)  
 27 [field performance of a tunable diode laser absorption spectrometer for analysis of carbon](#)  
 28 [isotopes of CO<sub>2</sub> in forest air, \*Atmospheric Chem. Phys.\*, 8, 5263–5277, 2008.](#)

29 [Schimel, D. T., Kittel, G. F., Running, S., Monson, R., Turnispeed, A. and Anderson, D.:](#)  
 30 [Carbon sequestration studied in western U.S. mountains, \*Eos Trans AGU\*, 83\(40\), 445–449,](#)  
 31 [2002.](#)

32 [Scott-Denton, L. E., Sparks, K. L. and Monson, R. K.: Spatial and temporal controls of soil](#)  
 33 [respiration rate in a high elevation, subalpine forest, \*Soil Biol. Biochem.\*, 35, 525–534, 2003.](#)

34 [Sellers, P. J., Randall, D. A., Collatz, G. J., Berry, J. A., Field, C. B., Dazlich, D. A., Zhang, C.,](#)  
 35 [Collelo, G. D. and Bounoua, L.: A revised land surface parameterization \(SiB2\) for atmospheric](#)  
 36 [GCMs. Part I: Model formulation, \*J. Clim.\*, 9\(4\), 676–705, 1996.](#)

37 [Thornton, P. E. and Rosenbloom, N. A.: Ecosystem model spin up: Estimating steady state](#)  
 38 [conditions in a coupled terrestrial carbon and nitrogen cycle model, \*Ecol. Model.\*, 189\(1–2\),](#)  
 39 [25–48, doi:10.1016/j.ecolmodel.2005.04.008, 2005.](#)



Thornton, P. E., Law, B. E., Gholz, H. L., Clark, K. L., Falge, E., Ellsworth, D. S., Golstein, A. H., Monson, R. K., Hollinger, D., Falk, M., Chen, J. and Sparks, J. P.: Modeling and measuring the effects of disturbance history and climate on carbon and water budgets in evergreen needleleaf forests, *Agric. For. Meteorol.*, 113(1–4), 185–222, 2002.

Thornton, P. E., Lamarque, J. F., Rosenbloom, N. A. and Mahowald, N. M.: Influence of carbon-nitrogen cycle coupling on land model response to CO<sub>2</sub> fertilization and climate variability, *Glob. Biogeochem. Cycles*, 21, GB4018, doi:10.1029/2006GB002868, 2007.

Trolier, M., White, J. W. C., Tans, P. P., Masarie, K. A. and Gemery, P. A.: Monitoring the isotopic composition of atmospheric CO<sub>2</sub>: Measurements from the NOAA Global Air Sampling Network, *J. Geophys. Res. Atmospheres*, 101(D20), 25,897–25,916, 1996.

van der Velde, I. R., Miller, J. B., Schaefer, K., Masarie, K. A., Denning, S., White, J. W. C., Tans, P. P., Krol, M. C. and Peters, W.: Biosphere model simulations of interannual variability in terrestrial <sup>13</sup>C/<sup>12</sup>C exchange, *Glob. Biogeochem. Cycles*, 27(3), 637–649, doi:10.1002/gbc.20048, 2013.

Wehr, R. and Saleska, S. R.: An improved isotopic method for partitioning net ecosystem-atmosphere CO<sub>2</sub> exchange, *Agric. For. Meteorol.*, 214–215, 515–531, doi:10.1016/j.agrformet.2015.09.009, 2015.

White, J. W. C., Vaughn, B. H., Michel, S. E., University of Colorado and Institute of Arctic and Alpine Research (INSTAAR): Stable Isotopic Composition of Atmospheric Carbon Dioxide (<sup>13</sup>C and <sup>18</sup>O) from the NOAA ESRL Carbon Cycle Cooperative Global Air Sampling Network, 1990–2014, Version: 2015-10-26, Path: [ftp://aftp.emdl.noaa.gov/data/trace\\_gases/co2e13/flask/](ftp://aftp.emdl.noaa.gov/data/trace_gases/co2e13/flask/), 2015.

White et al.: Parameterization and Sensitivity Analysis of the Biome BGC Terrestrial Ecosystem Model: Net Primary Production Controls, [online] Available from: [http://secure.ntsg.umt.edu/publications/2000/WTRN00/White\\_2000.pdf](http://secure.ntsg.umt.edu/publications/2000/WTRN00/White_2000.pdf), 2000.

Wingate, L., Ogee, J., Burlett, R., Bosc, A., Devaux, M., Grace, J., Loustau, D. and Gessler, A.: Photosynthetic carbon isotope discrimination and its relationship to the carbon isotope signals of stem, soil and ecosystem respiration, *New Phytol.*, 188(2), 576–589, 2010.

Zaehle, S., Medlyn, B. E., De Kauwe, M. G., Walker, A. P., Dietze, M. C., Hickler, T., Luo, Y., Wang, Y. P., El Masri, B., Thornton, P., Jain, A., Wang, S., Warland, D., Weng, E., Parton, W., Iversen, C. M., Gallet-Budynck, A., McCarthy, H., Finzi, A., Hanson, P. J., Prentice, I. C., Oren, R. and Norby, R. J.: Evaluation of 11 terrestrial carbon-nitrogen cycle models against observations from two temperate Free-Air CO<sub>2</sub> Enrichment studies, *New Phytol.*, 202(3), 803–822, doi:10.1111/nph.12697, 2014.

Zarter, C. R., Demmig-Adams, B., Ebbert, V., Adamska, I. and Adams, W. W.: Photosynthetic capacity and light harvesting efficiency during the winter to spring transition in subalpine conifers, *New Phytol.*, 172(2), 283–292, doi:10.1111/j.1469-8137.2006.01816.x, 2006.

Zeng, X.: Global Vegetation Root Distribution for Land Modeling, *J. Hydrometeorol.*, 2(5), 525–530, doi:10.1175/1525-7541(2001)002<0525:GVRDFL>2.0.CO;2, 2001.

Zeng, X. and Decker, M.: Improving the Numerical Solution of Soil Moisture Based Richards Equation for Land Models with a Deep or Shallow Water Table, *J. Hydrometeorol.*, 10(1), 308–319, doi:10.1175/2008JHM1011.1, 2009.

Ainsworth, E. A. and Long, S. P.: What have we learned from 15 years of free air CO<sub>2</sub> enrichment (FACE)? A meta analytic review of the responses of photosynthesis, canopy properties and plant production to rising CO<sub>2</sub>, *New Phytol.*, 165(2), 351–372, doi:10.1111/j.1469-8137.2004.01224.x, 2005.

Andrews, S. F., Flanagan, L. B., Sharp, E. J. and Cai, T.: Variation in water potential, hydraulic characteristics and water source use in montane Douglas fir and lodgepole pine trees in southwestern Alberta and consequences for seasonal changes in photosynthetic capacity, *Tree Physiol.*, 32, 146–160, doi:10.1093/treephys/tp136, 2012.

Aranibar, J. N., Berry, J. A., Riley, W. J., Pataki, D. E., Law, B. E. and Ehleringer, J. R.: Combining meteorology, eddy fluxes, isotope measurements, and modeling to understand environmental controls of carbon isotope discrimination at the canopy scale, *Glob. Change Biol.*, 12(4), 710–730, 2006.

Arora, V. K., Boer, G. J., Friedlingstein, P., Eby, M., Jones, C. D., Christian, J. R., Bonan, G., Bopp, L., Brovkin, V., Cadule, P., Hajima, T., Ilyina, T., Lindsay, K., Tjiputra, J. F. and Wu, T.: Carbon Concentration and Carbon Climate Feedbacks in CMIP5 Earth System Models, *J. Clim.*, 26(15), 5289–5314, doi:10.1175/jcli-d-12-00494.1, 2013.

Ballantyne, A. P., Miller, J. B. and Tans, P. P.: Apparent seasonal cycle in isotopic discrimination of carbon in the atmosphere and biosphere due to vapor pressure deficit, *Glob. Biogeochem. Cycles*, 24, GB3018, doi:10.1029/2009GB003623, 2010.

Ballantyne, A. P., Miller, J. B., Baker, I. T., Tans, P. P. and White, J. W. C.: Novel applications of carbon isotopes in atmospheric CO<sub>2</sub>: What can atmospheric measurements teach us about processes in the biosphere?, *Biogeosciences*, 8(10), 3093–3106, 2011.

Bauerle, W. L., Oren, R., Way, D. A., Qian, S. S., Stoy, P. C., Thornton, P. E., Bowden, J. D., Hoffman, F. M. and Reynolds, R. F.: Photoperiodic regulation of the seasonal pattern of photosynthetic capacity and the implications for carbon cycling, *Proc. Natl. Acad. Sci. U. S. A.*, 109(22), 8612–8617, 2012.

Belmecheri, S., Maxwell, R. S., Taylor, A. H., Davis, K. J., Freeman, K. H. and Munger, W. J.: Tree ring  $\delta^{13}\text{C}$  tracks flux tower ecosystem productivity estimates in a NE temperate forest, *Environ. Res. Lett.*, 9(7), 74011, doi:10.1088/1748-9326/9/7/074011, 2014.

Boisvenue, C. and Running, S. W.: Simulations show decreasing carbon stocks and potential for carbon emissions in Rocky Mountain forests over the next century, *Ecol. Appl.*, 20(5), 1302–1319, 2010.

Bowling, D. R., Pataki, D. E. and Randerson, J. T.: Carbon isotopes in terrestrial ecosystem pools and CO<sub>2</sub> fluxes, *New Phytol.*, 178, 24–40, doi: 10.1111/j.1469-8137.2007.02342.x, 2008.

Bowling, D. R., Ballantyne, A. P., Miller, J. B., Burns, S. P., Conway, T. J., Menzer, O., Stephens, B. B. and Vaughn, B. H.: Ecological processes dominate the  $\delta^{13}\text{C}$  land disequilibrium

Formatted: Normal

Formatted: Font color: Auto, English (United States)

in a Rocky Mountain subalpine forest, *Glob. Biogeochem. Cycles*, 28(4), 2013GB004686, doi:10.1002/2013GB004686, 2014a.

Bowling, D. R., Ballantyne, A. P., Miller, J. B., Burns, S. P., Conway, T. J., Menzer, O., Stephens, B. B. and Vaughn, B. H.: Ecological processes dominate the  $^{13}\text{C}$  land disequilibrium in a Rocky Mountain subalpine forest, *Glob. Biogeochem. Cycles*, 28(4), 2013GB004686, doi:10.1002/2013GB004686, 2014b.

Bradford, M. A., Fierer, N. and Reynolds, J. F.: Soil carbon stocks in experimental mesocosms are dependent on the rate of labile carbon, nitrogen and phosphorus inputs to soils, *Funct. Ecol.*, 22(6), 964–974, doi:10.1111/j.1365-2435.2008.01404.x, 2008.

Braswell, B. H., Sacks, W. J., Linder, E. and Schimel, D. S.: Estimating diurnal to annual ecosystem parameters by synthesis of a carbon flux model with eddy covariance net ecosystem exchange observations, *Glob. Change Biol.*, 11, 335–355, doi:10.1111/j.1365-2486.2005.00897.x, 2005.

Brüggemann, N., Gessler, A., Kayler, Z., Keel, S. G., Badeck, F., Barthel, M., Boeckx, P., Buchmann, N., Brugnoli, E., Esperschütz, J., Gavrichkova, O., Ghashghaie, J., Gomez-Casanovas, N., Keitel, C., Knohl, A., Kuptz, D., Palacio, S., Salmon, Y., Uchida, Y. and Bahn, M.: Carbon allocation and carbon isotope fluxes in the plant-soil-atmosphere continuum: a review, *Biogeosciences*, 8(11), 3457–3489, doi:10.5194/bg-8-3457-2011, 2011a.

Brüggemann, N., Gessler, A., Kayler, Z., Keel, S. G., Badeck, F., Barthel, M., Boeckx, P., Buchmann, N., Brugnoli, E., Esperschütz, J., Gavrichkova, O., Ghashghaie, J., Gomez-Casanovas, N., Keitel, C., Knohl, A., Kuptz, D., Palacio, S., Salmon, Y., Uchida, Y. and Bahn, M.: Carbon allocation and carbon isotope fluxes in the plant-soil-atmosphere continuum: A review, *Biogeosciences*, 8(11), 3457–3489, 2011b.

Collatz, G. J., Ball, J. T., Griwet, C. and Berry, J. A.: Regulation of stomatal conductances and transpiration: a physiological model of canopy processes, *Agric. For. Meteorol.*, 54, 107–136, 1991.

Desai, A. R., Moore, D. J. P., Ahue, W. K. M., Wilkes, P. T. V., De Wekker, S. F. J., Brooks, B. G., Campos, T. L., Stephens, B. B., Monson, R. K., Burns, S. P., Quaife, T., Aulenbach, S. M. and Schimel, D. S.: Seasonal pattern of regional carbon balance in the central Rocky Mountains from surface and airborne measurements, *J. Geophys. Res.*, 116, G04009(4), doi:10.1029/2011JG001655, 2011.

Dlugokencky, E. J., Lang, P. M., Masarie, K. A., Crotwell, A. M. and Crotwell, M. J.: Atmospheric Carbon Dioxide Dry Air Mole Fractions from the NOAA ESRL Carbon Cycle Cooperative Global Air Sampling network, 1968–2014, Version: 2015-08-03, Path: [http://aftp.emdl.noaa.gov/data/trace\\_gases/co2/flask/surface/](http://aftp.emdl.noaa.gov/data/trace_gases/co2/flask/surface/), 2015.

Ehleringer, J. R., Buchmann, N. and Flanagan, L. B.: Carbon isotope ratios in belowground carbon cycle processes, *Ecol. Appl.*, 10(2), 412–422, 2000.

Epron, D., Bahn, M., Derrien, D., Lattanzi, F. A., Pumpanen, J., Gessler, A., Höglberg, P., Maillard, P., Dannoura, M., Gérant, D. and Buchmann, N.: Pulse labelling trees to study carbon allocation dynamics: a review of methods, current knowledge and future prospects, *Tree Physiol.*, 32(6), 776–798, doi:10.1093/treephys/tps057, 2012.

Farquhar, G. D., von Caemmerer, S. and Berry, J. A.: A Biochemical Model of Photosynthetic CO<sub>2</sub> Assimilation in Leaves of C<sub>3</sub> Species, *Planta*, 149, 78–90, 1980.

Farquhar, G. D., O'Leary, M. H. and Berry, J. A.: On the relationship between carbon isotope discrimination and the intercellular carbon dioxide concentration in leaves, *Aust. J. Plant Physiol.*, 9(2), 121–137, 1982.

Farquhar, G. D., Ehleringer, J. R. and Hubick, K. T.: Carbon isotope discrimination and photosynthesis, *Annu. Rev. Plant Physiol. Plant Mol. Biol.*, 40, 503–537, 1989.

Flanagan, L. B., Cai, T., Black, T. A., Barr, A. G., McCaughey, J. H. and Margolis, H. A.: Measuring and modeling ecosystem photosynthesis and the carbon isotope composition of ecosystem-respired CO<sub>2</sub> in three boreal coniferous forests, *Agric. For. Meteorol.*, 153, 165–176, 2012.

Francey, R. J., Allison, C. E., Etheridge, D. M., Trudinger, C. M., Enting, I. G., Leuenberger, M., Langenfelds, R. L., Michel, E. and Steele, L. P.: A 1000-year high-precision record of δ<sup>13</sup>C in atmospheric CO<sub>2</sub>, *Tellus*, 51B, 170–193, 1999.

Frank, D. C., Poulter, B., Saurer, M., Esper, J., Huntingford, C., Helle, G., Treyde, K., Zimmermann, N. E., Schleser, G. H., Ahlström, A., Ciais, P., Friedlingstein, P., Levis, S., Lomas, M., Sitch, S., Viovy, N., Andreu-Hayles, L., Bednarz, Z., Berninger, F., Boettger, T., D'Alessandro, C. M., Daux, V., Filot, M., Grabner, M., Gutierrez, E., Haupt, M., Hidasvuori, E., Jungner, H., Kalela-Brundin, M., Krapiec, M., Leuenberger, M., Loader, N. J., Marah, H., Masson-Delmotte, V., Pázdur, A., Pawelezyk, S., Pierre, M., Planells, O., Pukienė, R., Reynolds-Henne, C. E., Rinne, K. T., Saracino, A., Sonninen, E., Stievenard, M., Switsur, V. R., Szezepanek, M., Szychowska-Krapiec, E., Todaro, L., Waterhouse, J. S. and Weigl, M.: Water-use efficiency and transpiration across European forests during the Anthropocene, *Nat. Clim. Change*, 5(6), 579–583, doi:10.1038/nclimate2614, 2015.

Franks, P. J., Adams, M. A., Amthor, J. S., Barbour, M. M., Berry, J. A., Ellsworth, D. S., Farquhar, G. D., Ghannoum, O., Lloyd, J., McDowell, N., Norby, R. J., Tissue, D. T. and von Caemmerer, S.: Sensitivity of plants to changing atmospheric CO<sub>2</sub> concentration: From the geological past to the next century, *New Phytol.*, 197(4), 1077–1094, 2013.

Friedlingstein, P., Cox, P. M., Betts, R. A., Bopp, L., von Bloh, W., Brovkin, V., Cadule, P., Doney, S. C., Eby, M., Fung, I. Y., Bala, G., John, J., Jones, C. D., Joos, F., Kato, T., Kawamiya, M., Knorr, W., Lindsay, K., Matthews, H. D., Raddatz, T., Rayner, P., Reick, C., Roeckner, E., Schnitzler, K. G., Schnur, R., Strassmann, K., Weaver, A. J., Yoshikawa, C. and Zeng, N.: Climate-carbon cycle feedback analysis: Results from the C4MIP model intercomparison, *J. Clim.*, 19, 3337–3353, 2006.

Fung, I. Y., Field, C. B., Berry, J. A., Thompson, M. V., Randerson, J. T., Malmstrom, C. M., Vitousek, P. M., Collatz, G. J., Sellers, P. J., Randall, D. A., Denning, A. S., Badeck, F. and John, J.: Carbon-13 exchanges between the atmosphere and biosphere, *Glob. Biogeochem. Cycles*, 11(4), 507–533, 1997.

Greenland, D.: The Climate of Niwot Ridge, Front Range, Colorado, U.S.A., *Arct. Alp. Res.*, 21(4), 380–391, 1989.

Hogberg, P., Hogberg, M. N., Gottlicher, S. G., Betson, N. R., Keel, S. G., Metcalfe, D. B., Campbell, C., Schindlbacher, A., Hurry, V., Lundmark, T., Linder, S. and Nasholm, T.: High temporal resolution tracing of photosynthate carbon from the tree canopy to forest soil microorganisms, *New Phytol.*, 177(1), 220–228, 2008.

Hu, J., Moore, D. J. P., Burns, S. P. and Monson, R. K.: Longer growing seasons lead to less carbon sequestration by a subalpine forest, *Glob. Change Biol.*, 16(2), 771–783, doi:10.1111/j.1365-2486.2009.01967.x, 2010.

Katul, G. G., Ellsworth, D. S. and Lai, C. T.: Modelling assimilation and intercellular CO<sub>2</sub> from measured conductance: a synthesis of approaches, *Plant Cell Environ.*, 23(12), 1313–1328, doi:10.1046/j.1365-3040.2000.00641.x, 2000.

Keenan, T. F., Hollinger, D. Y., Bohrer, G., Dragoni, D., Munger, J. W., Schmid, H. P. and Richardson, A. D.: Increase in forest water use efficiency as atmospheric carbon dioxide concentrations rise, *Nature*, 499(7458), 324–327, doi:10.1038/nature12291, 2013.

Kolari, P., Lappalainen, H. K., Hänninen, H. and Hari, P.: Relationship between temperature and the seasonal course of photosynthesis in Scots pine at northern timberline and in southern boreal zone, *Tellus B*, 59(3), 542–552, doi:10.1111/j.1600-0889.2007.00262.x, 2007.

Lasslop, G., Reichstein, M., Papale, D., Richardson, A., Arneeth, A., Barr, A., Stoy, P. and Wohlfahrt, G.: Separation of net ecosystem exchange into assimilation and respiration using a light response curve approach: critical issues and global evaluation, *Glob. Change Biol.*, 16, 487–208, 2010.

Le Quéré, C., Moriarty, R., Andrew, R. M., Peters, G. P., Ciais, P., Friedlingstein, P., Jones, S. D., Sitch, S., Tans, P., Arneeth, A., Boden, T. A., Bopp, L., Bozec, Y., Canadell, J. G., Chini, L. P., Chevallier, F., Cosca, C. E., Harris, I., Hoppema, M., Houghton, R. A., House, J. I., Jain, A. K., Johannessen, T., Kato, E., Keeling, R. F., Kitidis, V., Klein Goldewijk, K., Koven, C., Landa, C. S., Landschützer, P., Lenton, A., Lima, I. D., Marland, G., Mathis, J. T., Metzl, N., Nojiri, Y., Olsen, A., Ono, T., Peng, S., Peters, W., Pfeil, B., Poulter, B., Raupach, M. R., Regnier, P., Rödenbeck, C., Saito, S., Salisbury, J. E., Schuster, U., Schwinger, J., Séférian, R., Segschneider, J., Steinhoff, T., Stocker, B. D., Sutton, A. J., Takahashi, T., Tilbrook, B., van der Werf, G. R., Viovy, N., Wang, Y. P., Wanninkhof, R., Wiltshire, A. and Zeng, N.: Global carbon budget 2014, *Earth Syst. Sci. Data*, 7(1), 47–85, doi:10.5194/essd-7-47-2015, 2015.

Leuning, R.: A critical appraisal of a combined stomatal-photosynthesis model for C<sub>3</sub> plants, *Plant Cell Environ.*, 18(4), 339–355, doi:10.1111/j.1365-3040.1995.tb00370.x, 1995.

Mao, J., Ricciuto, D. M., Thornton, P. E., Warren, J. M., King, A. W., Shi, X., Iversen, C. M. and Norby, R. J.: Evaluating the Community Land Model in a pine stand with shading manipulations and <sup>13</sup>C/<sup>12</sup>C labeling, *Biogeosciences*, 13(3), 641–657, doi:10.5194/bg-13-641-2016, 2016.

Martinelli, L. A., Almeida, S., Brown, I. F., Moreira, M. Z., Victoria, R. L., Sternberg, L. S. L., Ferreira, C. A. C. and Thomas, W. W.: Stable carbon isotope ratio of tree leaves, boles and fine litter in a tropical forest in Rondonia, Brazil, *Oecologia*, 114(2), 170–179, 1998.

1 McDowell, N. G., Allen, C. D. and Marshall, L.: Growth, carbon isotope discrimination, and  
2 drought-associated mortality across a *Pinus ponderosa* elevational transect, *Glob. Change Biol.*,  
3 16(1), 399–415, 2010.

4 Medvigy, D., Wofsy, S. C., Munger, J. W., Hollinger, D. Y. and Moorcroft, P. R.: Mechanistic  
5 scaling of ecosystem function and dynamics in space and time: Ecosystem Demography model  
6 version 2, *J. Geophys. Res. Biogeosciences*, 114, G01002, doi:10.1029/2008JG000812, 2009.

7 Mitton, J. and Ferrenberg, S. M.: Mountain pine beetle develops an unprecedented summer  
8 generation in response to climate warming, *Am. Nat.*, 179(5), 1–9, 2012.

9 Monson, R. K., Turnipseed, A. A., Sparks, J. P., Harley, P. C., Scott-Denton, L. E., Sparks, K.  
10 and Huxman, T. E.: Carbon sequestration in a high-elevation, subalpine forest, *Glob. Change*  
11 *Biol.*, 8, 459–478, 2002.

12 Monson, R. K., Sparks, J. P., Rosentiel, T. N., Scott-Denton, L. E., Huxman, T. E., Harley, P.  
13 C., Turnipseed, A. A., Burns, S. P., Backlund, B. and Hu, J.: Climatic influences on net  
14 ecosystem CO<sub>2</sub> exchange during the transition from wintertime carbon source to springtime  
15 carbon sink in a high-elevation, subalpine forest, *Oecologia*, 146, 130–147–5–169–2, 2005.

16 Oleson et al.: Technical Description of version 4.5 of the Community Land Model (CLM),  
17 [online] Available from:  
18 [http://www.cesm.ucar.edu/models/cesm1.2/clm/CLM45\\_Tech\\_Note.pdf](http://www.cesm.ucar.edu/models/cesm1.2/clm/CLM45_Tech_Note.pdf), 2013.

19 Parton, W. J., Hanson, P. J., Swanston, C., Torn, M., Trumbore, S. E., Riley, W. and Kelly, R.:  
20 ForCent model development and testing using the Enriched Background Isotope Study  
21 experiment, *J. Geophys. Res. Biogeosciences*, 115(G4), G04001, doi:10.1029/2009JG001193,  
22 2010.

23 Peñuelas, J., Canadell, J. G. and Ogaya, R.: Increased water use efficiency during the 20th  
24 century did not translate into enhanced tree growth, *Glob. Ecol. Biogeogr.*, 20(4), 597–608,  
25 doi:10.1111/j.1466-8238.2010.00608.x, 2011.

26 Reichstein, M., Falge, E., Baldocchi, D., Papale, D., Aubinet, M., Berbigier, P., Bernhofer, C.,  
27 Buchmann, N., Gilmanov, T., Granier, A., Grunwald, T., Havrankova, K., Ilvesniemi, H.,  
28 Janous, D., Knohl, A., Laurila, T., Lohila, A., Loustau, D., Matteucci, G., Meyers, T., Miglietta,  
29 F., Ourival, J. M., Pumpanen, J., Rambal, S., Rotenberg, E., Sanz, M., Tenhunen, J., Seufert,  
30 G., Vaccari, F., Vesala, T., Yakir, D. and Valentini, R.: On the separation of net ecosystem  
31 exchange into assimilation and ecosystem respiration: review and improved algorithm, *Glob.*  
32 *Change Biol.*, 11(9), 1424–1439, 2005.

33 Ricciuto, D. M., Davis, K. J. and Keller, K.: A Bayesian calibration of a simple carbon cycle  
34 model: The role of observations in estimating and reducing uncertainty, *Glob. Biogeochem.*  
35 *Cycles*, 22, GB2030, doi:10.1029/2006GB002908, 2008.

36 Ricciuto, D. M., King, A. W., Dragoni, D. and Post, W. M.: Parameter and prediction  
37 uncertainty in an optimized terrestrial carbon cycle model: Effects of constraining variables and  
38 data record length, *J. Geophys. Res. Biogeosciences*, 116(G1), G01033,  
39 doi:10.1029/2010JG001400, 2011.

Formatted: Normal

Richardson, A. D., Williams, M., Hollinger, D. Y., Moore, D. J. P., Dail, D. B., Davidson, E. A., Scott, N. A., Evans, R. S., Hughes, H., Lee, J. T., Rodrigues, C. and Savage, K.: Estimating parameters of a forest ecosystem C model with measurements of stocks and fluxes as joint constraints, *Oecologia*, 164(1), 25–40, 2010.

Roden, J. S. and Ehleringer, J. R.: Summer precipitation influences the stable oxygen and carbon isotopic composition of tree-ring cellulose in *Pinus ponderosa*, *Tree Physiol.*, 27(4), 491–501, 2007.

Rubino, M., Etheridge, D. M., Trudinger, C. M., Allison, C. E., Battle, M. O., Langenfelds, R. L., Steele, L. P., Curran, M., Bender, M., White, J. W. C., Jenk, T. M., Blunier, T. and Francey, R. J.: A revised 1000-year atmospheric  $\delta^{13}\text{C}$ -CO<sub>2</sub> record from Law Dome and South Pole, Antarctica, *J. Geophys. Res. Atmospheres*, 118(15), 8482–8499, doi:10.1002/jgrd.50668, 2013.

Saurer, M., Siegwolf, R. T. W. and Schweingruber, F. H.: Carbon isotope discrimination indicates improving water use efficiency of trees in northern Eurasia over the last 100 years, *Glob. Change Biol.*, 10(12), 2109–2120, doi:10.1111/j.1365-2486.2004.00869.x, 2004.

Saurer, M., Spahni, R., Frank, D. C., Joos, F., Leuenberger, M., Loader, N. J., McCarroll, D., Gagen, M., Poulter, B., Siegwolf, R. T. W., Andreu-Hayles, L., Boettger, T., Dorado Liñán, I., Fairchild, I. J., Friedrich, M., Gutierrez, E., Haupt, M., Hiltunen, E., Heinrich, I., Helle, G., Grudd, H., Jalkanen, R., Levanič, T., Linderholm, H. W., Robertson, I., Sonninen, E., Treydte, K., Waterhouse, J. S., Woodley, E. J., Wynn, P. M. and Young, G. H. F.: Spatial variability and temporal trends in water use efficiency of European forests, *Glob. Change Biol.*, 20(12), 3700–3712, doi:10.1111/gcb.12717, 2014.

Schaeffer, S. M., Miller, J. B., Vaughn, B. H., White, J. W. C. and Bowling, D. R.: Long-term field performance of a tunable diode laser absorption spectrometer for analysis of carbon isotopes of CO<sub>2</sub> in forest air, *Atmospheric Chem. Phys.*, 8, 5263–5277, 2008.

Schimel, D. T., Kittel, G. F., Running, S., Monson, R., Turnispeed, A. and Anderson, D.: Carbon sequestration studied in western U.S. mountains, *Eos Trans AGU*, 83(40), 445–449, 2002.

Scott-Denton, L. E., Sparks, K. L. and Monson, R. K.: Spatial and temporal controls of soil respiration rate in a high-elevation, subalpine forest, *Soil Biol. Biochem.*, 35, 525–534, 2003.

Sellers, P. J., Randall, D. A., Collatz, G. J., Berry, J. A., Field, C. B., Dazlich, D. A., Zhang, C., Collelo, G. D. and Bounoua, L.: A revised land surface parameterization (SiB2) for atmospheric GCMs. Part I: Model formulation, *J. Clim.*, 9(4), 676–705, 1996.

Thornton, P. E. and Rosenbloom, N. A.: Ecosystem model spin-up: Estimating steady-state conditions in a coupled terrestrial carbon and nitrogen cycle model, *Ecol. Model.*, 189(1–2), 25–48, doi:10.1016/j.ecolmodel.2005.04.008, 2005.

Thornton, P. E., Law, B. E., Gholz, H. L., Clark, K. L., Falge, E., Ellsworth, D. S., Golstein, A. H., Monson, R. K., Hollinger, D., Falk, M., Chen, J. and Sparks, J. P.: Modeling and measuring the effects of disturbance history and climate on carbon and water budgets in evergreen needleleaf forests, *Agric. For. Meteorol.*, 113(1–4), 185–222, 2002.



Thornton, P. E., Lamarque, J. F., Rosenbloom, N. A. and Mahowald, N. M.: Influence of carbon-nitrogen cycle coupling on land model response to CO<sub>2</sub> fertilization and climate variability, *Glob. Biogeochem. Cycles*, 21, GB4018, doi:10.1029/2006GB002868, 2007.

Trolier, M., White, J. W. C., Tans, P. P., Masarie, K. A. and Gemery, P. A.: Monitoring the isotopic composition of atmospheric CO<sub>2</sub>: Measurements from the NOAA Global Air Sampling Network, *J. Geophys. Res. Atmospheres*, 101(D20), 25,897-25,916, 1996.

van der Velde, I. R., Miller, J. B., Schaefer, K., Masarie, K. A., Denning, S., White, J. W. C., Tans, P. P., Krol, M. C. and Peters, W.: Biosphere model simulations of interannual variability in terrestrial <sup>13</sup>C/<sup>12</sup>C exchange, *Glob. Biogeochem. Cycles*, 27(3), 637-649, doi:10.1002/gbc.20048, 2013.

Wehr, R. and Saleska, S. R.: An improved isotopic method for partitioning net ecosystem-atmosphere CO<sub>2</sub> exchange, *Agric. For. Meteorol.*, 214-215, 515-531, doi:10.1016/j.agrformet.2015.09.009, 2015.

White, J. W. C., Vaughn, B. H., Michel, S. E., University of Colorado and Institute of Arctic and Alpine Research (INSTAAR): Stable Isotopic Composition of Atmospheric Carbon Dioxide (<sup>13</sup>C and <sup>18</sup>O) from the NOAA ESRL Carbon Cycle Cooperative Global Air Sampling Network, 1990-2014, Version: 2015-10-26, Path: [ftp://ftp.cmdl.noaa.gov/data/trace\\_gases/co2e13/flask/](ftp://ftp.cmdl.noaa.gov/data/trace_gases/co2e13/flask/), 2015.

White et al.: Parameterization and Sensitivity Analysis of the Biome-BGC Terrestrial Ecosystem Model: Net Primary Production Controls, [online] Available from: [http://secure.nts.g.umn.edu/publications/2000/WTRN00/White\\_2000.pdf](http://secure.nts.g.umn.edu/publications/2000/WTRN00/White_2000.pdf), 2000.

Wingate, L., Ogee, J., Burlett, R., Bose, A., Devaux, M., Grace, J., Loustau, D. and Gessler, A.: Photosynthetic carbon isotope discrimination and its relationship to the carbon isotope signals of stem, soil and ecosystem respiration, *New Phytol.*, 188(2), 576-589, 2010.

Zachle, S., Medlyn, B. E., De Kauwe, M. G., Walker, A. P., Dietze, M. C., Hickler, T., Luo, Y., Wang, Y. P., El Masri, B., Thornton, P., Jain, A., Wang, S., Warland, D., Weng, E., Parton, W., Iversen, C. M., Gallet-Budynek, A., McCarthy, H., Finzi, A., Hanson, P. J., Prentice, I. C., Oren, R. and Norby, R. J.: Evaluation of 11 terrestrial carbon-nitrogen cycle models against observations from two temperate Free-Air CO<sub>2</sub> Enrichment studies, *New Phytol.*, 202(3), 803-822, doi:10.1111/nph.12697, 2014.

Zarter, C. R., Demmig-Adams, B., Ebbert, V., Adamska, I. and Adams, W. W.: Photosynthetic capacity and light harvesting efficiency during the winter to spring transition in subalpine conifers, *New Phytol.*, 172(2), 283-292, doi:10.1111/j.1469-8137.2006.01816.x, 2006.

Zeng, X.: Global Vegetation Root Distribution for Land Modeling, *J. Hydrometeorol.*, 2(5), 525-530, doi:10.1175/1525-7541(2001)002<0525:GVRDFL>2.0.CO;2, 2001.

Zeng, X. and Decker, M.: Improving the Numerical Solution of Soil Moisture-Based Richards Equation for Land Models with a Deep or Shallow Water Table, *J. Hydrometeorol.*, 10(1), 308-319, doi:10.1175/2008JHM1011.1, 2009.



1  
2  
3  
4  
5  
6  
7  
8  
9  
10  
11  
12  
13

14 Table 1. List of symbols used.

Symbol	Description	Unit or Unit Symbol
$\alpha_{psa}$	Fractionation factor ( $R_a/ R_{GPP}$ )	dimensionless
$\beta_t$	Soil water stress parameter (BTRAN)	dimensionless
$\Delta_{canopy}$	photosynthetic carbon isotope discrimination	‰
$\delta^{13}C$	$^{13}C/^{12}C$ isotope composition (relative to VPDB)	‰
$\delta_{atm}$	$\delta^{13}C$ of atmospheric $CO_2$	‰
$\delta_{ER}$	$\delta^{13}C$ of ecosystem respiration	‰
$\delta_{GPP}$	$\delta^{13}C$ of net photosynthetic assimilation	‰
$\Gamma^*$	$CO_2$ compensation point	Pa
$A_c$	Enzyme-limiting rate of photosynthetic assimilation	$\mu mol\ m^{-2}\ s^{-1}$
$A_j$	Light-limiting rate of photosynthetic assimilation	$\mu mol\ m^{-2}\ s^{-1}$
$A_p$	Product-limiting rate of photosynthetic assimilation	$\mu mol\ m^{-2}\ s^{-1}$
$A_n$	net photosynthetic assimilation	$\mu mol\ m^{-2}\ s^{-1}$
$A$	<u>gross photosynthetic assimilation</u>	<u><math>\mu mol\ m^{-2}\ s^{-1}</math></u>
$Resp_d$	Leaf-level <del>dark</del> respiration	$\mu mol\ m^{-2}\ s^{-1}$
$a_{R25}$	Specific activity of Rubisco at 25°C	$\mu mol\ g^{-1}\ Rubisco\ s^{-1}$
$b$	Minimum stomatal conductance	$\mu mol\ m^{-2}\ s^{-1}$
$CF_{alloc}$	Actual carbon allocated to biomass (N-limited)	$gC\ m^{-2}\ s^{-1}$
$CF_{av\_alloc}$	Maximum carbon available for allocation to biomass	$gC\ m^{-2}\ s^{-1}$
$CF_{GPPpot}$	Potential gross primary production (non N-limited)	$gC\ m^{-2}\ s^{-1}$
$c_a$	Atmospheric $CO_2$ <u>partial</u> pressure	Pa
$c_i$	Leaf <del>inter</del> cellular $CO_2$ <u>partial</u> pressure	Pa
$c_i^*$	Leaf intracellular $CO_2$ <u>partial</u> pressure, (N-limited)	Pa
$c_s$	Leaf surface $CO_2$ <del>-partial</del> pressure	Pa
$e_l$	Saturation vapor pressure	Pa
$e_s$	Water vapor pressure at leaf surface	Pa
$E_T$	<u>Ecosystem</u> <del>Leaf</del> Transpiration	$\mu mol\ m^{-2}\ s^{-1}$
ER	Ecosystem respiration	$\mu mol\ m^{-2}\ s^{-1}$
GPP	Gross primary productivity (photosynthesis)	$\mu mol\ m^{-2}\ s^{-1}$
$F_{LNR}$	Fraction of leaf nitrogen within Rubisco	$gN\ Rubisco\ g^{-1}\ N$
$F_{NR}$	Total Rubisco mass per nitrogen mass within Rubisco	$g\ Rubisco\ g^{-1}\ N\ Rubisco$
$f_{df}$	$V_{cmax}$ scaling factor	dimensionless
$f_{dreg}$	Nitrogen photosynthetic downregulation factor	dimensionless

$g_b$	Leaf boundary layer conductance	$\mu\text{mol m}^{-2} \text{s}^{-1}$
$g_s$	Leaf stomatal conductance	$\mu\text{mol m}^{-2} \text{s}^{-1}$
$h_s$	Leaf surface <b>relative</b> humidity	$\text{Pa Pa}^{-1}$
$K_c$	<b>CO<sub>2</sub></b> Michaelis-Menten constant	$\text{Pa}$
$K_o$	<b>O<sub>2</sub></b> Michaelis-Menten constant	$\text{Pa}$
$LE$	Latent heat flux	$\text{W m}^{-2}$
$m$	Stomatal slope (Ball Berry conductance model)	dimensionless
$Na$	Leaf nitrogen concentration	$\text{gN m}^{-2}$ leaf area
$NEE$	Net ecosystem exchange	$\mu\text{mol m}^{-2} \text{s}^{-1}$
$NPP$	Net primary production	$\mu\text{mol m}^{-2} \text{s}^{-1}$
$o_i$	O <sub>2</sub> atmospheric partial pressure	$\text{Pa}$
$PFT$	Plant functional type	N/A
$P_{atm}$	Atmospheric pressure	$\text{Pa}$
$R_a$	Isotopic ratio of canopy air	$^{13}\text{C}/^{12}\text{C}$
$R_{GPP}$	Isotopic ratio of net photosynthetic assimilation	$^{13}\text{C}/^{12}\text{C}$
$R_{VPDB}$	Isotopic ratio of Vienna Pee Dee Belemnite standard	$^{13}\text{C}/^{12}\text{C}$
$r$	Fraction of roots (for $\beta_i$ )	dimensionless
$V_{cmax25}$	Maximum carboxylation rate at 25°C	$\mu\text{mol m}^{-2} \text{s}^{-1}$
$V_{cmax}$	Maximum carboxylation rate at leaf temperature	$\mu\text{mol m}^{-2} \text{s}^{-1}$
$VPD$	Vapor pressure deficit	$\text{Pa}$
$w$	Plant wilting factor (for $\beta_i$ )	dimensionless
$WUE$	Water use efficiency, ground area basis	$\frac{\mu\text{mol gC}}{\text{mol gH}_2\text{O}} \text{s}^{-1}$
$iWUE$	Intrinsic water use efficiency, leaf area basis	$\frac{\mu\text{mol gC}}{\text{mol gH}_2\text{O}} \text{s}^{-1}$

Formatted: Subscript

Formatted: Subscript

1 Table 2. CLM 4.5 model formulation description based upon timing of nitrogen limitation.  
 2 Pre-photosynthetic and post-photosynthetic nitrogen limitation are achieved through  $V_{cmax25}$   
 3 calibration (equation 175) and  $f_{dreg}$  (equation 87) respectively.

Formulation	Pre-Photosynthetic Nitrogen Limitation	Post-Photosynthetic Nitrogen Limitation	Impacts <del>on</del> $c_i/c_a$ & discrimination	Impacts <del>on</del> stomatal conductance $g_s$ and $A_n$
<i>Limited nitrogen (default)</i>	Yes (weak)	Yes, $f_{dreg} > 0$	Yes	No
<i>Unlimited nitrogen</i>	Yes (strong)	No, $f_{dreg} = 0$	Yes	Yes
<i>No downregulation discrimination</i>	Yes (weak)	Yes, $f_{dreg} > 0$	No	No

Formatted: Font: Italic

Formatted: Font: Italic, Subscript

Formatted: Font: Italic

Formatted: Font: Italic, Subscript

1 Table 3. CLM 4.5 key parameter values for all model formulations

Parameter	Description	Value	Units
<i>froot_leaf</i>	new fine root C per new leaf C	0.5	gC gC <sup>-1</sup>
<i>froot_cn</i>	fine root (C:N)	55	gC gN <sup>-1</sup>
<i>leaf_long</i>	leaf longevity	5	years
<i>leaf_cn</i>	leaf (C:N)	50	gC gN <sup>-1</sup>
<i>lflitcn</i>	leaf litter (C:N)	100	gC gN <sup>-1</sup>
<i>slatop</i>	specific leaf area (top canopy)	0.007	m <sup>2</sup> gC <sup>-1</sup>
<i>stem_leaf</i>	new stem C per new leaf C	2	gC gC <sup>-1</sup>
<i>mp</i>	stomatal slope	9	
<i>croot_stem</i>	coarse root: stem allocation	0.3	gC gC <sup>-1</sup>
<i>deadwood_cn</i>	dead wood (C:N)	500	gC gN <sup>-1</sup>
<i>livewood_cn</i>	live wood (C:N)	50	gC gN <sup>-1</sup>
<i>flnr</i>	fraction of leaf nitrogen within Rubisco enzyme	0.0509	gN gN <sup>-1</sup>
<i>decomp_depth_e_folding</i>	controls soil decomposition rate with depth	20	m

2

3



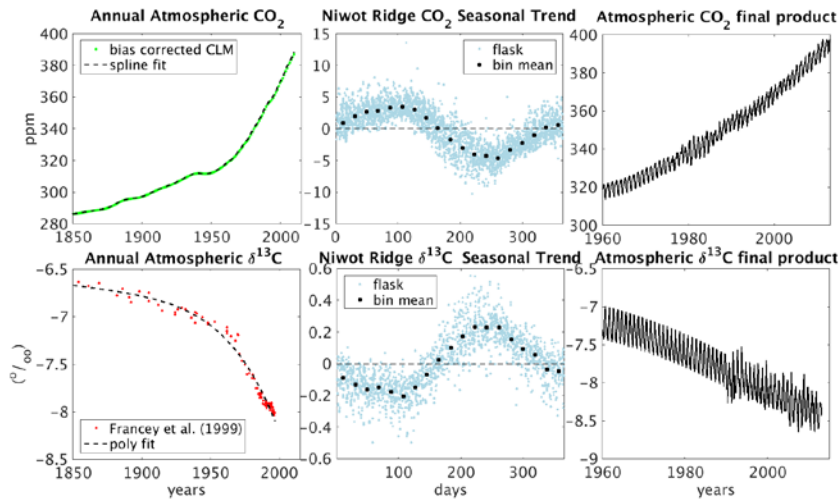


Figure 24. Niwot Ridge synthetic data product for atmospheric CO<sub>2</sub> concentration ( $c_a$ ) (top row) and  $\delta^{13}\text{C}$  of CO<sub>2</sub> ( $\delta_{\text{atm}}$ ) (bottom row). The final time series (right column) was used as a boundary condition for CLM, and created by combining the annual trends reported by Francey et al. (1999) adjusted for Niwot Ridge (left column) with the mean seasonal cycles measured at Niwot Ridge (middle column).

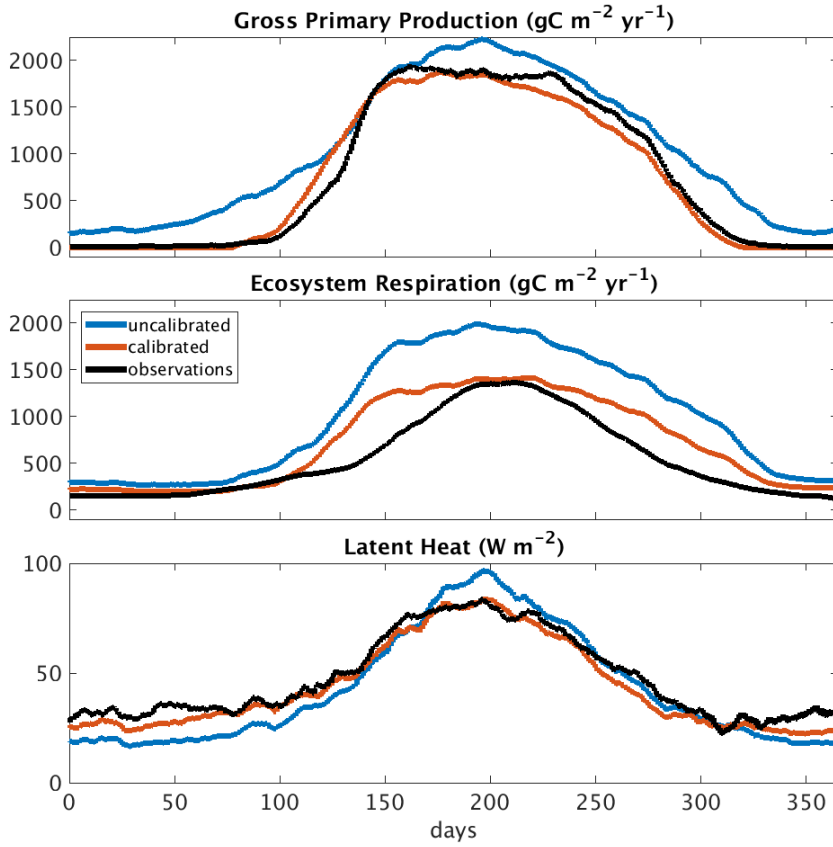


Figure 32. Seasonal averages (1999-2013) of simulated and observed land-atmosphere fluxes for A) gross primary production (GPP) B) ecosystem respiration (ER) and C) latent heat (LE) for the *limited nitrogen* simulation. The ‘observations’ are taken from the Ameriflux L2 processed eddy covariance flux tower data, partitioned into GPP and ER using the method of Reichstein et al. (2005). The *uncalibrated* simulation represents the CLM simulation without  $V_{max}$  scaling and the *calibrated* simulation represents the CLM run using the  $V_{max}$  scaling approach.

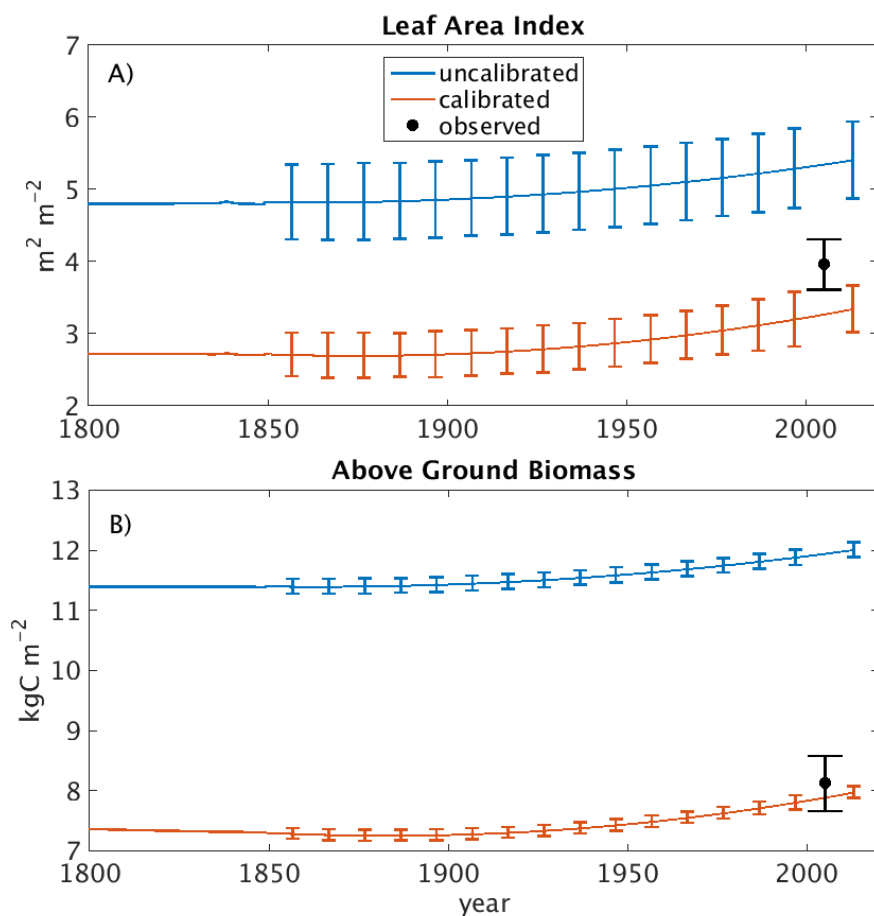


Figure 43. Simulation of A) leaf area index and B) above ground biomass for both uncalibrated and calibrated ( $V_{\text{cmax}}$  downscaled, *limited nitrogen*) simulation. Observations are from Bradford et al. (2008) with uncertainty bars representing standard error. Uncertainty bars on simulated runs represent 95% confidence of biomass variation as a result of cycling the site level meteorology observations.



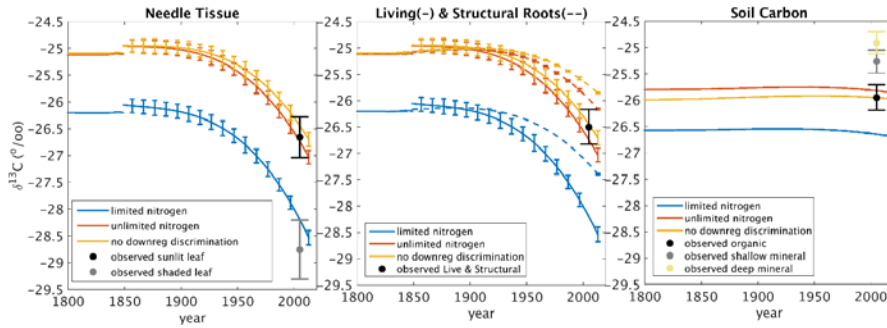


Figure 54. Simulation of  $\delta^{13}\text{C}$  of bulk needle tissue, bulk roots and bulk soil carbon. A description of model formulations are provided in Table (2). Uncertainty bars for simulations represent 95% confidence intervals of  $\delta^{13}\text{C}$  variation as a result of cycling the site level meteorology observations. The observed values are from Schaeffer et al. (2008) with uncertainty bars representing standard error. Solid lines and dashed lines in middle panel represent living roots and structural roots respectively.

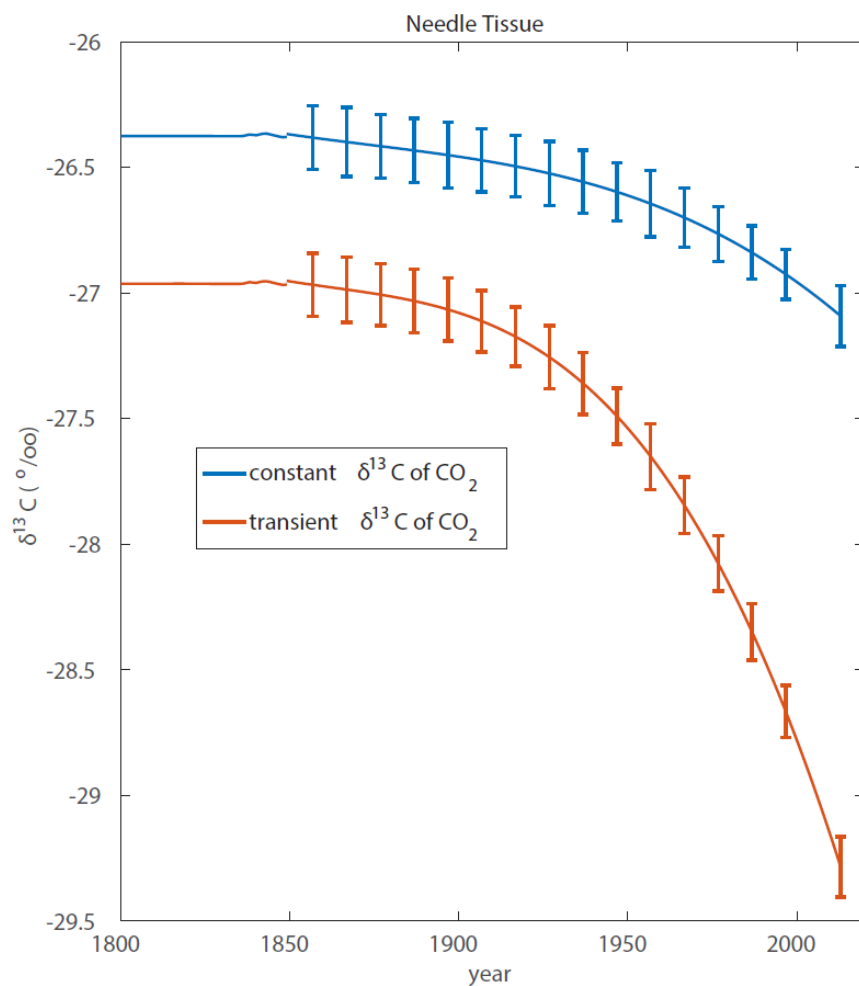


Figure 65. Simulation of  $\delta^{13}\text{C}$  of needle tissue using the *limited nitrogen* (default) CLM run. In the *constant  $\delta^{13}\text{C}$  of  $\text{CO}_2$  ( $\delta_{\text{atm}}$ )* simulation the model boundary condition was -6 ‰, whereas the *transient  $\delta_{\text{atm}}$*  simulation varied over time (Figure 24).

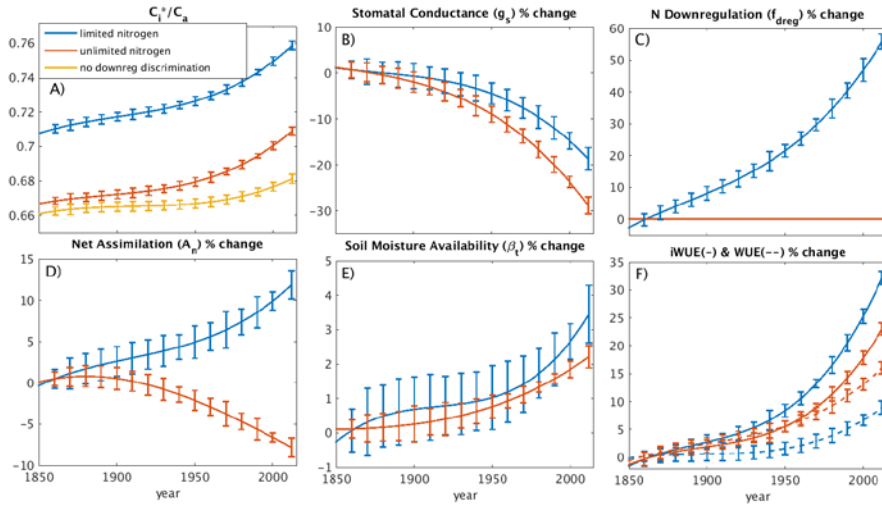


Figure 76. Diagnostic model variables that explain the discrimination trends (Figure 54) for the three model formulations as described in Table (2) for A)  $c_i^*/c_a$ , B)  $g_s$ , C)  $f_{dreg}$ , D)  $A_n$ , E)  $\beta_s$ , and F) the water use efficiency (WUE) and intrinsic water use efficiency (iWUE). Where the *no downregulation discrimination* simulation is not shown, it was identical to the *limited nitrogen* simulation. Uncertainty bars represent 95 % confidence intervals of diagnostic variable variation as a result of cycling the site level meteorology observations. The dashed lines represent WUE and the solid lines represent iWUE in panel F.

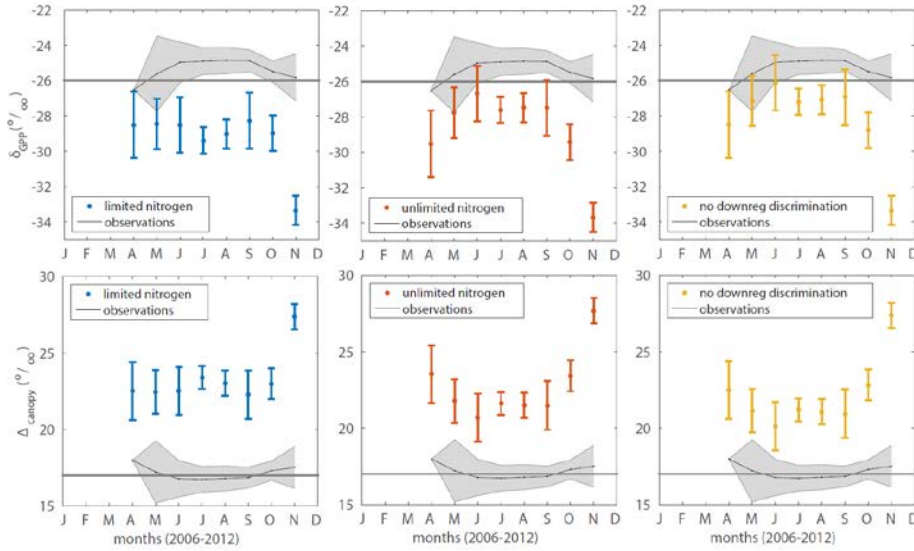


Figure 87. The seasonal pattern of photosynthetic discrimination as shown through  $\delta_{GPP}$  (top row) and  $\Delta_{canopy}$  (bottom row). Uncertainty bars represent 95% confidence bounds of simulated monthly average values from 2006-2012. Gray-shaded observation bounds represent 95% confidence intervals of ‘observed’ monthly average values based upon isotopic mixing model using Reichstein et al. (2005) partitioning of net ecosystem exchange flux described by (Bowling et al. 2014). The horizontal lines at  $\delta^{13}C$  of -26 ‰ (top row) and 17 ‰ (bottom row) are included for reference.

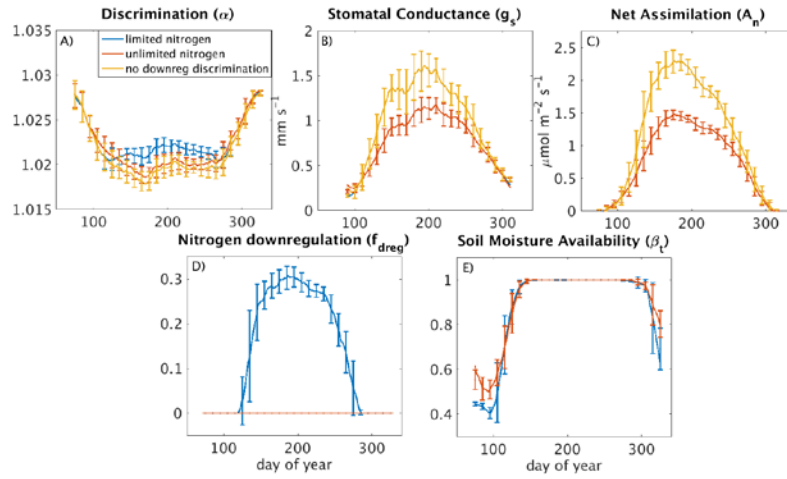


Figure 98. The seasonal pattern of discrimination (panel A) and diagnostic variables that explain the discrimination pattern in Figure (87). The individual tiles provide behavior from days 75-325 for A)  $\alpha_{psn}$ , B)  $g_s$ , C)  $A_n$ , D)  $f_{dreg}$ , and E)  $\beta_i$ . Where the *no downregulation discrimination* model simulation is not shown, it is identical to the *limited nitrogen* simulation. Uncertainty bars represent 95 % confidence intervals of inter-annual variation from 2006-2012.

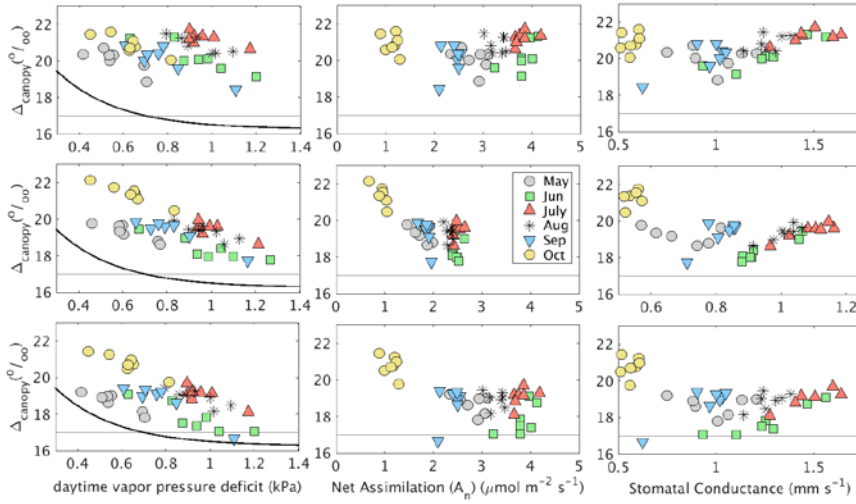


Figure 109. Relationship between monthly average photosynthetic discrimination and monthly average vapor pressure deficit (1<sup>st</sup> column),  $A_n$  (2<sup>nd</sup> column) and  $g_s$  (3<sup>rd</sup> column) from 2006-2012. The rows represent the *limited nitrogen* (row 1), *unlimited nitrogen* (row 2), and *no downregulation discrimination* (row 3) simulations. The black line in the 1<sup>st</sup> column is based on exponential fitted line from observed relationship at Niwot Ridge (Bowling et al. 2014). The horizontal lines represent  $\delta^{13}\text{C}$  of 17 ‰ and are included for reference.